Summer 2018

Hydrodynamics related performance evaluation of Upflow Moving Bed Hydrotreater reactor (MBR) using developed experimental methods and CFD simulation

Vineet Alexander

Department: Chemical and Biochemical Engineering

HYDRODYNAMICS RELATED PERFORMANCE EVALUATION OF UPFLOW MOVING BED HYDROTREATER REACTOR (MBR) USING DEVELOPED EXPERIMENTAL METHODS AND CFD SIMULATION

by

VINEET ALEXANDER

A DISSERTATION

Presented to the Graduate Faculty of the

MISSOURI UNIVERSITY OF SCIENCE AND TECHNOLOGY

In Partial Fulfillment of the Requirements for the Degree

DOCTOR OF PHILOSOPHY

in

CHEMICAL ENGINEERING

May 2018

Approved by

Muthanna Al-Dahhan, Advisor
Joseph Smith
Parthasakha Neogi
Joontaek Park
Joshua Schlegel

PUBLICATION DISSERTATION OPTION

This dissertation consists of the following four articles which will be submitted for publication as follows:

Paper I: Pages 8-32 are intended for submission to Flow Measurement and Instrumentation Journal.

Paper II: Pages 33-65 are intended for submission to Chemical Engineering Science Journal.

Paper III: Pages 66-94 are intended for submission to American Institute of Chemical Engineering (AIChE) Journal.

Paper IV: Pages 95-119 are intended for submission to American Institute of Chemical Engineering (AIChE) Journal.

ABSTRACT

Upflow Moving Bed Hydrotreater (MBR) reactor is used for hydrotreating resid crude oil. It is a two-phase upflow reactor having a catalyst bed with conical bottom, and plena. At industrial conditions the reactor is not performing at its best and encountering issues such as hot spots, catalyst agglomeration inside the catalyst bed leading to frequent shutdown of the reactor. The root cause of these problems are linked to the improper hydrodynamics inside the catalyst bed. To investigate this, the industrial scale MBR is scaled down to a pilot scale and indicative and key hydrodynamic parameters are investigated using developed experimental methods and CFD simulation.

The local hydrodynamics is quantified using an experimental technique called two-tip optical probe (TTOP). Developed algorithms for TTOP to derive the local phase saturations, velocities, backmixing, maldistribution using the time series data of the probe. The results indicates high maldistribution zones inside the catalyst bed and found convincing evidence to link this to the conical design and plena of MBR.

Overall Gas and Liquid dispersion/Mixing in the catalyst bed is investigated by tracer studies using a developed methodology based on residence time distribution (RTD), Convolution, Regression, and Catalyst Bed Models based on axial dispersion and wave model. Good gas/liquid dispersion is seen at the industrial scaled down operating condition.

A CFD model is developed for the lower plenum of MBR and validated with gamma ray densitometry (GRD) for radial profile of line average phase volume fraction. The simulation indicates that the current design of lower plenum is enabling a dominant movement of phases only in the central region outlets of this plenum. A modification of the current design proves to perform better in terms of movement of phases along entire outlets of the lower plenum.

ACKNOWLEDGMENTS

The first and foremost acknowledgment goes to my advisor Prof. Muthanna Al-Dahhan. I would like to thank him for being a constant source of support and guidance during my Ph.D. life. I always admired him for his passion and dedication towards his research activities and towards his responsibilities as a department chair. His out of box thinking, never give up attitude, hard-working style, and good work ethics always inspired me.

I would like to thank my committee members Dr. Joseph Smith, Dr. Parthasakha Neogi, Dr. Joonataek Park, and Dr. Joshua Schlegel, for their thorough evaluation and critical review of my Ph.D. research.

I wish to acknowledge my research group for their cooperation and helpful discussions to advance my work. A special thanks to Dean Lenz, his in-depth understanding and helpfulness with troubleshooting, ensured smooth functioning of my work. I am also grateful to office staffs Marlene Albrecht, Emily Filkins, Dawn Schacht, and former staffs Krista Welschmeyer, Morgan Coonrod, and Julia Burnette.

A sincere thanks to my friends Sarah Joseph, Kannan Suresh Kumar, Albin Thomas, Malweka Sree Vishnupuram and many other friends I made during my PhD life. You guys made this an enjoyable and memorable journey.

Lastly, I would like to thank the most important people in my life, my parents, Alexander Kunjapay and Mariamma Cherian. This achievement is possible only due to their hard work and blessings, and this dissertation belongs to them.

TABLE OF CONTENTS

Page

LIST OF ILLUSTRATIONS

PAPER IV

LIST OF TABLES

SECTION

1. INTRODUCTION

Hydrotreatment is a process in which hydrocarbon feed stream are catalytically treated with hydrogen for removal of unwanted contents. Heavy liquid stream such as crude oil or resid oil contains a lot of contaminants in the form of organometallic compounds and heavy metals which tend to deactivate catalyst at hydroprocessing conditions (Kramer *et al.*, 1994). Strict environmental regulation, severe crude oil deterioration and product demand shift towards lighter fuel have taken a movement towards improvement in hydroprocessing technology and catalyst (Scheuerman *et al.*, 1993a). Improved hydrotreaters have an enormous impact on resid oil treatment as refiners can have utmost feed flexibility with the maximum conversion.

The three-phase fluidized bed is one of the reactor configuration used in many H-oil processes like hydrogenation and hydrodesulfurization of residual oil (Jena *et al.*, 2008a). Other configuration includes upflow movement of hydrogen and oil with catalyst bed moving downward, this ensures high packing density and maximum conversion but can result in metal plugging and catalyst deactivation (Kramer *et al.*, 1994). Upflow moving packed or slightly expanded bed with a conical bottom, industrially known as Upflow Moving Bed Reactor (MBR) is a new configuration of the reactor for hydrotreatment.

1.1. UPFLOW MOVING BED REACTOR (MBR)

Upflow moving bed reactor has plena and catalyst bed section. The plena are subdivided as lower and upper plenum. The catalyst bed section has a conical support structure, and it demarcates plena from catalyst bed. Lower plenum is gas-liquid distributor

section having a deflector and chimneys with side holes attached to a plate distributor, which provide a gas pocket on top of the lower plenum. This design of lower plenum is very standard in the industry for upflow case. It is because the gas pocket acts as pressure surge dampener which may arise due to varying operating conditions and it also provides good distribution of gas-liquid to upper chambers (Kramer *et al.*, 1994). Under proper design conditions the gas flow through side holes of the tubes and mixes with the incoming liquid from the bottom hole or inlet of chimney and fed as a spray to upper plenum. Upper plenum is filled with passive spheres. There are skirts which are attached to the conical bottom. This arrangement of upper plenum claimed to provide good distribution of gas and liquid, and it feeds as annular ring of gas-liquid into the catalyst bed section which is supported by a conical bottom structure. This cone is enlarging upwards and have holes size small enough to prevent catalyst plugging and large enough to minimize the pressure drop across the cone (Bachtel *et al.*, 1996).

Moving Bed Reactor (MBR) is a new technology for hydrotreaters which incorporates provision for continuous replacement of spent catalyst and feeding of fresh catalyst simultaneously under operating conditions. Under hydrotreatment conditions, the catalyst gets deactivated and becomes heavy and eventually move downs towards the conical bottom due to discharge catalyst and adding new catalyst (Krantz *et al.*, 2002). There is a pipe having a diameter substantially larger than the catalyst attached to the conical bottom for removal of spent catalyst. The removal is done under laminar conditions to prevent disturbance in the bed (Kramer *et al.*, 1994). The spent catalyst is regenerated and either mixed with the fresh catalyst or fed alone to the top of the column in a similar laminar fashion to avoid disturbances in bed. The catalyst removal is usually done once or twice in a week and in small increments. Hence, MBR offers an efficient way of utilizing the catalyst and provision of removal of spent catalyst without shutdown. The maximum linear velocity of reactants is kept such that overall bed expansion is less than 10 percent (Kramer *et al.*, 1994). Hence, under normal conditions, the bed behaves as slightly expanded or packed

bed. It is mostly used as a replacement for fixed bed hydrodemetallization (HDM) reactor which acts as a guard reactor to fixed bed residual desulfurization (RDS) unit (Scheuerman *et al.*, 1993a). MBR reactors can handle feed with higher metal content which is relatively cheaper feed. Highly contaminated or heavy feed is hydrotreated with HDM catalyst in MBR for metal removal then fed to fixed bed RDS unit having HDS catalyst. Overall it should increase the run length of HDS catalyst. To summarize, MBR technology provide refiners capability of handling feed with varying degree of contaminant, increased the life cycle of fixed bed catalyst, reduced catalyst consumption.

Problems Associated with MBR: The MBR reactor as per design shall work to enhance and improve the performance of overall hydroprocessing unit of ressidum oil treatment. In fact, its replacement with fixed bed HDM as a guard reactor proved non-beneficial for refiners. It is mainly due to various issues encountered at industrial scale during operation of MBR. The usual problems which are met regularly in the refinery are as follows.

- Coke deposition in catalyst bed and on the side holes of the tubes in lower plenum
- Increased pressure drop either at distributor assembly or in the outlet or both, and hence the increase in overall pressure drop.
- Occasional difficulty in controlling reactor temperature
- Disturbance in the catalyst bed
- Variation in product quality
- Shortening cycle of fixed bed reactor
- Emergency shutdown

No clear pattern of these problems is observed. However, coke deposition is the major issue among them. Coke deposition can directly lead to other problems listed, like it can cause pressure drop increase, hot spots result in catalyst agglomeration and variation in temperature, catalyst deactivation, and eventually emergency shutdown. Manual scraping is required to remove coke deposits and to bring back MBR to normal safe working conditions.

1.2. MOTIVATION

Efficient working of MBR has huge positive impact on hydroprocessing technology for treating heavy ressidum oil. The major advantage is to handle feed with heavy metal contents which are available for a relatively cheaper price. It helps to produce clean fuel, and nowadays the major shift in product demand is towards lighter fuel and MBR is capable of achieving it efficiently and inexpensively. For efficient working of MBR, the major checklist are as follows

- Uniform flow distribution of gas-liquid in catalyst bed section
- Appropriate catalyst to ensure maximum conversion
- Minimum random motion and back mixing of the catalyst
- Good mixing of phases along the catalyst bed
- The maximum linear velocity of feed to limit bed expansion to 10 percent

These working conditions are never evaluated and quantified in MBR reactor. The primary cause of coke deposition is flow irregularities and improper distribution of gas-liquid in catalyst bed section and plenums. Hydrotreatment conditions are usually at 212^oF to 1200^oF and pressure of 20 to 300 atm (Kramer *et al.*, 1994), at these conditions, the gas deprivation at local void space inside catalyst can cause thermal cracking and hence coke formation on the catalyst. Coke deposition can cause thermal hot spots and catalyst

agglomeration. Hence, it is essential to study the hydrodynamics of MBR and evaluate the performance of current MBR. In literature, there are no hydrodynamic data available for the reactor of the configuration of MBR. The closest reference to follow is with the upflow three phase packed bed [(Benneker *et al.*, 1996), (Collins *et al.*, 2017), (Gutsche and Bunke, 2008), (Iliuta *et al.*, 1998), (Ji *et al.*, 2015), (Saroha and Khera, 2006)], upflow three phase slightly expanded bed [(Hu *et al.*, 2001), (Wang *et al.*, 2006b), (Wang *et al.*, 2006a), (Xie *et al.*, 2013), (Yun *et al.*, 2004), (Yun *et al.*, 2005)], upflow three phase fluidized bed [(Fraguío *et al.*, 2006), (Jena *et al.*, 2008a), (Lee *et al.*, 2001), (Safoniuk *et al.*, 2002), (Zhang *et al.*, 1998)] but again these reactor configurations are significantly different mainly with respect to conical bottom structure of MBR.

1.3. OBJECTIVES

The primary objective of this work is to advance understanding the hydrodynamics in MBR reactor at industrial best conditions and at various operating flow rate, by scaling it down to pilot plant scale. This study will enhance the understanding of working and design of this reactor, and helps refiners to make a better decision in selecting this hydrotreater reactor for their needs. Various objectives to accomplish primary objectives are as follows.

Objective 1: Designing, construction, and commissioning of cold-flow unit of MBR

In this task, the industrial MBR is scaled-down to pilot plant scale. The scaling down is approached in such a way to make dynamic and geometrical similarities between Industrial and Pilot-scale. The details of scaling down procedure can be found in the appendix A.

Objective 2: Local saturations, local phase velocities, local backmixing, and local maldistribution investigation in packed bed of pilot-scale MBR

A method (algorithm) is developed for Two-tip optical probe (TTOP) to extract local liquid and gas saturations, local liquid and gas velocities, local maldistribution of phases, and local backimixing of phases from two-phase flow packed bed reactor. This study quantifies the local behavior of phases inside the void space of catalyst bed packing. The detailed information about the procedure to obtain local hydrodynamic parameter from TTOP is shown in appendix B. The experiments are conducted at industrial scaled down flow condition.

Objective 3: Gas phase dispersion/mixing investigation in the catalyst bed section of pilot scale MBR

The gas phase dispersion/mixing in the catalyst bed of MBR is investigated using advanced gas tracer technique. The experimental setup is designed in such a way to extract out the gas phase signal. A multiple injection and one sampling at reactor outlet is performed to obtain RTDs of various section of MBR. Then these RTDs are evaluated using a developed methodology based on convolution, regression, and ADM as catalyst bed Model. The ADM parameters (D_g and Pe) quantifies mixing parameter of gas phase in catalyst bed section of MBR. The experiments are conducted at various flow rates plus the scaled down conditions

Objective 4: Liquid phase dispersion/mixing investigation in the catalyst bed of pilot-scale MBR

The liquid phase mixing in catalyst bed section is investigated using advanced liquid tracer technique. The RTDs are obtained for various section of MBR using a two-injection and one-detection method. The obtained RTDs are evaluated using a developed methodology based on convolution, regression, and Wave Model (WM). WM parameters (D_l and Pe) quantifies mixing behavior in the catalyst bed section of MBR. The experiments are conducted at various flow rates of phases including the scaled down experimental condition.

Objective 5: Phase mass distribution based performance evaluation of lower plenum of pilot-scale MBR using CFD

In this task, CFD model is developed for lower plenum of MBR. The lower plenum consists of deflector, chimneys and distributor plates. This study will quantify the effect of the deflector on this part of MBR reactor. This kind plenum are widely used in industries for upflow case. The validation of the CFD code is done by the radial profile of line average volume fraction obtained from Gamma-Ray Densitometry (GRD). A new design of lower plenum is also proposed based on modified deflector which shows improved performance in terms of mass distribution.

PAPER

I. LOCAL HYDRODYNAMICS INVESTIGATION OF INDUSTRIAL SCALED DOWN UPFLOW MOVING BED HYDROTREATER (MBR) REACTOR USING TWO-TIP OPTICAL PROBE

Vineet Alexander[1], Hamza Albazzaz[2], Muthanna Al-Dahhan[*,3]

[1,*]Department of Chemical & Biochemical Engineering,

Missouri University of Science and Technology, Rolla, MO-65409

[2]Kuwait Institute for Scientific Research (KISR), Safat, Kuwait

[3]Cihan University, Erbil, Iraq

Email:[1]vaxt8@mst.edu, * aldahhanm@mst.edu

ABSTRACT

Upflow Moving Bed Hydrotreater (MBR) is used in refineries as guard reactor to fixed bed residual desulfurization (RDS) reactor. At the industrial scale, the reactor is facing issues of coking, catalyst agglomeration, hotspots in the catalyst bed leading to emergency shutdown. These problems are directly linked with the local flow maldistribution inside the catalyst packing of MBR. The local maldistribution is investigated on a scaled-down MBR and at scaled-down industrial flow condition using an experimental technique called Two-Tip Optical Probe (TTOP), which gives local phase saturations, phase velocities, backmixing and maldistribution at voids of two-phase flow packed bed. TTOP is invasive technique and is placed in local void space at different radial, and axial locations along the catalyst bed. The results indicate highly fluctuating phase saturations inside the catalyst bed, with zones having very low to high gas or liquid saturations, these conditions are prone to facilitate the significant issues seen at the industrial MBR. The local phase backmixing and local

maldistribution is more on the expanded part of the bed. The severity in fluctuating local saturations and local maldistribution is associated with improper design of key components of MBR.

Keywords: Local Hydrodynamics, Two-Tip Optical Probe, Moving Bed Reactor, Maldistribution

1. INTRODUCTION

Hydrotreatment is a standard process in refineries to treat heavy crude oil with hydrogen on hydrotreating catalyst for reducing sulfur, aromatics, and nitrogen from oil. This process is usually done in the two-phase flow fixed bed reactor configuration, but the impurities (metals) present in crude oil to tend to deactivate catalyst fast and leads to frequent shutdown for catalyst removal. Severe crude oil deterioration, strict environmental regulation, and rapid demand for cleaner and light fuel emphasized the need for new technologies for hydrotreatment (Scheuerman *et al.*, 1993). Upflow moving bed hydrotreater reactor (MBR) is a new technology for hydrotreating and is usually used as guard reactor to fixed bed residual desulfurization (RDS) reactor. MBR reactor has hydrodemetallization catalyst (HDM) which treats crude oil in the presence of hydrogen for metal and organometallic removal, and treated oil is fed to RDS reactor. Efficient working of MBR has an enormous effect on entire hydrotreatment process, as it enables refiners to handle feed with varying degree of contaminants, increases the life cycle of fixed bed RDS catalyst, and overall reduced catalyst consumption (Kramer *et al.*, 1994).

MBR has a catalyst bed with the conical bottom, gas-liquid deflector, plenum, gas-liquid distributor (from lower plenum to the conical surrounding compartment), and compartment surrounding the conical bottom (upper plenum) packed with passive spheres. The operation of this reactor is in upflow manner, with resid oil and hydrogen move up at a combined maximum linear velocity at which the bed expansion is less than 10% by volume (Bruce *et al.*, 1999). Detail design and working of MBR is explained in section 2.

The specialty of MBR is the conical bottom, which facilitates the removal of spent catalyst without shutdown, then removed spent catalyst is either regenerated or mixed with fresh catalyst and fed towards the top of the bed. At industrial condition, the removal would be conducted once in a week and in small increments, the bed in all other times behaves as two-phase upflow packed with slight expansion at the top. The bed at industrial conditions is facing drastic issues such as hot spots, coking, and catalyst agglomeration, eventually forced shutdown. These problems are local in nature and originate at pores scale level, and is directly linked to either maldistribution of phases at the void space of packed bed or the type of catalyst related to coking reaction. In this study we focus on root cause of maldistribution of phases. Hence, It necessitates the study of local hydrodynamics in MBR and to identify the flow distribution along the bed for the present configuration of MBR at the industrial operating condition.

Local hydrodynamics are usually quantified in a multiphase system by measuring the gas bubble properties such as holdups, saturation, chord length, interfacial area and local liquid velocities and holdups. There are various measurement techniques to quantify local phenomena and are primarily classified as invasive and noninvasive techniques. The most common invasive techniques are needle probes (optical/conductivity), heat transfer probes, ultrasound probes [(Boyer *et al.*, 2002), (Dominic *et al.*, 2014)].The noninvasive techniques can be classified as photographic, particle tracking(PIV), radiography(X-Ray), resonance based (MRI, NMR) (Boyer *et al.*, 2002). These techniques are mostly implemented on the gas-liquid system, and not so frequently on gas-liquid-solid or gas-solid system. There are limited studies on local flow dynamics inside the packed bed.

(Salleh *et al.*, 2014) developed X-Ray Digital Image Radiography (DIR) with particle tracking velocimetry and investigated local liquid velocities in gas-liquid downflow packed bed of internal diameter 4.5 cm and height 40cm. (Johns *et al.*, 2000) and (Sederman *et al.*, 1997) used Magnetic Resonance Imaging (MRI) to investigate the local liquid hydrodynamics (flow regime, velocities) on 4.6 cm diameter and length 70 cm packed bed

column operating in downflow mode. (Götz *et al.*, 2002) used NMR technique to find the local liquid velocities and dispersion parameters in small scale liquid downflow packed bed. (Sankey *et al.*, 2009) and (Mantle *et al.*, 2001) used MRI in two-phase upflow through packed bed of 4cm diameter and 50 cm length to investigate the local liquid velocities, flow profile and pores size. (Collins *et al.*, 2017) used MRI to study gas phase hydrodynamics on a 4.3 cm diameter and length 80 cm two-phase upflow packed bed reactor. All the literature mentioned above is limited to small-scale diameter, as these measurement techniques (X-Ray, MRI, and NMR) are not feasible for large diameter reactor. Electrical Capacitance Tomography (ECT) can be applied to slightly larger scale reactor, (Hamidipour and Larachi, 2010) used it on 5.3 cm diameter and 80 cm length packed bed column to study the liquid dynamics in both two-phase upflow and downflow mode. (Chen *et al.*, 2017) used ECT to study gas phase dynamics (mean bubble size) in two-phase upflow packed bed reactor of diameter 14cm and height of 100cm. The advantage of all the techniques mentioned above is that its noninvasive and the major disadvantages are its implementation is limited by the size of the column, operating condition (low gas holdup) and high operating cost (Boyer *et al.*, 2002). These disadvantages make it harder to implement in pilot or industrial scale reactor as flow monitoring and measurement device. The alternatives to these techniques are intrusive in nature.

(Schubert *et al.*, 2010) developed wire mesh sensors (WMS) and implemented on 10 cm diameter and 111.4 cm length packed bed column operating in two-phase downflow mode, to investigate liquid saturation distribution in the bed. The issue with this technique is that its highly intrusive nature, as sensors occupy a significant amount of cross-section. Optical probes are less intrusive and are widely used in the multiphase system in the form of single tip, two-tips, four tips, especially in gas-liquid system (Xue, 2004). (Li *et al.*, 2012) has given a detailed review on the application of optical probe sensors in multiphase reactors. The advantage of optical probe sensors is its small size and harsh environment tolerance (Boyer *et al.*, 2002), which makes it a good technique to investigate

packed bed local hydrodynamics. (Mena *et al.*, 2008) used single point optical probe developed by (Cartellier and Barrau, 1998) to study gas residence time and velocity in a gas-liquid-solid systems, with solids loading limited to 30% by volume. Their algorithms are developed for the single probe orientation, where probe tip are pointing towards the upward flowing phases. This particular orientation is not feasible for two-phase packed bed. (Abdul Rahman, 2017) came up with two-tip optical probe (TTOP) design which is compatible with two-phase packed bed operating in either upflow and downflow mode, they used the procedure mentioned in appendix B to obtain local gas/liquid saturation and local gas/liquid velocities in a trickle bed reactor, they validated TTOP for local liquid velocity with X-ray DIR (Salleh *et al.*, 2014).

In this study TTOP is used to investigate the local hydroynmaics in MBR, and additional hydrodynamic parameters local backmixing and local maldistribution is also measured along with local gas/liquid saturations and local gas/liquid velocities. Appendix B shows the procedure to determine these parameters.

The objective of this study is to implement TTOP at various radial and axial location inside the packed bed part of the pilot-scale MBR at scaled-down experimental conditions and to investigate the performance of the catalyst bed in terms of measured parameters at these conditions.

2. EXPERIMENTAL SETUP

Industrial Moving bed hydrotreater reactor (MBR) has been scaled down to pilot-scale. The scaling down is based on matching the hydrodynamic and geometric similarity between the industrial scale and pilot scale reactor. The reactor has a catalyst bed section which has a conical bottom, and plena. The plena is divided into lower and upper plenum by a distributor plate that consists of chimneys. The lower plenum is a gas-liquid distributor (Bruce *et al.*, 1999), which includes deflector and chimneys. The deflector is the inlet to the lower plenum and then to the reactor at its bottom. The chimneys are at the top of lower

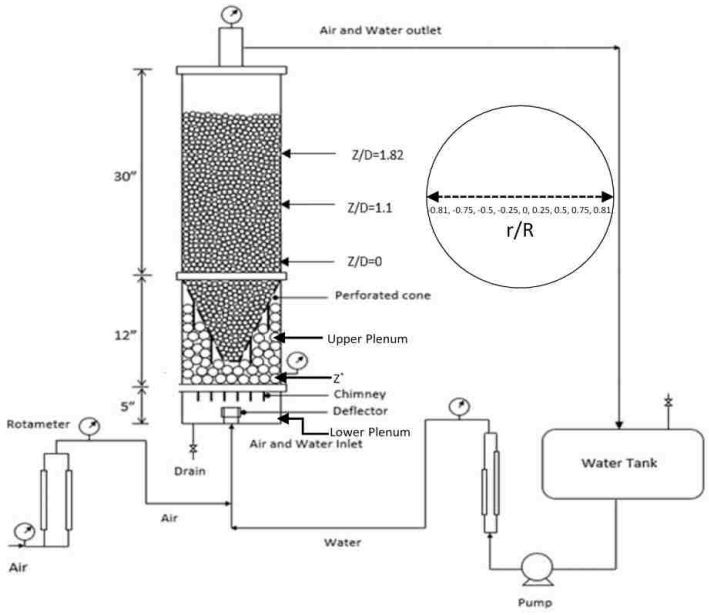

Figure 1. Schematic diagram of scaled down MBR setup for local hydrodynamics study

plenum, attached to the distributor plate in a triangular pitch. The chimney is a hollow pipe with an inlet- exit holes and additional side hole on chimneys just below the exit hole. The exit holes of the chimney are screwed to the holes of the distributor plate, and this hole is the exit of lower plenum and inlet to the upper plenum as the compartment surrounding the conical section of the bed. The upper plenum is space filled with tightly packed passive spheres and is between the conical bottom of the catalyst bed and the lower plenum. The upper plenum is a packed bed type gas-liquid distributor, and its exit boundary is with the conical bottom of the bed. The conical bottom has holes in a circular pitch and along the length of enlarging diameter of the cone and holes at the base of the cone. These holes are the inlet to the catalyst bed in the conical base of the bed which is attached to the cylindrical bed. The catalyst bed section is filled with industrial hydrotreating catalyst, which is 3mm in diameter and porous. Table 1 shows the specification of the scaled down MBR. The experimentation done in this study is in cold flow manner, and the gas and liquid phase are air and room temperature water, respectively. The pumps are used to push the phases

into the reactor, and rotameters control it. Both gas and liquid are fed in a pre-mixed state to the deflector inlet of the lower plenum. The phases enter the plena and distribute and moves in an upward manner through the catalyst bed and exits at the reactor outlet, and the outlet pipe extends to the water tank. The water tank is attached to a water pump to recycle liquid and the tank is open to atmosphere to vent out the air. The reactor operates at scaled-down experimental condition (Table 1), and at these conditions, the catalyst bed behaves as upflow packed bed with slight expansion at the top of the reactor. The liquid scaled-down experimental condition is obtained by matching the Liquid Hourly Space velocity (volumetric flow rate of liquid/bulk catalyst volume) at industrial condition with lab scale condition for a catalyst mass of 30 kg. The gas scaled down condition is obtained by equating gas to liquid volumetric flow ratio of industrial condition with the lab-scale condition. The scaled down operating conditions are shown in Table 1. The primary focus of this study is to understand the local phase saturations, local velocities, local backmixing, and local maldistribution at various locations inside the catalyst bed and to identify its relation with the design of the reactor. Hence various local measurement zones are selected at various radial and axial locations along the packed region of the catalyst bed as shown in Figure 1 and Table 1.

3. MEASUREMENT TECHNIQUE: TWO-TIP OPTICAL PROBE (TTOP)

The optical probes are widely used to distinguish gas-liquid phase and its due to light propagation behavior inside the probes which follows Snell's law. It states that when light travels from the optically dense medium (High refractive index) to optical lesser dense medium (Lower refractive index), and the light falls at angle greater than the critical angle at the plane of the interface, then light will be totally reflected back to the optically denser medium. In all other cases, the light will refract. The total internal reflection or backscattering phenomena of optical probe became the foundation for its use as measurement technique to identify gas-liquid interface (Li *et al.*, 2012). The sensitive

Table 1. Experimental setup specification, operating conditions, measurement zones for optical probe study

Parameters	Value/Range	Comment
Column Diameter	11 inch	
Column Height	46.46 inch	
Bed Height	24.8 inch	Height from top of the cone to the top of the bed at no flow rate
Catalyst	3 mm Diameter	Bulk Density (570 Kg/m^3)
Scaled Down Liquid Flow Rate	0.0175 cm/sec	By matching LHSV of industrial and scaled down reactor
Scaled Down Gas Flow Rate	7.7 cm/sec	By matching Gas/liquid volumetric flow rate of industrial and scaled down reactor
Measurement zone (radial-r/R)	r/R=[-0.81,-0.75,-0.5,-0.25,0,0.25,0.5,0.75,0.81]	r(distance form the center to measurement zone), R (Radius of the reactor)
Measurement zone (axial-z/D)	z/D=[0,1.1,1.82], and Z^*	z(distance form the top of conical bottom), D (Diameter of the bed)

part of the tips is made into a conical shape which ensures the conditions necessary for the light traveling inside the probe to reflect back when gas is in contact and refracts when liquid is contact [(Boyer *et al.*, 2002), (Choi and Lee, 1990)]. This reflection phenomenon is utilized to distinguish gas-liquid phase.

The optical probe used in this study is manufactured by thor labs, the optical cable has a quartz glass core of diameter 200 μm (micrometer), and a protective layer of silicon cladding and teflon making a total diameter of 600 μm. The protective layer is removed at

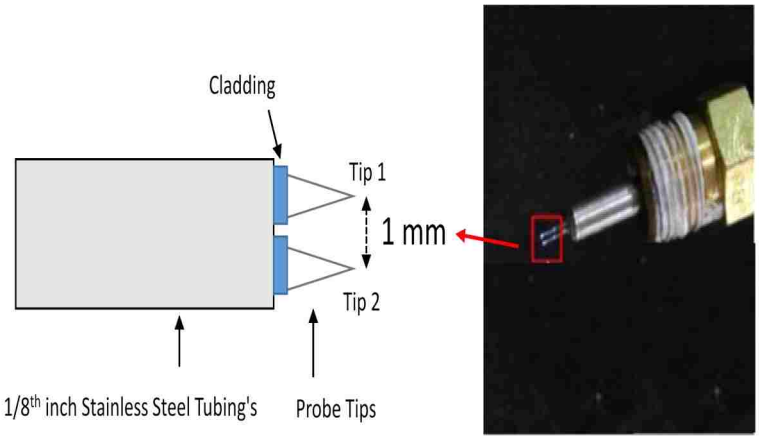

Figure 2. Design of two-tip optical probe (TTOP)

one end of the fiber optic cable, and exposed quartz glass core is made into the shape of conical tip (Xue, 2004). The detailed procedure to manufacture optical probes can be found in [(Abdul Rahman, 2017) (Xue, 2004)].

Figure 2 shows the design of TTOP, and procedure of (Abdul Rahman, 2017) is followed to design and manufacture two-tip optical probe (TTOP). Two optic fiber cables are taken and glued to 1/8 inch stainless steel tubings, and the distance between the two tips are 1mm, as shown in the Figure 2. Tips are named as upper and lower tip, with upper will always be at the higher axial location than the lower tip. The other end of the fiber optics cables are attached to a light source emitting a 680 nm wavelength light from LED, the transmitted light travels to the probe and illuminates the conical tip (Figure 2), this assembly is placed in the local void space positions inside the bed of the MBR, and if the gas phase is in contact, light reflects back due to total internal reflection, and retraces its path back in fiber optics, and falls on the photodiode. The photodiode will generate voltages signal, which is sampled at a frequency of 40Khz using a data acquisition system (Power DAQ PD2-MFS-8-1M/12). When liquid touches the tip, the light refracts, and photodiode generates the base voltage. Hence, based on the movement of phases in the vicinity of the probe tips, step-up or step-down type signals are obtained as shown in the Figure 3. The

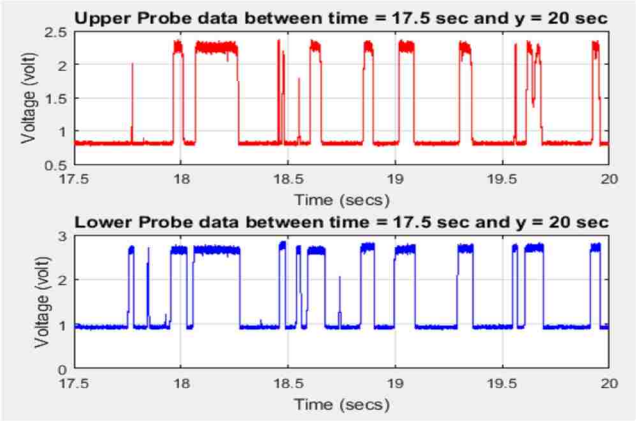

Figure 3. Raw signal of TTOP

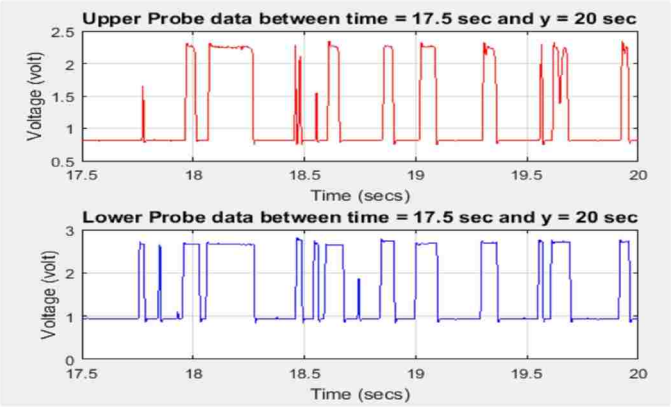

Figure 4. Filtered signal of TTOP

two separate signal depicts the time series of two optical probe tips. The larger voltage peaks depict the windows of the time frame of gas phase on the probe tip and similarly, the base voltage slots show the time of liquid phase on the probe tip. The raw signals are passed through a second-order butterworth filter to remove electronic noises, and the obtained signals are shown in the Figure 4.

The above time series is normalized to obtain perfect step-up and step down of signals, as shown in the Figure 5. The normalization is done using the method as shown in appendix B. Normalization is vital, as it gives the times at which interphase of gas-

Figure 5. Normalized signal of TTOP

liquid crosses the tip, and windows of the time frame of liquid and gas touching the tips. These time series are used to calculate local phase saturations, local phase velocities, local backmixing, and local maldistribution from the two-tip optical probe.

3.1. Local Phase Saturations Measurements. The saturation of any phase in a two-phase flow packed bed reactor at the local void is the amount of volume occupied by a particular phase with respect to the entire void volume. It is similar to local holdup but only confined to local void space, and this does not account the volume occupied by the solid phase. Hence it is defined as ratio of volume of a phase per volume of void. The ergodic hypothesis states that volume average is equivalent to time average for the flowing system. Hence, the local gas saturation is the ratio of time spent by the gas phase on the probe tip to the total time of measurement (Equation-1). The liquid saturation is one minus gas saturation (Equation-1), as the probe only senses the gas-liquid phase flowing in the void space.

$$\beta_{g,local} = \frac{t_{G,Local}}{t_{L,Local} + t_{G,Local}} \tag{1}$$

Local liquid Saturation = 1-$\beta_{g,local}$

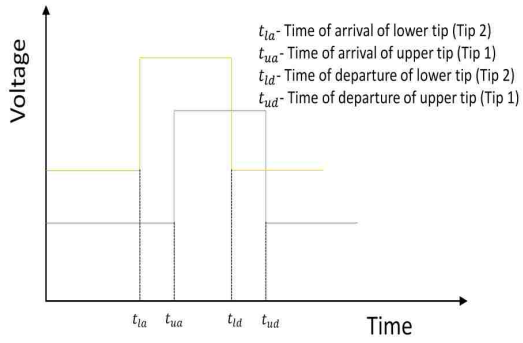

Figure 6. Schematic of matched bubble signals used for velocity measurement

Whereas, $t_{G,Local}$ and $t_{L,Local}$ is the time spent by the gas and liquid phase respectively on the probe tips. These time parameter are obtained from the normalized time series signal (Figure 5) , Two tips of the optical probe gives two time series data, which is combined to give one saturation values for either phase.

3.2. Local Phase Velocities Measurements. To obtain velocity parameters from the normalized signal (Figure 5), the signals needs to be matched to identify the same bubble touching the tips, and then by finding the delay time and using the distance between the tips, phase velocities are obtained. To match the signal, the bubble tracking and matching algorithm, explained in appendix B is implemented. This algorithm tracks all the bubbles and uses every matched bubble signal for velocity parameter evaluation. The Figure 6 shows the schematic of one such matched bubble out of all the matched bubble in the time series data.

Local gas velocities are obtained from the equation 2. Where, t_{la} is the time at which a gas bubble or gas slug arrives at the tip of lower optical probe, and t_{ua} time at which the same gas bubble or slugs arrive at the upper tip. The time difference $(t_{ua} - t_{la})$ is the delay time of the signal to travel a distance of 1mm between the tips.

$$V_{g,local} = \frac{1mm}{t_{ua} - t_{la}} \tag{2}$$

The liquid velocity is calculated using equation (3). Where, $t_{ld}$is the time at which a gas bubble or gas slug departs the lower tip and t_{ud} is the time which the same gas bubble or gas slug departs the upper tip. The time difference ($t_{ud} - t_{ld}$) gives the delay time of liquid phase to travel a distance of 1mm between the tips.

$$V_{L,local} = \frac{1mm}{t_{ud} - t_{ld}} \tag{3}$$

The algorithm (appendix B) gives the velocities of all the matched signal for both gas and liquid velocities. Hence a velocity distribution of both gas and liquid in the range from negative to positive values are obtained at a local location for any particular flow rates of phases.

3.3. Local Backmixing Measurement. The backmixing for any phase inside a reactor is defined by the intensity of flow reversal of phases at a particular location. The occurrences of negative velocities during velocity calculations are seen when the flow of phases are reversed due to the local force field causing backpressure. Hence, by quantifying the occurrences of negative velocities in terms of percentage, will indicate the extent of back-mixing. This information can be used to compare the back-mixing zones inside various local locations of the packed bed.

3.4. Local Maldistribution Measurement. Globally a good distributed system will have a uniform flow distribution cross-sectional and over the entire volume of the reactor, and for good distribution locally such as the void space of catalyst bed, the same principle applies. Hence, the local maldistribution occurs when there is flow irregularities in the void volume for MBR. These cases occur for the transient times when the signal (Figure 4) obtained from the two-tips of optical probe does not match to find the gas velocity or we can call it zero gas velocity conditions. These condition mainly occur when the entire void space is either filled with liquid or gas phase, or gas bubble are deviating without touching both the tips, these condition represents maldistribution locally and are not good in terms of

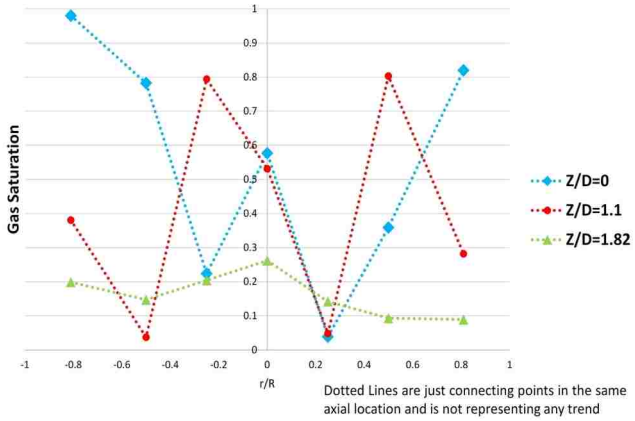

Figure 7. Gas saturation at various radial and axial location of MBR at experimental scaled down conditions shown in Table 1

catalyst utilization in these local zones. Zero velocities are obtained from the gas velocity calculation by following the method as shown in appendix B. The zero velocities quantified in terms of percentage of occurrences will indicate the extent of maldistribution.

4. RESULTS

4.1. Local Phase Saturations at Local Locations. Figure 7 shows the saturation values of gas phase at various local locations inside the packed bed. Figure 7 also gives good indication of liquid saturations at local zones, which is one minus of gas saturations. The results indicate that there is large fluctuation in saturation values all along the packed bed, and it clearly indicates the extent of maldistribution. There are zones with more than 90% gas saturation (Z/D=0, r/R=-0.81) and less than 5% gas saturation [(Z/D=0, -r/R=0.25) (Z/D=1.1, -r/R=-0.5)]. Only central region and towards the bottom of the bed [(r/R=0, Z/D=0,1.1)], shows the gas saturation values in the range of 0.5-0.6, which indicates a good local distribution of both gas and liquid phase. On observing saturation values along radial locations, the fluctuations is seen quite significant, and its extent is seen maximum at the bottom of the reactor. Gas saturation is seen more towards the wall region at the bottom of

the bed (Z/D=0), and it may be due to the conical bottom of the bed, which is pushing the gas towards the wall region of the bed. (Toukan, 2017) conducted the GRD studies on the same reactor (MBR) and at the experimental scaled down condition (Table 1), and found line average gas holdup at wall region is higher than those at the other radial locations at the bottom (Z/D=0) of the bed. Towards the top in the packed bed region (Z/D=1.82) of the bed the distribution is seen to improve radially, and is due to slight expansion of the bed along the axial height (Yun *et al.*, 2005), this allows more space for liquid and gas to redistribute along the radial location of the bed.

4.2. Investigation of the Local Phase Velocities at Local Locations. The phase velocity measurements show there is distribution of velocities at a local point. The distribution of either gas or liquid phase velocities are usually depicted in the form of histogram (Figure 8).

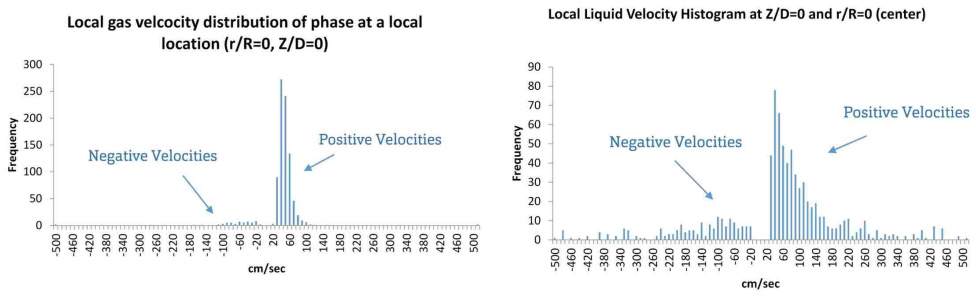

(a) (b)

Figure 8. Histogram plot of phase velocities at r/R=0 and Z/D=0 (a) gas velocities (b) liquid velocities at experimental scaled down conditions shown in Table 1

Figure 8 shows the velocity distribution of gas phase (a) and liquid phase (b), at location (Z/D=0,r/R=0) for the scaled down flow conditions. The X-axis shows the bands of velocities in cm/sec, and Y-axis shows the number of occurrences of the velocities of each matched signal in respective velocity band. The velocity distribution shows positive velocities, which is the velocity of upward moving phases. It also shows negative velocity, which is the velocity of downward moving phases due to flow reversal. The average of all

the positive velocities obtained at a local point for a particular flow condition is reported as average upward velocity, and similarly, the negative velocity average is reported as average downward velocity.

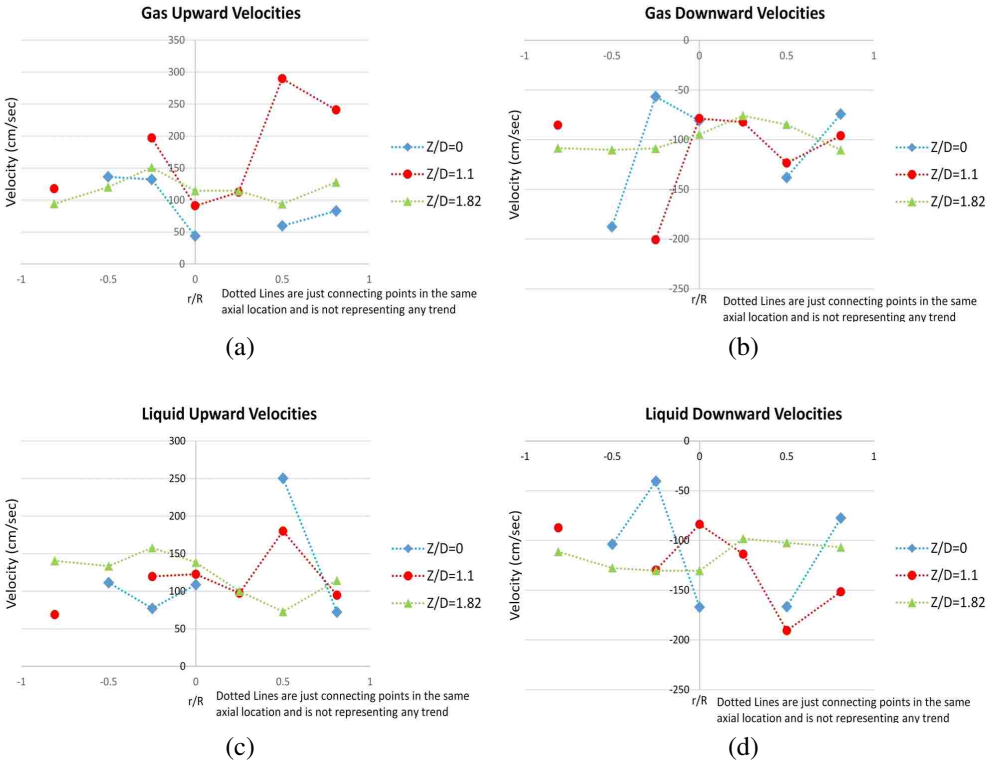

Figure 9. Phase velocities at various local location of MBR at scaled down experimental condition shown in Table 1

Figure 9 shows the local velocities of phases at various local locations inside the bed for the scaled-down experimental condition. At the locations [(Z/D=0, r/R=0.81,0.25) and (Z/D=1.1, r/R=-0.5)], no velocities are obtained, it is due to the local flow conditions at these locations which failed to provide matching bubble signals to obtain velocities. These zones also show very high and low gas saturation values (Figure 7). At scaled-down experimental condition, the flow regime is found to be in pulse flow, as observed visually at the walls, and on comparison with flow regime map of gas- liquid upflow packed bed reactor (Rao *et al.*, 2011). At pulse flow, the gas and liquid slugs move along the void region of the packed bed, and hence the TTOP gives the velocity of gas/liquid slugs moving in upward or

downward direction for the scaled down operating conditions. Figure 9 shows the average velocities of gas/liquid slugs moving in an upward and downward direction at various local locations, at the scaled down experimental conditions. It is seen that the velocity values of gas and liquid are similar, and this phenomenon is linked with the pulsing flow of phases, where the dispersed gas phase dictates the local hydrodynamics of continuous phase. The velocity values for both phases are varying in the range of 50-250 cm/sec in both upward and downward direction. (Sankey *et al.*, 2009) observed for two-phase downflow the local velocities can go up to 100 times superficial velocities. The higher velocities are seen in Figure 9a at location (Z/D=1.1, r/R=0.5) and Figure 9c at location (Z/D=0, r/R=0.5) and it may be due to channeling effect. (Sederman *et al.*, 1997) and (Sankey *et al.*, 2009) observed channeling effect and a corresponding increase in phase velocities at the local location of the packed bed. Figure 9b and Figure 9d shows the negative velocities of phase which arises due to the countercurrent flow of phase [(Sederman *et al.*, 1997), (Sankey *et al.*, 2009)], and it mainly arises due to the backpressure zones created at local void space due to bed structure and flow conditions, creating recirculation of phases. Figure 9 also indicates the radial velocity fluctuation is much less in the top region of packed bed (Z/D=1.82), and is due to slight expansion, which redistributes gas and liquid in radial direction, as observed from saturation plot (Figure 7) for the axial level (Z/D=1.82).

4.3. Local Backmixing at Local Locations. Local backmixing is calculated based on the number of occurence of negative gas velocities. At the location (r/R and Z/D=0) for experimental scaled down condition, the backmixing in terms of gas phase (Figure 8a) is around 6.8%. Similarly, Figure 10 shows the extent of backmixing at different local locations. The information is missing for location for [(Z/D=0, r/R=0.25,-0.81) and (Z/D=1.1, r/R=-0.5)], as we do not have gas velocity values at these locations (Figure 9). Backmixing is mainly due to the force field creating a backpressure zone which recirculates phases. Figure 10 indicates that the backmixing is seen less in the central region and overall its increases as we move up the bed. This kind of behavior is mainly due to two

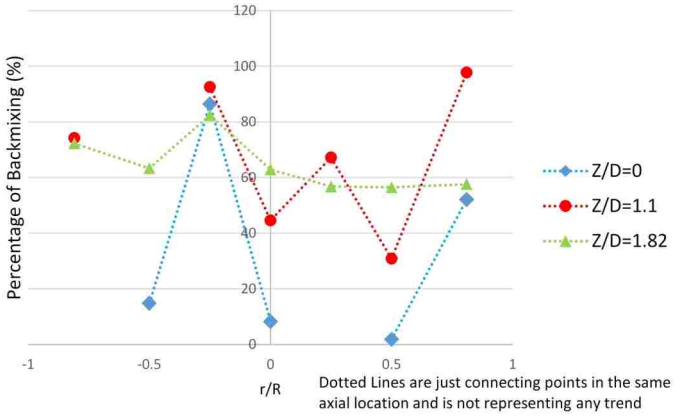

Figure 10. Local backmixing of phases based on zero gas velocities at scaled down experimental condition shown in Table 1

phenomena, the bed expansion along the axial height, which results in local recirculation zones (Muroyama and Fan, 1985), and the force field translating up from the plena towards the bed. Bacmixining is seen very low (Z/D=0 and r/R=0), indicating good push of gas and liquid upward through this place and on moving upward, the pressure drops and can result in backflow.

4.4. Local Maldistriubtion at Local Locations. The Figure 11 shows the histogram plot of gas velocities with addition of occurrences of zero velocity. For the case shown in Figure 11, the local maldistribution is 65.2%.

Figure 12 shows the local maldistribution plot for experimental scaled down conditions. The lower values of maldistribution indicate better catalyst utilization at these locations. The plot indicates a relative way of understanding the catalyst utilization along various local location inside the packed bed. In the Figure 12 the lowest maldistribution is seen at the bottom of the bed (Z/D=0) at (r/R=-0.5, 0, 0.5), it indicates the catalyst utilization is better at these places compared to other local locations inside the bed. Even there are spots of 100 percent maldistribution (Z/D=0, r/R=-0.81, 0.25) and (Z/D=1.1, r/R=-0.5), at these locations we do not have velocities (Figure 9) and has either very high or low gas saturation (Figure 7). These are the problem causing zones with low catalyst utilization

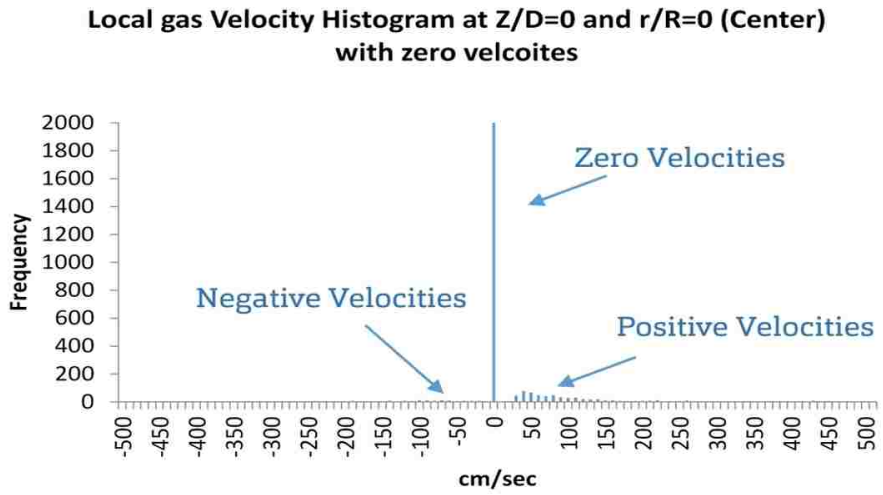

Figure 11. Local gas velocity histogram at Z/D=0 and r/R=0 for scaled down experimental conditions shown in Table 1

and can drastically affect the overall performance of the catalyst bed. Overall the Figure 12 indicates that the local maldistribution is increasing as we move up the reactor. Hence, it can be inferred that in tightly packed bed, the catalyst utilization is much better than slightly loose packing. It is also seen, that at the bottom of the bed (Z/D=0), which is tightly packed, the local maldistribution values are higher (r/R=-0.81,-0.25, 0.25, 0.81). This behavior is due to highly fluctuation flow behavior at the bottom of the bed along the radial direction, as also observed from the Figure 7, which shows highly fluctuating saturations values at Z/D=0. This behavior is directly linked to the flow distribution translating from the plena to the catalyst bed section. The optimum working condition of the bed for desired performance is the lower values of maldistribution and similar values at different radial and axial locations along the bed. It can be achieved by tightly packing the bed and with a good distribution of phases along the cross-sectional plane of the bed.

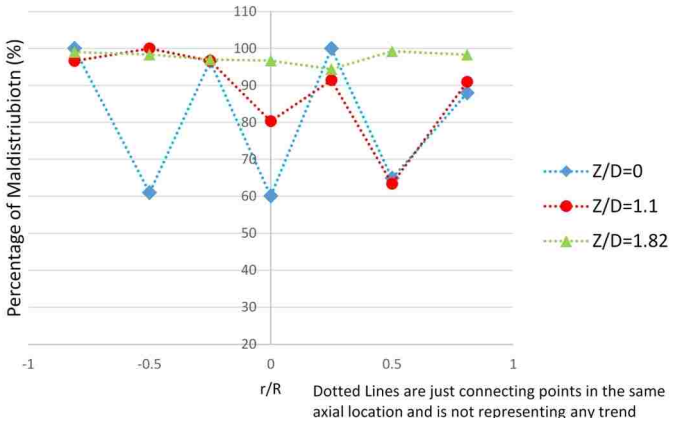

Figure 12. Local maldistribuition plot at various location inside the packed bed for scaled down experimental condition

5. DISCUSSION

The major issues with the industrial upflow moving bed reactor is catalyst agglomeration and hotspot formation inside the catalyst bed of the reactor. Now, it is evident from the Figure 7, the flow maldistribution as the major cause of these problems. It is seen that there are points within the bed where gas saturation values are greater than 100% and less than 5%, in the first cases void zones are liquid deprived and in the second case it is gas deprived. In less gas zones and at the high temperature and pressure of hydrotreating conditions, the liquid feed comprised of hydrocarbon cracks (thermal cracking), and carbon residues stick to catalyst particle (coking) and reduces its activity (Absi-Halabi *et al.*, 1991). In less liquid zones, and at hydrotreatment condition can generate hot spots on the catalyst surface and can lead to catalyst agglomeration (Dudukovic and Mills, 2014). Figure 7 data shows the highest maldistribution is seen at the bottom of the reactor (Z/D=0) with high gas region towards the wall, and very low gas region (r/R=0.25). Coking and catalyst agglomeration can start from these locations and easily spread along, creating reduced conversion, larger pressure drop and uneven temperature distribution along the reactor, and eventually shut down. The whole design of MBR is to facilitate removal of spent catalyst without shutdown, and these

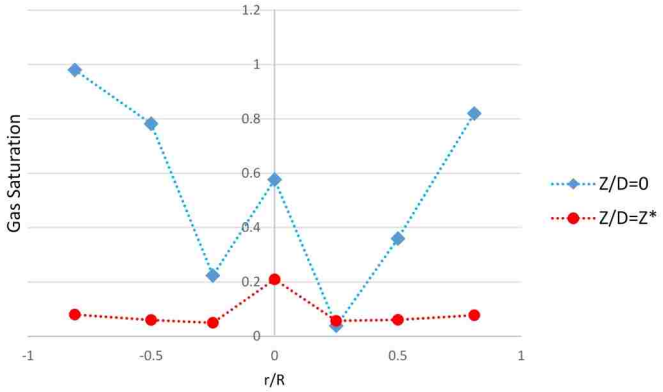

Figure 13. Comparison of radial plot of gas saturations at Z/D=0 and Z/D= Z* at scaled down experimental condition shown in Table 1

extreme maldistribution cases reduces its purpose. These local maldistributions can occur due to bed structure but are mainly due to the force field and flow profile of phases generated by the plena towards the catalyst bed. To investigate the effect of the conical bottom and gas-liquid distributor on the flow profile of phases, TTOP is implemented just below the conical bottom at location Z* (Figure 1) in the upper plenum section.

Figure 13 shows the comparison of the radial profiles of gas saturation at locations below the conical bottom and above the conical bottom. The profile at Z* indicates that the gas is coming out as a fountain from the central region of the gas-liquid distributor. Hence the distributor design needs modification to spread the phases evenly along the cross-sectional area of its outlet. Upon comparison with the results at (Z* and Z/D=0) which it will carry on whole the flow moving upward, it indicates that the conical bottom is pushing the gas towards the wall region and making extreme flow maldistribution condition at the bottom level (Z/D=0). Hence, the conical bottom needs design modification which can translate the exact radial flow profile generated at bottom of the conical part (Z/D=Z*) to the top of the conical bottom or bottom of the bed (Z/D=0).

6. REMARKS

Local hydrodynamics are investigated for a scaled-down pilot scale upflow moving bed hydrotreater (MBR) reactor using an experimental technique called two-tip optical probe (TTOP). TTOP gives local phase saturations, local phase velocities, local backmixing, and local maldistribution, and is implemented at various radial, and axial locations along the catalyst bed for experimental scaled down operating condition. Local phase saturation results indicate randomized behavior with many local locations having very high and low phase saturation in the bed. Phase velocities results indicate the distribution of velocity at a single point, with negative and positive velocities. Overall both local backmixing and local maldistribution are increasing along the axial height of the bed. The gas saturation radial behavior below the conical bottom of the catalyst bed indicates the lower plenum is pushing the phases in the central region, and on comparing the radial behavior of gas saturation with radial behavior at the top of the conical bottom, shows the cone is pushing the gas towards the wall. For improved performance in terms of local hydrodynamics, which is based on catalyst utilization, the bed shall be tightly packed with uniform flow distribution along the cross-sectional plane at the different axial location of the bed. The plena design needs to be modified to provide uniform flow distribution at the inlet of the catalyst bed.

REFERENCES

Abdul Rahman, M. F. B., *Investigation of local velocities and phase holdups, and flow regimes and maldistribution identification in a trickle bed reactor*, Ph.D. thesis, Rolla, 2017.

Absi-Halabi, M., Stanislaus, A., and Trimm, D., 'Coke formation on catalysts during the hydroprocessing of heavy oils,' Applied Catalysis, 1991, **72**(2), pp. 193 – 215, doi:https://doi.org/10.1016/0166-9834(91)85053-X.

Boyer, C., Duquenne, A. M., and Wild, G., 'Measuring techniques in gas liquid and gas liquid solid reactors,' Chemical Engineering Science, 2002, **57**, pp. 3185–3215, doi:https://doi.org/10.1016/S0009-2509(02)00193-8.

Bruce, E. R., Bruce, E. S., and Parimi, K., 'Gas pocket distributor for hydroprocessing a hydrocarbon feed stream,' US Patent, US5885534A, 1999.

Cartellier, A. and Barrau, E., 'Monofiber optical probes for gas detection and gas velocity measurements: Conical probes,' International Journal of Multiphase Flow, 1998, **24**(8), pp. 1265–1294, doi:https://doi.org/10.1016/S0301-9322(98)00032-9.

Chen, Z., Yang, J., Ling, D., Liu, P., Ilankoon, I. M. S. K., Huang, Z., and Cheng, Z., 'Packing Size Effect on the Mean Bubble Diameter in a Fixed Bed under Gas-Liquid Concurrent Upflow,' Industrial and Engineering Chemistry Research, 2017, **56**(45), pp. 13490–13496, doi:https://doi.org/10.1021/acs.iecr.7b00123.

Choi, K. H. and Lee, W. K., 'Comparison of probe methods for measurement of bubble properties,' Chemical Engineering Communications, 1990, **91**(1), pp. 35–47, doi:https://doi.org/10.1080/00986449008940700.

Collins, J. H. P., Sederman, A. J., Gladden, L. F., Afeworki, M., Douglas Kushnerick, J., and Thomann, H., 'Characterising gas behaviour during gas-liquid co-current up-flow in packed beds using magnetic resonance imaging,' Chemical Engineering Science, 2017, **157**, pp. 2–14, doi:https://doi.org/10.1016/j.ces.2016.04.004.

Dominic, P., Arturo, M., and Valois, P., 'Bubble characteristics measured using a monofibre optical probe in a bubble column and freeboard region under high gas holdup conditions,' Chemical Engineering Science, 2014, doi:https://doi.org/10.1016/j.ces.2014.02.024.

Dudukovic, M. P. and Mills, P. L., 'Chapter one - challenges in reaction engineering practice of heterogeneous catalytic systems,' in A. G. Dixon, editor, 'Modeling and Simulation of Heterogeneous Catalytic Processes,' volume 45 of *Advances in Chemical Engineering*, pp. 1 – 40, Academic Press, 2014, doi:https://doi.org/10.1016/B978-0-12-800422-7.00001-7.

Götz, J., Zick, K., Heinen, C., and König, T., 'Visualisation of flow processes in packed beds with NMR imaging: determination of the local porosity, velocity vector and local dispersion coefficients,' Chemical Engineering and Processing: Process Intensification, 2002, **41**(7), pp. 611–629, doi:https://doi.org/10.1016/S0255-2701(01)00185-4.

Hamidipour, M. and Larachi, F., 'Characterizing the liquid dynamics in cocurrent gas-liquid flows in porous media using twin-plane electrical capacitance tomography,' Chemical Engineering Journal, 2010, **165**(1), pp. 310–323, doi:https://doi.org/10.1016/j.cej.2010.08.058.

Johns, M. L., Sederman, A. J., Bramley, A. S., Gladden, L. F., and Alexander, P., 'Local transitions in flow phenomena through packed beds identified by MRI,' AIChE Journal, 2000, **46**(11), pp. 2151–2161, doi:https://doi.org/10.1002/aic.690461108.

Kramer, D. C., Stangeland, B. E., Smith, D. S., McCall, J. T., Scheuerman, G. L., and Bachtel, R. W., 'Apparatus for an on-stream particle replacement system for countercurrent contact of a gas and liquid feed stream with a packed bed,' US Patent, US5302357A, 1994.

Li, X., Yang, C., Yang, S., and Li, G., 'Fiber-optical sensors: Basics and applications in multiphase reactors,' Sensors (Switzerland), 2012, **12**(9), pp. 12519–12544, doi: https://doi.org/10.3390/s120912519.

Mantle, M. D., Sederman, A. J., and Gladden, L. F., 'Single-and two-phase flow in fixed-bed reactors: MRI flow visualisation and lattice-Boltzmann simulations,' Chemical Engineering Science, 2001, **56**(2), pp. 523–529, doi:https://doi.org/10.1016/S0009-2509(00)00256-6.

Mena, P. C., Rocha, F. A., Teixeira, J. A., Sechet, P., and Cartellier, A., 'Measurement of gas phase characteristics using a monofibre optical probe in a three-phase flow,' Chemical Engineering Science, 2008, **63**(16), pp. 4100–4115, doi: https://doi.org/10.1016/j.ces.2008.05.010.

Muroyama, K. and Fan, L.-S., 'Fundamentals of gas-liquid-solid fluidization,' AIChE Journal, 1985, **31**(1), pp. 1–34, doi:https://doi.org/10.1002/aic.690310102.

Rao, A. V. R., Kumar, R. K., Sankarshana, T., and Khan, A., 'Identification of flow regimes in a concurrent gas liquid upflow through packed beds,' Chemical Engineering & Technology, 2011, **34**(11), pp. 1909–1917, doi:https://doi/org/10.1002/ceat.201100070.

Salleh, K. A. M., Lee, H. K., and Al-Dahhan, M. H., 'Local liquid velocity measurement in trickle bed reactors (TBRs) using the x-ray digital industrial radiography (DIR) technique,' Measurement Science and Technology, 2014, **25**(7), doi: https://doi.org/10.1088/0957-0233/25/7/075401.

Sankey, M., Holland, D., Sederman, A., and Gladden, L., 'Magnetic resonance velocity imaging of liquid and gas two-phase flow in packed beds,' Journal of Magnetic Resonance, 2009, **196**(2), doi:https://doi.org/10.1016/j.jmr.2008.10.021.

Scheuerman, G. L., Johnson, D. R., Reynolds, B. E., Bachtel, R. W., and Threlkel, R. S., 'Advances in Chevron RDS technology for heavy oil upgrading flexibility,' Fuel Processing Technology, 1993, **35**(1), pp. 39–54, doi:http://doi.org/10.1016/0378-3820(93)90084-H.

Schubert, M., Kryk, H., and Hampel, U., 'Slow-mode gas/liquid-induced periodic hydrodynamics in trickling packed beds derived from direct measurement of cross-sectional distributed local capacitances,' Chemical Engineering and Processing: Process Intensification, 2010, **49**(10), pp. 1107–1121, doi: https://doi.org/10.1016/j.cep.2010.08.004.

Sederman, A. J., Johns, M. L., Bramley, A. S., Alexander, P., and Gladden, L. F., 'Magnetic resonance imaging of liquid flow and pore structure within packed beds,' Chemical Engineering Science, 1997, **52**(14), pp. 2239–2250, doi: https://doi.org/10.1016/S0009-2509(97)00057-2.

Toukan, A. J., 'Hydrodynamics of a co-current gas liquid uplfow in a moving packed bed reactor with porous catalyst,' 2017, **MS thesis**.

Xue, J., *Bubble Velocity, Size and Interfacial Area Measurements in Bubble Columns*, Ph.D. thesis, 2004.

Yun, J., Yao, S. J., and Lin, D. Q., 'Variation of the local effective axial dispersion coefficient with bed height in expanded beds,' Chemical Engineering Journal, 2005, **109**(1), pp. 123–131, doi:https://doi.org/10.1016/j.cej.2005.03.015.

II. GAS PHASE DISPERSION/MIXING INVESTIGATION IN GAS-LIQUID UPFLOW MOVING BED HYDROTREATER REACTOR (MBR) USING DEVELOPED GAS TRACER TECHNIQUE AND METHOD BASED ON CONVOLUTION/ REGRESSION

Vineet Alexander[1], Hamza Albazzaz[2], Muthanna Al-Dahhan[*,3]

[1,*]Department of Chemical & Biochemical Engineering,

Missouri University of Science and Technology, Rolla, MO-65409

[2]Kuwait Institute for Scientific Research (KISR), Safat, Kuwait

[3]Cihan University, Erbil, Iraq

Email:[1]vaxt8@mst.edu, [*] aldahhanm@mst.edu

ABSTRACT

Gas dispersion studies has been executed for the catalyst bed section of a scaled-down industrial Moving Bed Hydrotreater Reactor (MBR). Gas dispersion/mixing is one of the critical design parameter concerning mass transfer and reactor performance, and is never evaluated in MBR. The catalyst bed of MBR is modeled using Axial Dispersion Model (ADM) and its parameters gas dispersion coefficient (D_g) and peclet number (Pe) are estimated using Residence Time Distribution (RTD) and implementing a methodology based on convolution and regression. Additionally, dimensionless variance (σ_D^2) for the catalyst bed is also measured using RTDs first and second moments to compare with the findings of ADM model. This study is conducted at the varying flow rates of gas and liquid including scaled down operating conditions. The results of D_g, Pe, and σ_D^2 indicate that bed behaves as a packed bed for low liquid flow rate and moves towards with three-phase fluidized bed for increasing liquid flow rate. Overall the gas phase behavior is seen to be in

plug flow for all the operating conditions, with relatively high dispersion/mixing in packed bed state. Scaled down flow conditions is seen to be best in terms of gas dispersion/mixing and catalyst utilization.

Keywords: Residence Time Distribution (RTD), Moving Bed Reactor (MBR), Gas Tracer, Gas Dispersion Coefficient, Peclet Number, Axial Dispersion Model (ADM)

1. INTRODUCTION

Uplfow moving bed reactor is a hydrotreater and used for removal heavy metal content from crude oil. It is usually a replacement for fixed bed Hydrodemetalization reactor, which is guard reactor to the fixed bed residual desulfurization (RDS) unit (Toukan *et al.*, 2017). This reactor has a catalyst bed section having a conical bottom and plena below the cone. The operating parameters are upflow movement of resid oil and hydrogen over hydrodemetalization catalyst (HDM), with flow conditions to limit the bed expansion to 10 percent of catalyst bulk volume (Bruce *et al.*, 1999) . The specialty of MBR is the conical bottom, which enables removal of spent catalyst under operation, this increases the run time of the reactor without shutdown. At industrial conditions, the catalyst removal takes place few times per week and that too in small increment, rest all time the reactor behaves as upflow packed bed or expanded bed. It is usually operated at a low linear velocity of the mixed feed to avoid substantial expansion (or contraction) of the bed (Bruce *et al.*, 1999). The expanded bed or ebullated bed can improve the distribution of phases cross-sectionally but is usually not preferred due to increased catalyst attrition, bed mixing, increased reactor length for the desired conversion (Bruce *et al.*, 1999) at these conditions.

The major problems seen for this kind of reactor at industrial scale are catalyst coking, agglomeration, and early shutdown. The primary factors for these unwanted phenomena is maldistribution of phases (Bruce *et al.*, 1999) which can result in unwanted mixing behavior of phases or the coke reaction related to catalyst type and its reaction, which is the least studied reaction, but this study focus is mixing. The mixing of a phase within the

reactor is conventionally classified as micromixing and macromixing (Shah *et al.*, 1978). Micromixing is the mixing occurring at the molecular level, and it depends on the intimacy of two nearby molecules. Micromixing parameter such as molecular diffusion is hard to estimate using experimental measurement technique. The macromixing phenomena is at a scale where the individual phase can be considered as an entity moving with convective dispersion and bulk flow and dispersing along axial, radial and angular direction. It is not feasible to measure the local velocity field profile at every possible local position within the reactor to quantify macromixing. Therefore, RTD concept is used, where a tracer is injected and detected a the boundaries of test section and obtained RTD curve quantifies the dispserion/mixing in terms of its spread (Iliuta *et al.*, 1998). RTD's are comprehended using mass balance model having dispersion coefficient parameter, which lumps the non-ideality in terms of the convective dispersion and molecular diffusion, which dictates the spread in the RTD curve. Dispersion coefficient is an important design parameter, as the performance of any reactor depends on inter and intraparticle rate process for heat and mass transfer which is directly related to the mixing of phases. Hence, it is essential to determine the dispersion parameters and to integrate it with the intrinsic kinetics and other mass, and heat transfer parameters to yield reactor design and models, that account for certain extent of non ideality (Shah *et al.*, 1978). The knowledge of gas phase dispersion/mixing quantified in terms of dispersion coefficient is useful, as in most of the mathematical model for upflow packed or fluidized bed the axial dispersion and film diffusion describe the bulk phase mass transfer (Koh *et al.*, 1998).

There are no studies in the open literature on gas dispersion/mixing study in MBR reactor having a conical bottom. The closest possible literature is for gas mixing studies in upflow packed bed [(Valenz *et al.*, 2010), (Benneker *et al.*, 1996), (Delgado, 2006)], and expanded/fluidized bed (Muroyama and Fan, 1985), due to bed behavior of MBR from packed bed to three phase fluidized bed based on the flow conditions of the phases. All these studies used RTD concept and obtained dispersion coefficient using either moment

method or modeling the test section with appropriate mass balance model having dispersion parameter. In moment method, the second moment (variance) of the RTD (Saroha and Khera, 2006) is matched with the equation of variance for different boundary conditions (Levenspiel and Smith, 1957). In reactor modeling approach, the obtained RTD is fitted for mixing parameters of a model describing the mass flow behavior inside the test section. At macromixing level, the extreme flow conditions can be modeled using plug flow for no mixing/dispersion, and CSTR for completely mixed flow (Shah *et al.*, 1978). If the flow is not much deviating from the plug flow, then Axial Dispersion Model (ADM) and its many derivatives are the most common model used to describe the flow behavior [(Shah *et al.*, 1978), (Iliuta *et al.*, 1998)].

In many cases, such as in hydrotreaters, the area of interest (catalyst bed) is accompanied by additional volumes (plena). Here, by injecting tracer at the inlet and detecting at the outlet of the enitre reactor will not give the required RTD information of the test section (catalyst bed). In these instances one injection and two-point measurement methods are implemented.

In one injection and two-point measurement method, is an injection-sampling concept in which an injected tracer at the inlet of the reactor is sampled before and after the test section, and the difference in the variance of the two obtained RTD gives the effective dispersion coefficient of the test section. It is based on the assumption that the spreading of tracer or variance of the curve is linearly changing along the reactor [(Levenspiel and Smith, 1957), (Edwards and Richardson, 1968))]. (Valenz *et al.*, 2010) used this approach with a step input to find the mixing of gas phase in a two-phase packed bed column.

(Han, PhD Thesis, 2007) advanced one injection and two-point detection method by integrating this injection-sampling concept with convolution and regression principle. In this approach the test section is modeled with appropriate model and the solution of the model is considered as the RTD response of the test section, the response of the test section is convoluted with the RTD signal sampled at the inlet. The convoluted signal is theoretical

RTD at the outlet of the test section based on the model parameters and for the inlet boundary condition obtained by sampling at inlet of test section. The theoretical output response is regressed with actual output response obtained from sampling of tracer at the outlet of test section for minimum error to estimate mixing parameters. (Han, PhD Thesis, 2007) implemented this method on a slurry bubble column reactor and (Abdulmohsin and Al-Dahhan, 2016) followed this approach on pebble bed reactor to obtain dispersion parameters of gas phase in plenum and bed zone (test section) of these reactors. They also measured the RTD curve along the radial profile at the inlet of the bed section and found similar curves radially. The significance of this radial study is that it shows the tracer from the plenum is evenly distributing to the bed section. The one injection and two-point measurement method is not applicable to the cases where the plenum are not evenly distributing the phases to the bed section. As a single point measurement at the outlet of the plena does not represent the actual flow behavior of the plena. The similar scenario is observed in MBR due to conical bottom of the catalyst bed (test section) and complex internal of plena.

The solution to this problem is an alternative injection-sampling concept called two-point/multiple injections and one detection method. In which the tracer is injected at inlet and outlet of the test section and detected at the outlet of the reactor after a mixing cup to ensure even distribution of tracer at the detection cross-sectional plane (Carleton *et al.*, 1967). (Midoux and Charpentier, 1972) used this method and compared with one injection and two-point detection method, and found both method yield similar results when experimental RTDs are interpreted with theoretical models using dankwerts boundary.

This study focuses on investigating the gas mixing behavior at various flow condition in the catalyst bed section of MBR reactor. The approach followed is a injection-sampling concept based on multiple injection and one detection method along with convolution-regression principle approach proposed by (Han, PhD Thesis, 2007). This objective is achieved by developing a gas tracer experimental facility for MBR based on the experimental facility developed by (Han, PhD Thesis, 2007) for slurry bubble column reactor and

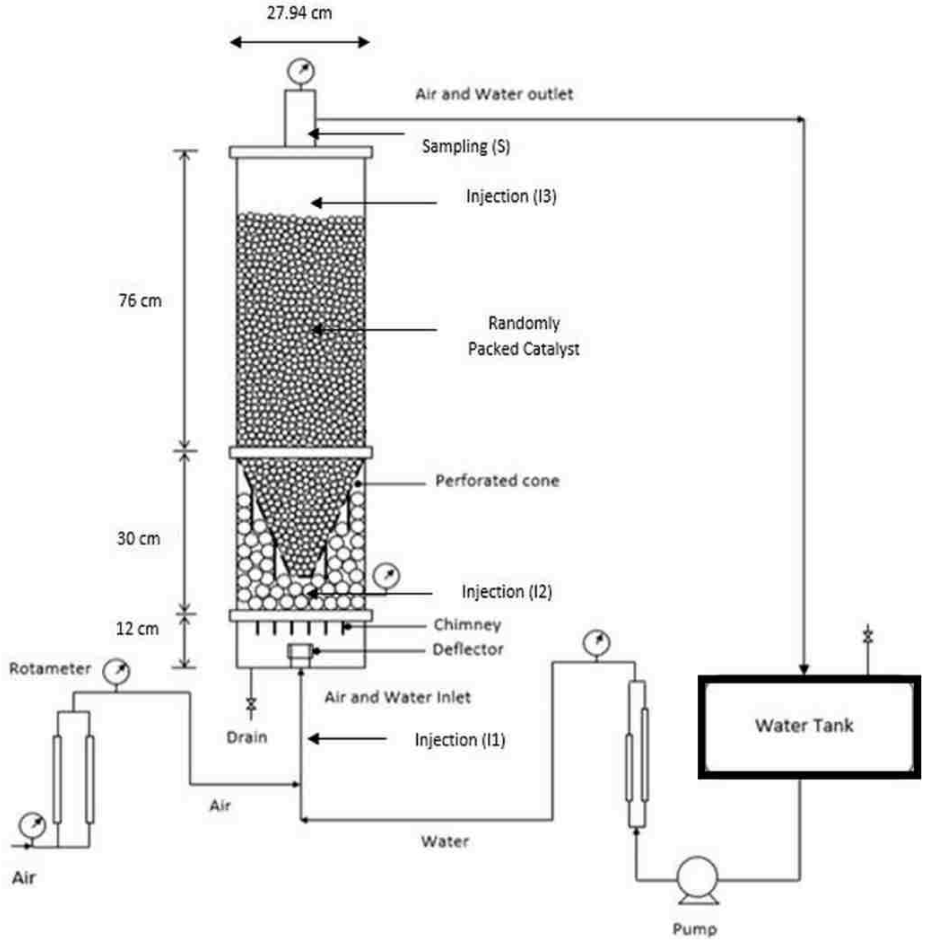

Figure 1. Schematic diagram of scaled down MBR setup for gas dynamics studies

(Abdulmohsin and Al-Dahhan, 2016) for pebble bed reactor. This experimental facility has multiple injections and one sampling port and provisions to obtain the RTD curve only for gas phase from the two-phase upflow at different sections of the MBR. The RTDs of different sections along with ADM and Ideal CSTR-PFR model for packed bed and plena respectively, is used with convolution-regression to estimate dispersion/mixing parameters of catalyst bed section.

2. EXPERIMENTAL SETUP

The experimental set-up of the moving bed hydrotreater (MBR) reactor is scaled down to pilot-plant scale from industrial scale based on hydrodynamic and geometric similarity. The scaled down flow operating condition is obtained by matching the LHSV and gas-liquid volumetric flow rate ratio with the industrial operating conditions.

The schematic of the pilot plant scale reactor is shown in Figure 1. The reactor is a plexiglass column of height 118 cm and the internal diameter of 29.7 cm. It is divided into three sections by distributor plate and conical bottom. The parts below conical bottom are called plena, and it is further divided into lower and upper plenum. The lower plenum consists of the deflector and 19 chimneys. The chimneys are attached to the distributor in triangular pitch and have an additional side hole opening just below the distributor plate (Figure 1). The upper plenum is the compartment between the conical bed and the upper plenum wall which is tightly packed with passive spheres to cover the entire region between the conical bottom and distributor plate. Above the conical bottom is bed section, which is the region from conical base to the top of the bed at cylindrical column, It is filled with 3mm industrial grade HDM (Hydrodemetallization) catalyst. The conical bottom is perforated, and perforations are small enough to avoid catalyst plugging. At industrial operation, the catalyst withdrawal is facilitated through the cone.

The ancillaries for the reactor are gas and liquid rotameters, liquid pump, and water tank. This reactor operates in upflow state, with premixed gas-liquid which is under control by rotameters are fed mixed into the deflector of the lower plenum. For scaled down operating conditions the flow profile inside the lower plenum will have a gas pocket around the chimneys side hole. The gas penetrates through the side hole, and liquid enters through main hole of chimney at its bottom both are mixed below the distributor and ejects as a spray to upper plenum. The passive spheres in the upper plenum distribute the incoming phases and are fed to the bed section through the perforated cone. The distributed stream maintains

Table 1. Reactor design parameters and experimental condition for gas dispersion/mixing study

Parameters	Value/Range	Comment
Column Diameter	27.94 cm	
Column Height	118 cm	
Bed Height	63 cm	Height from top of the cone to the top of the bed at no flow rate
Catalyst	3 mm Diameter	Bulk Density (570 Kg/m^3)
Liquid (Water) Superficial Velocity	0.01 to 0.4 cm/sec	
Gas (Air) Superficial Velocity	1.28 to 5.13 cm/sec	
Scaled Down Liquid Flow Rate	0.0175 cm/sec	By matching LHSV of industrial and scaled down reactor
Scaled Down Gas Flow Rate	7.7 cm/sec	By matching Gas/liquid volumetric flow rate of industrial and scaled down reactor

the bed in packed or expanded bed state based on the flow conditions. For scaled-down operating condition, the bed behaves as packed bed with slight expansion at the top of the bed.

In this study, the gas dispersion is investigated by varying flow rate of gas and liquid and at the scaled-down experimental condition. The dimensions of the experimental setup and operating conditions used in this study are shown in the Table 1.

3. GAS DYNAMIC TRACER TECHNIQUE FOR EVALUATION OF THE RESIDENCE TIME DISTRIBUTION (RTD) OF THE GAS PHASE IN THE GAS-LIQUID UPFLOW MBR

The residence time distribution (RTD) concept is developed long time ago for flow evaluation of reactor by developing a model for the reactor and quantification by RTD [(Danckwerts, 1953), (Levenspiel and Smith, 1957), (Simcik *et al.*, 2012)]. Its simplicity has made it an useful part of engineering applications, but simplicity lies within a particular range of applications such as single phase small-scale reactors. The complication arises when the multiphase flow is encountered; it can be difficult to separate a phase from a mixture and analyze them for tracer for RTD determination (Simcik *et al.*, 2012). The trouble increases when reactors have plena, and the RTD is only needed for the reactor-bed section, where the conversion occurs. To overcome these difficulties, (Han, PhD Thesis, 2007) developed dynamic gas tracer experimental and mathematical approach for slurry bubble column. The developed dynamic gas tracer experimental technique and a mathematical approach for a slurry bubble column reactor is used and implemented by (Abdulmohsin and Al-Dahhan, 2016) on a pebble bed reactor. Here we extend this to upflow moving bed reactor (MBR). The developed tracer technique for MBR can separate gas phase from the mixture of gas-liquid.

3.1. Dynamic Gas Tracer Technique. Figure 2 shows the components of the gas tracer technique. Gas tracer is analyzed using a Thermal Conductivity Detector (TCD-Gow MAC 20 series) (Figure 2a). Helium is used as a gas tracer, which is non-reactive, non-transferable to liquid phase (Han, PhD Thesis, 2007), and having the physical property similar to the gas phase (air) (Shah *et al.*, 1978). Different kind of gas tracer are used for RTD studies based on the detection equipment and is summarized by (Shah *et al.*, 1978). Nitrogen (Figure 2b) is reference gas for the TCD. Water pump (Figure 2c) removes tracer laden gas-liquid mixture out of the reactor. In house developed Gas-liquid separator (Figure

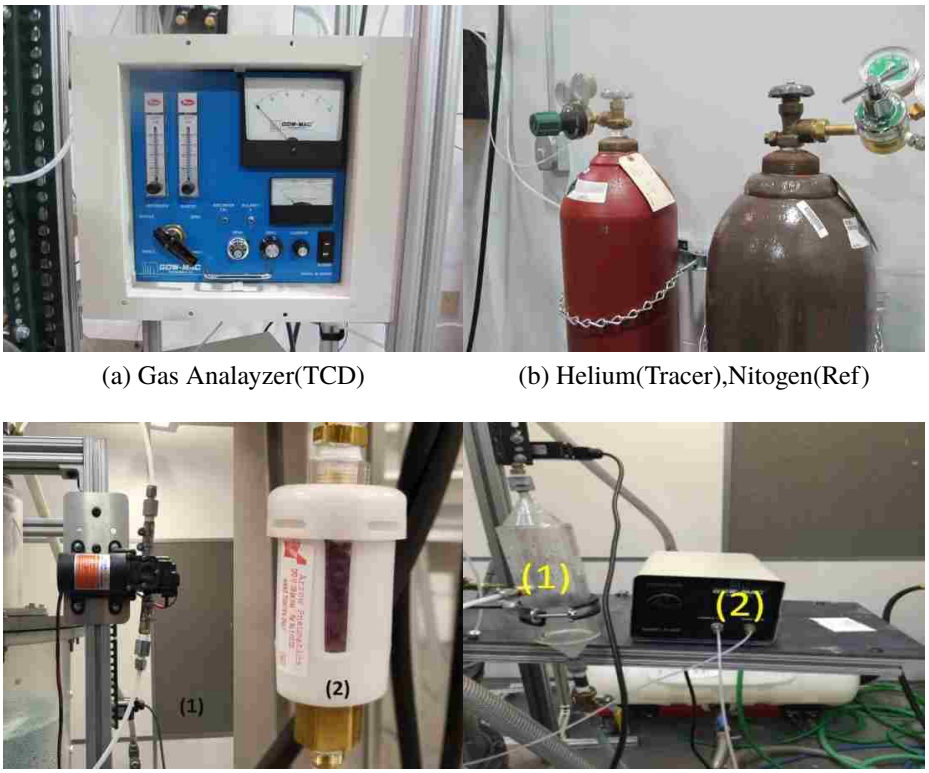

(a) Gas Analayzer(TCD) (b) Helium(Tracer),Nitogen(Ref)

(c) 1-Water Pump, 2-Moisture Remover (d) 1-Gas-liq Seperator, 2-Air Pump

Figure 2. Gas tracer components

2d (1)) separates gas from the liquid using a gas-pump (Figure 2d) and before gas pump there is a moisture remover (Figure 2c). These components along with data acquisition system (Gow-Mac) and reactor forms gas dynamic tracer system.

3.2. Gas Tracer System of MBR. Figure 3 shows the gas tracer system of MBR. Helium is injected through injection tubes (I1, I2, I3), detailed explanation of the injection and sampling is given in section 4.1. Compressed helium gas cylinder (Figure 2b) is connected to a solenoid valve using nylon tube (0.5 inches), and the connection continues to injection points. The solenoid valve is controlled by a digital timer and set for 0.5 sec opening interval; this provides a pulse injection. The tracer sticks to the gas phase and follows its path along with the liquid phase. The gas-liquid mixture enters into mixing cup as shown in the Figure 3, and after that, sampling (S) of the mixture is done using sampling

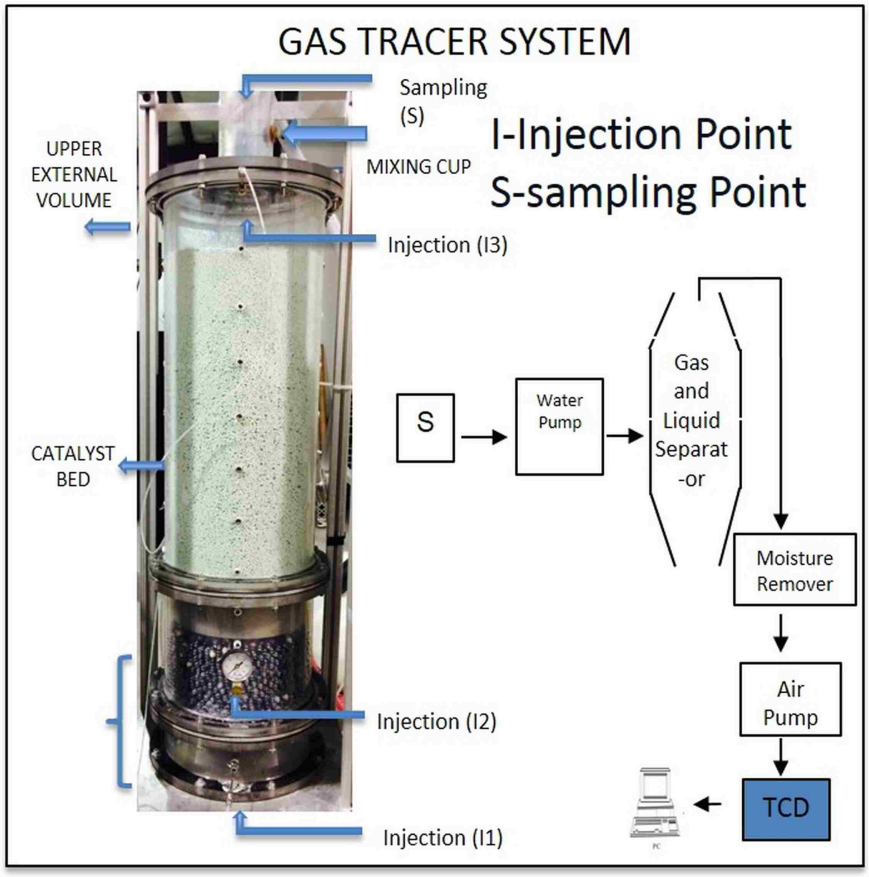

Figure 3. Gas dynamic tracer system of MBR

tubes and water pump (Figure 2c), which draws out the mixture and feeds into an in-house developed gas-liquid separator (Figure 2c). This pump creates a suction to remove gas phase from the separator and then it passed through a moisture remover (Figure 2c), and then only gas phase to the TCD (Figure 2a). The thermal conductivity of the helium mixed in the gas phase is compared with the reference gas (Nitrogen) for TCD. The helium mixture in gas has higher thermal conductivity than reference gas, and TCD response as voltage signal is linear with the concentration of helium in the air. Response from the TCD is amplified and recorded as time series at a sampling frequency of 10 Hz. Each injection will give respective RTD and will be used all together in developed methodology to determine gas dispersion parameter of the catalyst bed alone.

Table 2. Injection and sampling assembly of MBR for gas dynamics study

Measurement	Injection	Sampling	Dispersion Zones
C(1)	I1	S	**Zone(1)**: Plena + CatalystBed + Upper external Volume + Sampling Line (measurement Volume)
C(2)	I2	S	**Zone(2)**: Catalyst Bed + Upper External Volume + Sampling Line (measurement volume)
C(3)	I3	S	**Zone(3)**: Upper External Volume + Sampling Line (Measurement Volume)

4. METHODOLOGY TO MEASURE GAS DISPERSION IN CATALYST BED SECTION OF MBR

A methodology is developed based on the injection-sampling concept called multiple injection and one detection method, and a mathematical approach based on convolution and regression proposed and implemented by (Han, PhD Thesis, 2007). This particular method is developed for upflow moving bed reactor (MBR), but this method can be applied to any multiphase reactors with plena.

4.1. Injection and Sampling Assembly. Injection-sampling assembly is designed in a way to have one point measurement (S) with three injections (I1, I2, I3) as shown in the Figure 3. Table 2 shows the zones covered by each injection and sampling point. The injection (I1) is at the bottom of the reactor and just below the plenum section, injection (I2) is below the conical bottom, and injection (I3) is just above the catalyst bed as shown in the Figure 3. The sampling (S) at the top of the reactor. The measurement C(1) (I1-S) gives RTD of the entire reactor which includes the plena, catalyst bed section, upper external volume from above the bed to sampling point, sampling assembly, and measurement system line.

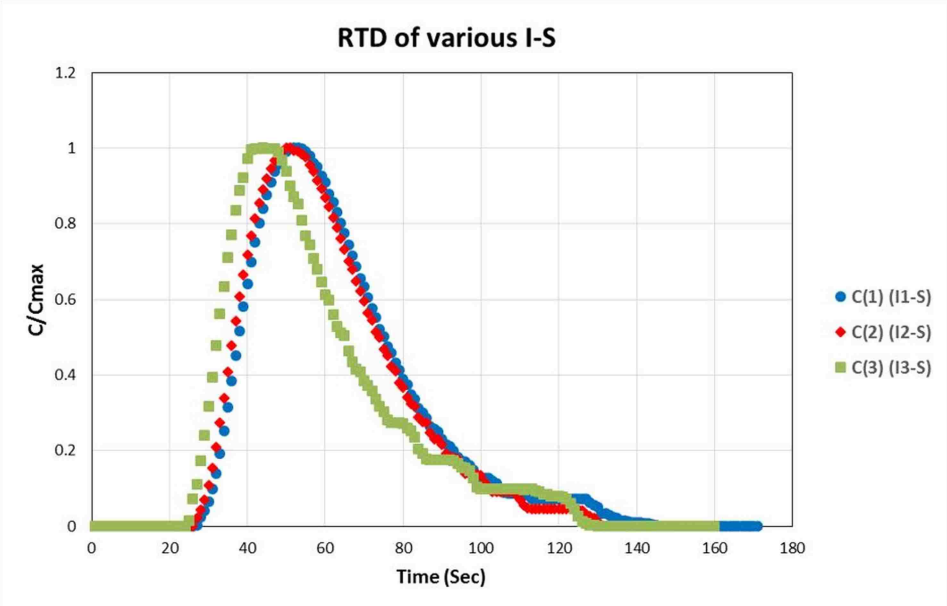

Figure 4. RTD of various injection-sampling at scaled experimental conditions

The measurement C(2) (I2-S) gives the RTD of zones other than plena, and measurement C(3) (I3-S) gives the RTD of the zones other than plena and catalyst bed section. The RTDs of each section are plotted in Figure 4 for industrial scale down conditions.

The shape of the RTD curve depends on the type of injection and flowing structure (Shah *et al.*, 1978). The injections are usually of the pulse, imperfect pulse, step, sinusoidal, ramp and parabolic in nature (Shah *et al.*, 1978). In the majority of the studies, mixing characteristics of phases are investigated using pulse injection (Shah *et al.*, 1978). In our case, we injected tracer as pulse, and if the reactor mixing behavior is between pulse and perfectly mixed CSTR, then the response of the system for pulse injection will be of Gauss Jordan distribution type (Shah *et al.*, 1978), as also observed from the Figure 4. The RTD curves are usually plotted by normalizing it with its peak value [(Yun *et al.*, 2005), (Han, PhD Thesis, 2007), (Abdulmohsin and Al-Dahhan, 2016)] and are used to determine

holdups, mass transfer parameters, and linear isotherms parameters (Yun *et al.*, 2005), the same is done here. The plots are normalized based on the maximum concentration for each RTD signal.

4.2. Convolution and Regression Approach to Estimate Gas Dispersion in Catalyst Bed of MBR. Convolution principle is widely used to get the RTD signal of the region which is accompanied by additional volume hence additional dispersion. Deconvolution in another mathematical way to extract out the signal of the interested zone by removing dispersion for additional volumes from the overall signal, but this method is usually not preferred in chemical engineering applications due to numerical instability (Han, PhD Thesis, 2007). Convolution integral shown by equation 1 is a mathematical way to obtain RTD of a system for any arbitrary input (Shah *et al.*, 1978). In equation 1, C_{in} in the inlet concentration or input and C_{out} is the response of the system and C^*_{out} is the output of this system for an inlet concentration profile of C_{in}. Both input (C_{in}) and system response (C_{out}) can be obtained by proposing a model and regression to estimate model parameters, or directly from experimental RTD for a Dirac pulse input.

$$C^*_{out} = \int_0^t C_{out}(t').C_{in}(t - t').dt' \tag{1}$$

The different regions of the reactor either additional volumes or zone of interest, can be modeled by simple or complex differential type model following diffusional type mixing or stage-wise macro-mixing model where mixing is described by perfectly staged regions (Iliuta *et al.*, 1998). The complexity of the model increases with its increase in parameter, and it tries to characterize the realistic flow pattern. Some of these models are summarized in the review of (Shah *et al.*, 1978).

The reactor shown in Figure 3 has three regions; catalyst bed section, plena (Additional volume), upper external space plus sampling line (Additional volume). ADM is the most commonly used model for the packed bed dispersion studies, here ADM is the assumed model for the catalyst bed with two parameters D_g (Dispersion coefficient) and

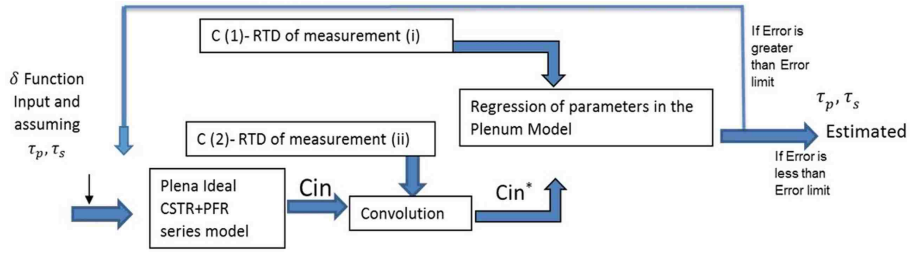

Figure 5. Schematic of convolution and regression approach to obtain parameters for plenum model

Gas Holdup (ϵ_g). Ideal CSTR plus PFR series is the assumed model for the plena (lower plenum, packed bed region between the conical bottom and distributor plate), as CSTR is the most commonly used model for plenum for upflow reactors ((Han, PhD Thesis, 2007)), and RTD experiment gives the response of upper external volume (I3-S Figure 4). Then a single point multiple injection methods (section 4.1) is implemented along with convolution and regression to get ADM parameters. ADM is solved by two-step process, In first step; by determining the concentration for inlet boundary condition for ADM, which is the solution of ideal CSTR+ PFR model (quantifies mixing in plena). In the second step; solving ADM numerically for the closed-closed boundary with inlet concentration from step 1, and parameters for regression. If the ADM or ideal CSTR plus PFR are not a valid model to quantify the gas mixing process in catalyst bed section and plena, then it fails during regression test.

4.3. Step 1: Procedure to Obtain Plenum Model Parameters and Inlet Boundary Condition for ADM. Figure 4.3 show the schematic of the procedure of step 1. The plena are taken as ideal CSTR and PFR (equation 2), and it has two parameters τ_p (Space time of PFR) and τ_s (Space time of CSTR), the parameters are at first assumed to initiate the run for step 1. The assumed parameters give C_{in}, which is theoretically input to the section zone-2 (Table 2).

$$C_{in}(t) = 0, t < \tau_p$$

$$C_{in}(t) = \left(\frac{e^{\frac{-(t-\tau_p)}{\tau_s}}}{\tau_s}\right), t > \tau_p \tag{2}$$

Applying convolution principle; C_{in} is the input to the Zone 2 (Table 2) and the response of the Zone-2 is measured by I2-S as shown in Figure 4, C(2) is obtained experimentally by (I2-S) (Figure 4)

$$C^*_{in} = \int_0^t C_{in}(t').C(2)(t-t').dt' \tag{3}$$

The convolution gives C^*_{in} (Figure 6) which is the theoretical output of the zone 2 (Table 2), for an input concentration of C_{in} which represents mixing behavior of gas in plena, as shown in Figure 6. Hence C^*_{in} represents the theoretical RTD of the entire reactor (Zone 1) as it comprises of Plena and Zone 2. Experimentally we have determined RTD for the whole reactor (Zone 1) $C(1)$ by I1-S. The regression of C(1) (experimental) and C^*_{in} (theoretical) for τ_p and τ_s yields these parameters for minimum error of averaged squared error in the time domain (equation 6). The n in equation 6 is the number of data points.

$$Error = \frac{1}{n}\sum_{j=1}^{n}[C^*_{in}(t_j) - C(1)(t_j)]^2 \tag{4}$$

Figure 7 shows the plot of theoretical output based on plena model and experimental output of the whole reactor for minimum error for the equation 6. The estimated regression parameter are τ_p (1sec) and τ_s (1sec) for scaled down operating conditions. The error in the equation for the estimated parameter at scaled down experimental conditions is 0.00041 and this indicates that the assumed model is valid enough to represent the gas mixing in plena. The regressed τ_p and τ_s parameter are plugged into equation 2, which is used as an initial concentration for inlet boundary condition of ADM.

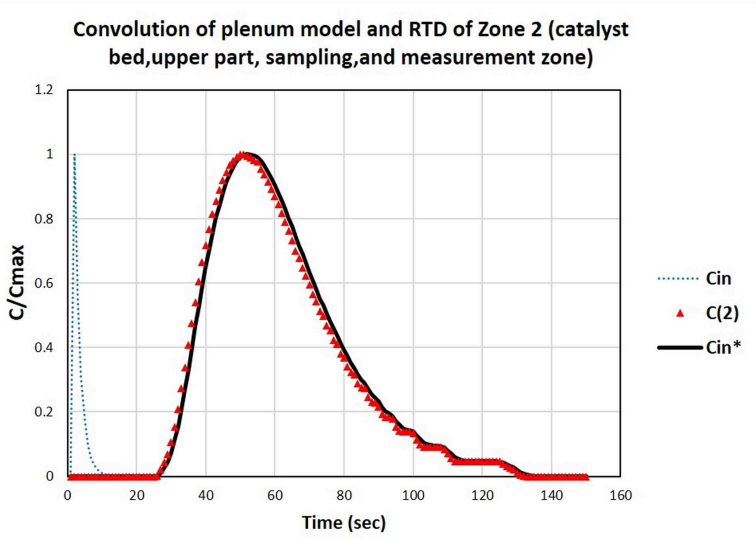

Figure 6. C_{in} (solution of plenum model; ideal CSTR+PFR), $C(2)$ (experimental response of zone-2 measured by I1-S), C_{in}^{*} (convoluted signal of C_{in} and $C(2)$)

4.4. Step 2: The Procedure to Obtain ADM Model Parameters using Step 1 Inlet Boundary Condition. The catalyst bed section shown in Figure 1 and Figure 3, is modeled using Axial dispersion model (equation 5) with boundary condition (equation 6 and 7). The parameter of ADM are D_g (gas dispersion coefficient) and ϵ_g (gas holdup). The ADM is solved numerically by plugging C_{in} in equation (6) from the C_{in} obtained from step 1 (Figure 5), and initiate the procedure (Figure 8) by assuming the parameters (D_g, and ϵ_g). The solution of ADM yields C_{out}, which is output of ADM for inlet concentration of plena as shown in Figure 9. In other words C_{out} is the theoretical RTD of plena plus catalyst bed section for dirac pulse input. C_{out} is also an theoretical input for Zone 3 (Table 2).

$$\frac{\partial C_g}{\partial t} = D_g \frac{\partial^2 C_g}{\partial Z^2} - \frac{U_g}{\epsilon_g} \frac{\partial C_g}{\partial Z} \tag{5}$$

Boundary Conditions:

$$Z = 0, U_g.C_{in} = U_g.C_g|_{z=0} - D_g \frac{\partial C_g}{\partial Z}|_{z=0} \tag{6}$$

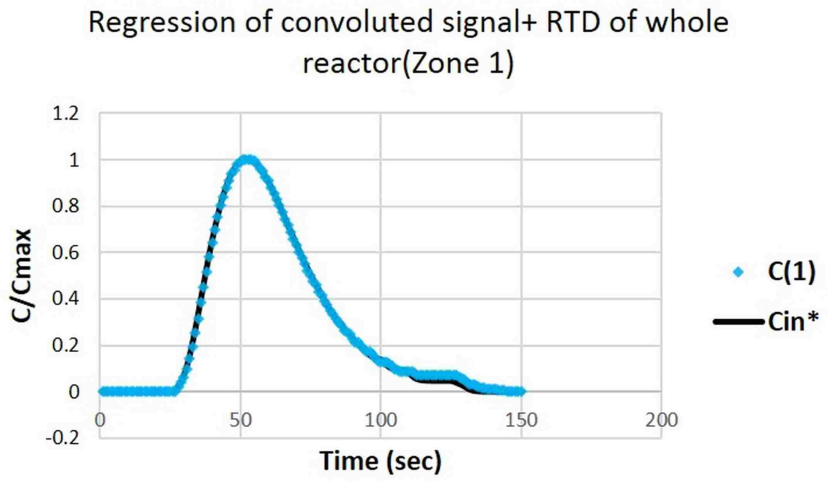

Figure 7. Regression of the theoretical output based on the plenum model (C_{in^*}) and the experimental output (C(1)) of the whole reactor for minimum error

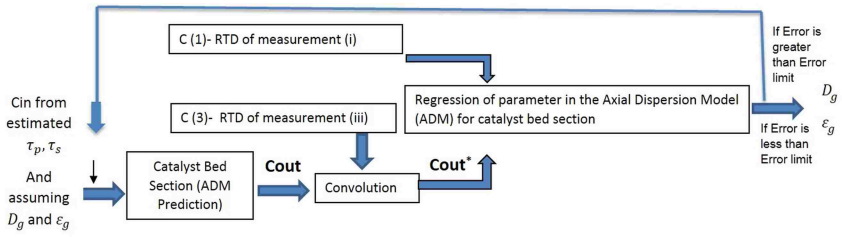

Figure 8. Schematic of convolution and regression approach to obtain parameters for ADM model using input profile C_{in}

Applying convolution principle (equation 8); C_{out} is the input to zone 3 and C(3) is experimental response of zone 3 obtained by I3-S (Figure 4).

$$Z = L, \frac{\partial C_g}{\partial z}|_{z=L} = 0 \tag{7}$$

The convoluted output C_{out^*} represents the output of the zone 3 for input profile C_{out}, (which represents the RTD of plenums plus catalyst bed section). Hence C_{out^*} represents the theoretical output of the entire reactor or zone 1. Experimental output of the zone-1 is obtained by C(1) (I1-S) (Figure 4).

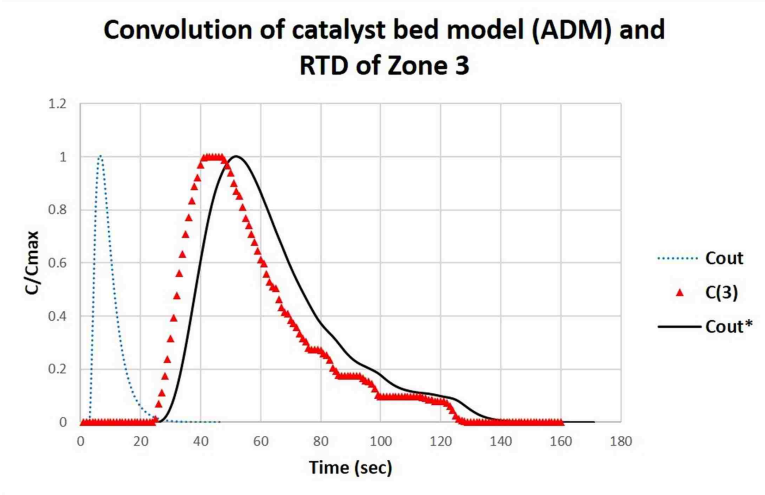

Figure 9. C_{out} (ADM solution of plenum model input), C(3) (experimental output of zone1), C_{out^*} (convoluted signal output of C_{out} and RTD of zone3)

The regression of C(1) (experimental) and C^*_{out}(theoretical) for D_g and ϵ_g yields these parameters for minimum error of averaged squared error in time domain (equation 9).

$$C_{out^*} = \int_0^t C_{out}(t').C_3(t - t').dt' \tag{8}$$

The two parameter regression by equation involves unconstrained regression of parameters (Yun *et al.*, 2005). One of the parameter (ϵ_g) is constrained between ϵ_{gmin} and ϵ_{gmax} as shown by equation 10, this improves accuracy and speed of regression calculation. Peclet number (Pe) is also estimated using equation 11.

$$Error = \frac{1}{n}\sum_{j=1}^{n}[C_{out^*}(t_j) - C(1)(t_j)]^2 \tag{9}$$

$$\epsilon_{gmin} = \frac{U * t_1}{L}, \epsilon_{gmax} = \frac{U * t_2}{L} \tag{10}$$

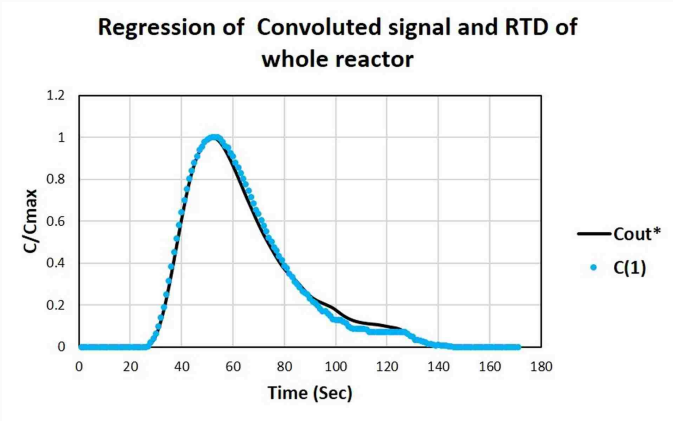

Figure 10. Regression plot of C_{out^*} (convoluted signal of ADM output and experimental output of zone-3 (I3-S)) and C(1) (experimental output of zone1) for minimum error

Whereas, U is superficial velocity of gas based on empty column, L is the linear distance between injection (I2 and I3), t_1 is time difference between first signal arriving for C(2) and C(3), and t_2 is the time difference between mean residence time (equation 19) for C(2) and C(3), ϵ_g is the gas holdup in packed bed, D_g is the gas dispersion coefficient.

$$Pe = \frac{U * L}{\epsilon_g * D_g} \tag{11}$$

Figure 10 shows the regression for minimum error of equation 9 for parameter D_g and ϵ_g The estimated regression parameters are D_g ($0.1 m^2/s$), ϵ_g (0.0823), and Pe (7.87) for scaled down operating conditions. The minimum error for experimental scaled down condition is 0.00051, which is lower than the tolerance limit of 0.001, and hence validates that the ADM is a valid model to represent gas dynamics in catalyst bed of MBR. This methodology is applicable for the catalyst bed section of the MBR reactor for gas dynamics investigation. In addition to these parameters, dimensionless variance (σ_D^2) is calculated for the bed section of MBR using the RTDs (Table 2) , which also indicates the degree of mixing, with σ_D^2 of zero indicates plug flow and σ_D^2 of one indicates complete mixing.

5. DIMENSIONLESS VARIANCE (TANK IN SERIES)

Tank in series is modeling concept, where n tanks are modeled as ideal CSTR in series for pulse injection of tracer. The theoretical residence time distribution (RTD) obtained from the model is regressed with experimental RTD of non-ideal reactor by varying the number of tank (n). Larger the value of n indicating the flow is towards plug flow and lower means the flow is towards CSTR. (Fogler, 2005) showed that equation 12 is the generalized RTD for n tank modeled as ideal CSTR in series.

$$E(t) = \frac{t^n}{(n-1)!\tau_i^n} e^{-t/\tau_i} \tag{12}$$

Where τ_i is the means residence time in single tank, n is the number of tank, and τ_i is equal to τ/n, and τ is mean residence time of entire reactor. Equation 12 is converted to dimensionless form $E(\theta)$ as shown in Equation 13.

$$E(\theta) = \tau E(\theta) = \frac{n(n\theta)^{n-1}}{(n-1)!} e^{-n\theta} \tag{13}$$

Where θ is the ratio of t and τ. The variance of equation 13 can be found using equation 14, which is called dimensionless variance (σ_D^2), and this dimensionless variance is equal to the ratio of variance (σ^2) and square of mean residence time (t_m).

$$\sigma_D^2 = \frac{\sigma^2}{{t_m}^2} = \int_0^\infty (\theta - 1)^2 E(\theta) d\theta \tag{14}$$

(Fogler, 2005) showed the solution of equation 14 is equal to the inverse of number of tanks (n), as shown in equation 15.

$$\sigma_D^2 = \frac{\sigma^2}{{t_m}^2} = \frac{1}{n} \tag{15}$$

This indicates if σ_D^2 is zero then n is infinity, which is the case for plug flow, and when σ_D^2 is one then is n is one, which means complete mixing. Dimensionless variance can be determined by RTD experiments, as it is the ratio of variance (σ^2) (second moment) and square of mean residence time (t_m) (first moment).

$$MeanResidenceTime(t_m) = \int_0^\infty E(t)tdt \tag{16}$$

$$Variance(\sigma^2) = \int_0^\infty (t - t_m)^2 E(t)dt \tag{17}$$

In our case, the area of interest is packed bed region, and its dimensionless variance is evaluated by finding the variance of RTD of zone 2 (t_{m2}) (Figure 4 and Table 2) and RTD of zone 3 (t_{m3}) (Figure 4 and Table 2) using the equation 16 and similarly the variance (σ_2^2 and σ_3^2) using equation 17. Volume of Zone 2 minus volume of zone 3 gives volume of bed , and as these moments are additive the bed variance will be ($\sigma_2^2 - \sigma_3^2$) and mean residence time in the bed will be ($t_{m2} - t_{m3}$). Hence the σ_D for the bed is calculated using equation 18.

$$\sigma_D^2(Bed) = \frac{(\sigma_2^2 - \sigma_3^2)}{(t_{m2} - t_{m3})^2} \tag{18}$$

Equation 18 shows the dimensionless variance of the gas phase in catalyst bed region and for scaled down experimental condition (Table 1), σ_D^2 is 0.232.

6. RESULTS AND DISCUSSION

Gas transport inside a reactor with packing is mainly occurring due to three mechanism; bulk flow due to pressure gradients, diffusion due to concentration gradients, and convective dispersion due to spatial velocity fluctuation (Pugliese *et al.*, 2012). The summation of last two parameters defines the dispersion/mixing of phase in the system. The

D_g values estimated from ADM equation is due to both molecular diffusion and convective dispersion (hydrodynamic mixing) (Edwards and Richardson, 1968). Hence, our focus of this study is to see dispersion/mixing behavior of gas in terms of D_g values. The value of D_g functionally depends on the ratio of the particle diameter to column diameter, fluid density and viscosity, superficial velocities of phases, ratio of the length of the reactor to the column diameter, particle size distribution, and effect of temperature (Delgado, 2006). In this study, we wanted to see the effect of superficial velocity on the dispersion coefficient (D_g), peclet number (Pe), and dimensionless variance ($\sigma_D{}^2$) in the catalyst bed section of MBR.

6.1. Effect of Flow Rate of Phases on Gas Dispersion Coefficient (D_g) for Catalyst Bed in MBR. Figure 11 shows the trend in D_g values for varying superficial velocity of the gas at low liquid superficial velocities (Figure 11a) and at high liquid superficial velocities (Figure 11b). Figure 11a shows that the Dg values are increasing with increase in gas flow rate and liquid flow rates, and this phenomenon is usually observed in packed bed reactor [(Edwards and Richardson, 1968), (Delgado, 2006), (Abdulmohsin and Al-Dahhan, 2016)]. To understand the effect of velocity on D_g in packed bed , let us look into the equation $D_l = D_m{}' + ud/Pe_L(\infty)$ [(Gunn and Pryce, 1969), (Edwards and Richardson, 1968), (Delgado, 2006)]. For packed bed, the estimated D_g is the summation of molecular diffusivity ($D_m{}'$) and dispersion due to turbulent or eddy motion of flow i.e, convection ($ud/Pe_L(\infty)$). At low particle Reynolds number; less than 1.8 for gases, molecular diffusivity plays a vital role (Edward 1968). On increasing the velocity, the flow moves towards the turbulent flow, and eddy diffusion plays a dominant role in gas transport due to spatial velocity variations and fluctuations. The dispersive component due to eddy diffusion ($ud/Pe_L(\infty)$), depends on interstitial velocity which in turn depends on packing structure, flow distribution, and flow rates. Hence, increase in flow rate increases the convective dispersion component ($ud/Pe_L(\infty)$), and also results in the increase in bubble breakage phenomena due to the interaction of gas bubbles with catalyst bed particles ((Briens and Ellis, 2005)). Hence, on

increasing gas flow rate, we observe wider bubble size distribution which results in wider spread of gas phase along the 3-dimensional space of catalyst bed and increased mixing due to the convective component of dispersion. Both of these mechanism leads to increase in the estimated D_g value with increase in gas flow rate. From dispersion/mixing point of view increasing the gas velocity at low liquid flow rate is good, as it increases the overall mixing, reduces channeling (Edwards and Richardson, 1968), provides better radial distribution (Abdulmohsin and Al-Dahhan, 2016). At scaled down experimental condition, visually, the bed is behaving in packed bed state with slight expansion at the top of the bed. The results (Figure 11a) also confirm that the bed is behaving as packed for these flow rates. The gas phase flow dynamics completely change when the bed starts to expand and which we observed for the higher flow rate of the liquid.

Figure 11b shows decreasing trend of D_g value with increase in both gas and liquid flow rates, which is complete opposite trend of the phenomena observed for packed bed case (Figure 11a). It shows the bed is not anymore in packed bed state and the bed expansion is significant at the higher flow rate of liquid (Yun *et al.*, 2005) which promote backmixing. It is seen that with the increase in gas and liquid velocities result in more expansion of the bed and bed flow dynamics move towards the 3-phase fluidized bed. At expanded bed conditions the gas phase can displace suspended solid phase and gas phase follows least resistance path, which results in a less cross-sectional distribution of gas phase at these conditions. Although overall the bed is at high turbulent condition due to movement of solid particles, but due to less spread of gas phase along the cross-section results in the reduction in estimated values of D_g. In terms of mixing this condition is not good for hydrotreating applications. As the bubbles try to coalesce and move without dispersing cross-sectionally, which results in inefficient utilization of catalyst. Hence it is desired to run this reactor at the conditions of packed bed with least and preferably no expansion of the bed. By looking at the trend of D_g value for expanded bed, it looks the flow is more towards the plug flow state. Usually in three-phase fluidized bed the gas phase flow as plug

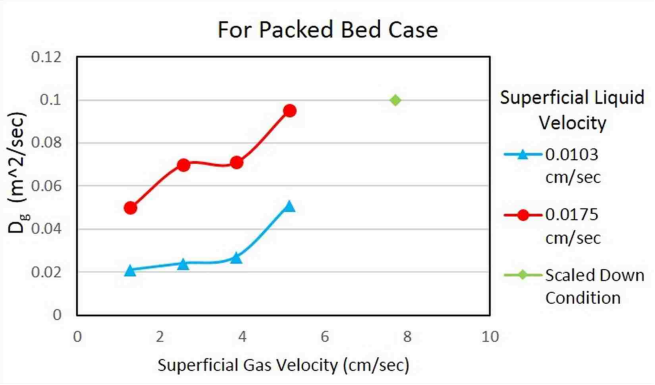

(a) Plots of D_g for varying flow rate of gas at low liquid velocity

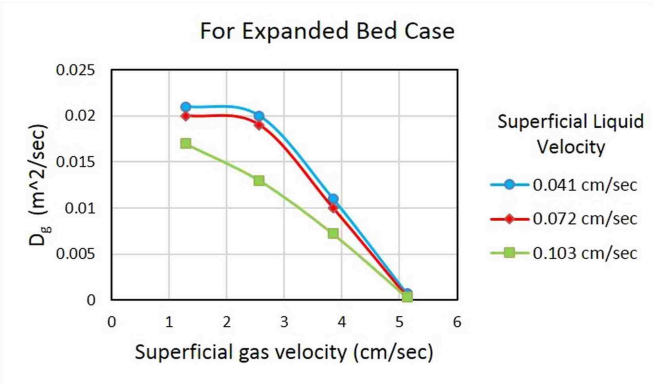

(b) Plots of D_g for varying flow rate of gas at high liquid velocity

Figure 11. Gas dispersion plot for varying flow rate of phases

flow with significant backmixing of the liquid phase (Fan *et al.*, 1987). To see how much deviation the gas flow is from plug flow, Pe and σ_D^2 evaluation is needed. To estimate Pe, ϵ_g values are needed. For three phase flow, ϵ_g is the function of flow rate and packing (Beg *et al.*, 93-103) and is one of the estimated parameter from the ADM equation 5 which is discussed in section 4.4, and its variation with flow conditions are measured to calculate Pe (Equation 11).

6.2. Effect of Flow Rate of Phases on the Gas Holdup (ϵ_g) in Catalyst Bed of MBR. From dispersion plot (Figure 11), we were able to identify the flow rates at which the bed behaves as packed and expanded bed, respectively. The gas holdup results are also shown for packed bed (Figure 12a) and for expanded bed (Figure 12b). Figure 12a shows

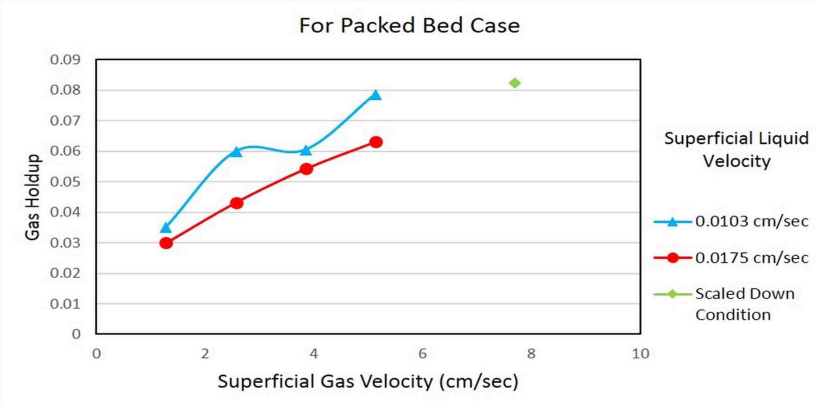

(a) The gas holdup plot for varying gas flow rate at low liquid flow rates

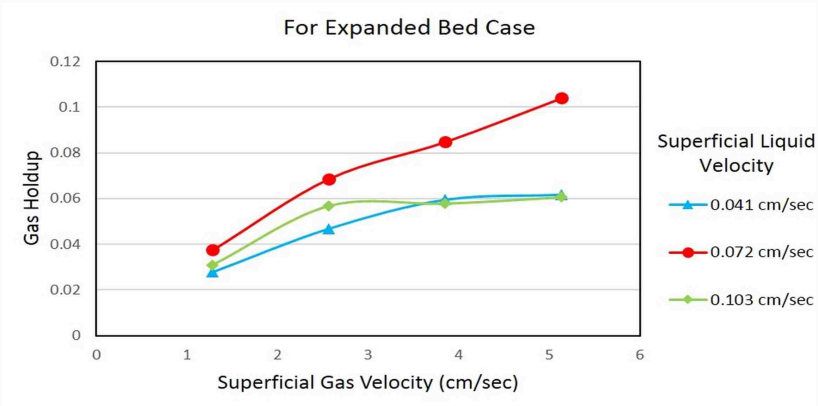

(b) The gas holdup plot for varying gas flow rate at high liquid flow rate

Figure 12. Gas holdup plot for varying flow rate of phases

that with the increase in gas flow rate there is an increase in the gas holdup and with the increase in liquid flow rate there is a decrease in the gas holdup. This behavior is expected in packed bed reactor (Collins *et al.*, 2017), as increasing gas flow rate results in better radial distribution of gas phase (Abdulmohsin and Al-Dahhan, 2016) and thus increasing the residence time of the gas phase, and increased residence time is equivalent to increase in the gas holdup for flowing system. When the liquid flow rate is increased, the gas phase moved out quickly and reduces the residence time hence reduces the gas holdup (Collins *et al.*, 2017).

Figure 12b shows the gas holdup at expanded bed state for varying flow rate of phases. The trend of the gas holdup is increasing with gas flow rate, similar to packed bed case. With the increase in liquid velocity, the trend is fluctuating. On increasing the liquid velocity form 0.0041 cm/sec to 0.072 cm/sec the gas holdp increases, and from increasing the liquid velocity from 0.072 cm/sec to 0.103 cm/sec the gas holdup decreases, this kind of trend is due to the degree of bed expansion. When the flow is increased from 0.0041 cm/sec to 0.072 cm/sec, the bed expands and reduces the solid concentration (Kumar *et al.*, 2012), which in turns increases the gas holdup, as much more voidage is available for gas to distribute. As the bed is in the expanded state, hence, we expected the gas holdup to increase further when the liquid velocity is increased from 0.072 cm/sec to 0.103 cm/sec, but the gas holdup decreased, and it is due to bed behavior shifts more towards the three-phase fluidized bed. At this state the bed is expanded, thus the solids are easily displaced by moving gas phase, and on increasing the gas velocity results in bubble coalescence and movement through least resistance path, which results in increased bubble rise velocity and further reduction in gas holdup [(Kumar *et al.*, 2012), (Jena *et al.*, 2008)].

For hydrotreating purpose, gas to liquid mass transfer on the catalyst surface is the rate-limiting step, and for high utilization of catalyst, high gas holdup at high solid concentration is required, which is observed at scaled down conditions. Based on the results this is occurring at low liquid and high gas flow rate where the bed is behaving as packed bed.

6.3. Effect of Flow Rate of Phases on Peclet Number (Pe) in Catalyst Bed of MBR. Using the D_g and ϵ_g values, Pe is calculated using equation 11. Pe is a dimensionless number which gives the information of the dominance of transport mechanism between bulk flow and dispersive force. Higher the Pe means bulk flow forces dominate the transport, and lower Pe indicate the dispersion dominates flow through the bed. Figure 13a shows the trend of Pe variation for varying flow rate of gas and liquid phase, and at these flow rates, the bed behaves as a packed bed. Figure 13b shows the trend of Pe variation with the

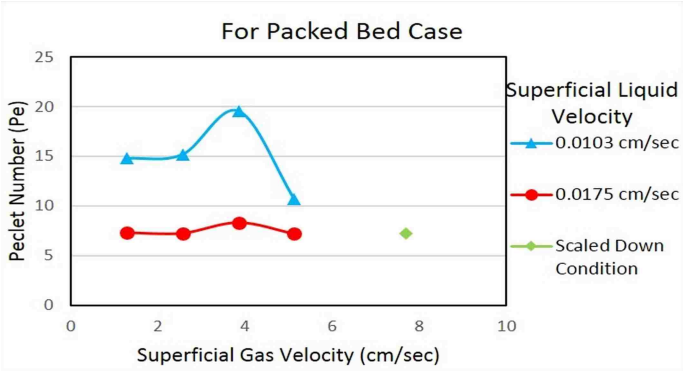

(a) Peclet Number plot for varying flow rate of gas at low liquid flow rate

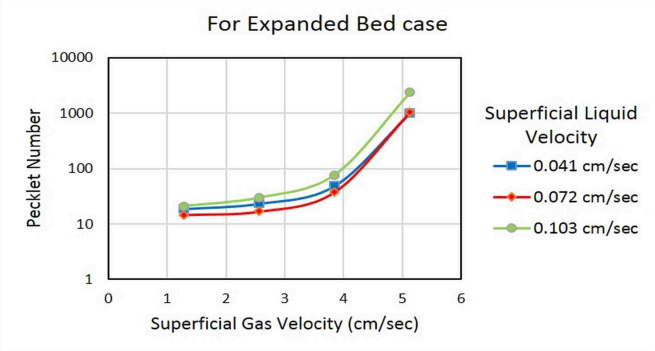

(b) Peclet Number plot for varying flow rate of gas at high liquid flow rate

Figure 13. Peclet number plot for varying flow rate of phases

varying flow rate of gas and liquid phase at which the bed is in the expanded state. Figure 13a trends show that the Pe is not varying much with the increase in gas flow rate and decreases with increase in liquid flow rate. With the increase in gas phase the dispersive forces are increases as observed in Figure 11a, but this increase is due to the convective dispersion component of (D_g). It indicates that at these flow rates the increase in disperse force is proportional to the increase in bulk flow force and making the Pe values almost constant. With the increase in liquid flow rate, the gas dispersion is increased, as observed in Figure 11a and Pe number is also increase (Figure 13). It means at similar gas flow rate for higher liquid flow rate dispersive forces are dominating for gas transport for packed bed case, which increases overall gas dispersion/mixing in the bed. Figure 13b trend shows

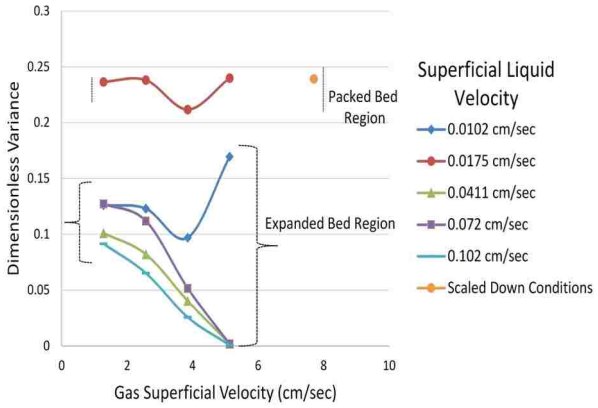

Figure 14. Dimensionless variance of gas phase in the catalyst bed for various flow conditions and scaled down conditions

that with increasing gas flow rate for any liquid flow rate, the Pe increases, which means bulk forces are dominating the transport mechanism. With increases in liquid flow rate, the Pe varies but is again depended on the degree of expansion. Overall as the bed moves towards 3 phase fluidized bed the Pe increases which means reduced dispersion/mixing of gas phase or moving towards plug flow.The results indicate that gas dispersion/mixing is better at packed state for higher liquid flow rate and at the higher gas flow rate. The scaled down conditions (Figure 13a) in terms of mixing is good, as it comes under the purview of packed bed with slight expansion at the top. At these flow rate, the gas mixing is good, but overall gas distribution is largely function of plena and bed packing. To confirm the findings from the results of D_g and Pe. A dimensionless variance (σ_D^2) is calculated for the bed section, which also indicates the dispersion/mixing behavior of phases.

6.4. Effect of Flow Rate of Phases on Dimensionless Number ($\sigma_D{}^2$) in Catalyst Bed of MBR. The dimensionless variance for the catalyst bed section is calculated from the RTDs using it moments (t_m, σ^2), as explained in the section 4.1. If its values is zero then it means the gas movement is in plug flow manner, and if its one then the flow is completely mixed. Figure 14 shows the dimensionless variance in the catalyst bed for various flow condition and at scaled down conditions and it also indicates packed/expanded

bed operating condition. Overall for all the flow condition the values are close to zero, indicating the gas flow is closer to plug flow. As for σ_D^2 less than 0.1 is usually considered to be in plug flow of packed bed reactor (Tang *et al.*, 2004). Relatively, gas dispersion/mixing is more in packed bed region, and in this region increasing liquid velocity and gas velocity increases dispersion/mixing, and in the expanded bed region the flow is moving closer to plug with increase of both gas and liquid velocities. The results are similar to what we observed from the results of Dispersion (Figure 11) and Peclet number (Figure 13). The gas dispersion/mixing is higher in the packed bed region and even for scaled down condition compared to the expanded bed regions.

7. REMARKS

Gas dispersion/mixing has been investigated for the catalyst bed section of the pilot-scale upflow moving bed hydrotreater reactor (MBR), using injection-sampling concept based on multiple injection and detection method, and a mathematical approach of convolution and regression, with appropriate model for catalyst bed and plena proposed by (Han, PhD Thesis, 2007). The catalyst bed is Modeled with Axial Dispersion Model (ADM), with its inlet boundary condition obtained from the Ideal CSTR plus PFR model of plena, these models are assumed first and validated based on the regression. This methodology is successfully implemented in the MBR at the scaled-down experimental condition and various other flow rates of phases.The dispersion plot indicates that at low liquid flow rates the D_g increases with increases in gas flow rate and decreases with increase in liquid flow rate, this trend is observed in packed bed state. At higher liquid flow rates the D_g is decreasing with increase in both gas and liquid flow rate, and this trend is observed in expanded bed state. Pe plot shows that the in packed bed state the flow is relatively dominated by the dispersive forces and in expanded bed state gas flow moves towards plug flow state with the increase in bed expansion. This is confirmed by calculating ${\sigma_D}^2$, which indicate overall the gas phase

flow is towards plug flow, but at expanded bed state the flow is more closer to plug flow. Hence, a good gas mixing is achieved for highest flow condition of phases where the bed expansion is minimum, and that is seen in the scaled-down experimental condition.

REFERENCES

Abdulmohsin, R. S. and Al-Dahhan, M. H., 'Axial dispersion and mixing phenomena of the gas phase in a packed pebble-bed reactor,' Annals of Nuclear Energy, 2016, **88**, pp. 100–111, doi:https://doi.org/10.1016/j.anucene.2015.10.038.

Beg, A., Hassan, M., and Naqvi, M., 'Hydrodynamics and mass transfer in a cocurrent packed column a theoretical study,' Chemical Engineering Journal and the Biochemical Engineering Journal, 93-103, **63**, pp. 1–2, doi:https://doi.org/10.1016/0923-0467(96)03080-1.

Benneker, A. H., Kronberg, A. E., Post, J. W., Van Der Ham, A. G. J., and Westerterp, K. R., 'Axial dispersion in gases flowing through a packed bed at elevated pressures,' Chemical Engineering Science, 1996, **51**(10), pp. 2099–2108, doi:https://doi.org/10.1016/0009-2509(96)00067-X.

Briens, L. A. and Ellis, N., 'Hydrodynamics of three-phase fluidized bed systems examined by statistical, fractal, chaos and wavelet analysis methods,' Chemical Engineering Science, 2005, **60**(22), pp. 6094–6106, doi:https://doi.org/10.1016/j.ces.2005.04.005.

Bruce, E. R., Bruce, E. S., and Parimi, K., 'Gas pocket distributor for hydroprocessing a hydrocarbon feed stream,' US Patent, US5885534A, 1999.

Carleton, A., Flain, R., Rennie, J., and Valentin, F., 'Some properties of a packed bubble column,' Chemical Engineering Science, 1967, **22**(12), pp. 1839 – 1845, doi:https://doi.org/10.1016/0009-2509(67)80214-8.

Collins, J. H. P., Sederman, A. J., Gladden, L. F., Afeworki, M., Douglas Kushnerick, J., and Thomann, H., 'Characterising gas behaviour during gas-liquid co-current up-flow in packed beds using magnetic resonance imaging,' Chemical Engineering Science, 2017, **157**, pp. 2–14, doi:https://doi.org/10.1016/j.ces.2016.04.004.

Danckwerts, P., 'Continuous flow systems: Distribution of residence times,' Chemical Engineering Science, 1953, **2**(1), pp. 1 – 13, doi:https://doi.org/10.1016/0009-2509(53)80001-1.

Delgado, J. M. P. Q., 'A critical review of dispersion in packed beds,' Heat and Mass Transfer/Waerme- und Stoffuebertragung, 2006, **42**(4), pp. 279–310, doi:https://doi.org/10.1007/s00231-005-0019-0.

Edwards, M. and Richardson, J., 'Gas dispersion in packed beds,' Chemical Engineering Science, 1968, **23**(2), pp. 109 – 123, doi:https://doi.org/10.1016/0009-2509(68)87056-3.

Fan, L. S., Bavarian, F., Gorowara, R. L., Kreischer, B. E., Buttke, R. D., and Peck, L. B., 'Hydrodynamics of gas-liquid-solid fluidization under high gas hold-up conditions,' Powder Technology, 1987, **53**(3), pp. 285–293, doi:http://doi.org/10.1016/0032-5910(87)80101-8.

Fogler, H. S., 'Elements of chemcial reaction engineering,' 2005, **4th Edition**.

Gunn, D. J. and Pryce, C., 'Dispersion in Packed Beds,' Trans Inst Chem Eng, 1969, **47**, pp. t341–t350.

Han, L., 'Hydrodynamics and mass transfer in slurry bubble column,' PhD Thesis, 2007.

Iliuta, I., Thyrion, F. C., and Muntean, O., 'Axial dispersion of liquid in gas-liquid cocurrent downflow and upflow fixed-bed reactors with porous particles,' Chemical Engineering Research and Design, 1998, **76**(1), pp. 64–72, doi: https://doi.org/10.1205/026387698524488.

Jena, H. M., Roy, G. K., and Meikap, B. C., 'Prediction of gas holdup in a three-phase fluidized bed from bed pressure drop measurement,' Chemical Engineering Research and Design, 2008, **86**(11), pp. 1301–1308, doi: http://doi.org/10.1016/j.cherd.2008.05.007.

Koh, J. H., Wankat, P. C., and Wang, N. H. L., 'Pore and surface diffusion and bulk-phase mass transfer in packed and fluidized beds,' Industrial and Engineering Chemistry Research, 1998, **37**(1), pp. 228–239.

Kumar, S., Kumar, R. A., Munshi, P., and Khanna, A., 'Gas hold-up in three phase co-current bubble columns,' Procedia Engineering, 2012, **42**, pp. 782–794, doi: https://doi.org/10.1016/j.proeng.2012.07.470.

Levenspiel, O. and Smith, W., 'Notes on the diffusion-type model for the longitudinal mixing of fluids in flow,' Chemical Engineering Science, 1957, **6**(4), pp. 227 – 235, ISSN 0009-2509, doi:https://doi.org/10.1016/0009-2509(57)85021-0.

Midoux, N. and Charpentier, J. C., 'On an experimental method of residence time distribution measurement in the fast flowing phase of a two-phase flow apparatus: Application to gas flow in gas-liquid packed column,' The Chemical Engineering Journal, 1972, **4**(3), pp. 287–290, doi:https://doi.org/10.1016/0300-9467(72)80026-1.

Muroyama, K. and Fan, L.-S., 'Fundamentals of gas-liquid-solid fluidization,' AIChE Journal, 1985, **31**(1), pp. 1–34, doi:https://doi.org/10.1002/aic.690310102.

Pugliese, L., Poulsen, T. G., and Andreasen, R. R., 'Relating Gas Dispersion in Porous Media to Medium Tortuosity and Anisotropy Ratio,' Water, Air, & Soil Pollution, 2012, **223**(7), pp. 4101–4118, doi:https://doi.org/10.1007/s11270-012-1176-7.

Saroha, A. K. and Khera, R., 'Hydrodynamic study of fixed beds with cocurrent upflow and downflow,' Chemical Engineering and Processing: Process Intensification, 2006, **45**(6), pp. 455–460, doi:https://doi.org/10.1016/j.cep.2005.11.005.

Shah, Y. T., Stiegel, G. J., and Sharma, M. M., 'Backmixing in gas-liquid reactors,' AIChE Journal, 1978, **24**(3), pp. 369–400, doi:https://doi.org/10.1002/aic.690240302.

Simcik, M., Ruzicka, M. C., Mota, A., and Teixeira, J. A., 'Smart rtd for multiphase flow systems,' Chemical Engineering Research and Design, 2012, **90**(11), pp. 1739–1749, doi:https://doi.org/10.1016/j.cherd.2012.03.014.

Tang, D., A., J., X., R., B., B., and S., S., 'Axial dispersion and wall effects in narrow fixed bed reactors: A comparative study based on rtd and nmr measurements,' Chemical Engineering & Technology, 2004, **27**(8), pp. 866–873, doi:10.1002/ceat.200402076.

Toukan, A., Alexander, V., Albazzaz, H., and Al-Dahhan, M., 'Identification of flow regime in a cocurrent gas-liquid uplfow moving packed bed reactor using gamma ray densitometry,' Chemical Engineering Science, 2017, **168**, pp. 380–390, doi:https://doi.org/10.1016/j.ces.2017.04.028.

Valenz, L., Rejl, F. J., and Linek, V., 'Gas and liquid axial mixing in the column packed with Mellapak 250Y, Pall rings 25, and intalox saddles 25 under flow conditions prevailing in distillation columns,' Industrial and Engineering Chemistry Research, 2010, **49**(20), pp. 10016–10025, doi:https://doi.org/10.1021/ie101092e.

Yun, J., Yao, S. J., and Lin, D. Q., 'Variation of the local effective axial dispersion coefficient with bed height in expanded beds,' Chemical Engineering Journal, 2005, **109**(1), pp. 123–131, doi:https://doi.org/10.1016/j.cej.2005.03.015.

III. LIQUID PHASE DISPERSION/MIXING INVESTIGATION IN GAS-LIQUID UPFLOW MOVING BED HYDROTREATER REACTOR (MBR) USING DEVELOPED LIQUID TRACER TECHNIQUE AND METHOD BASED ON CONVOLUTION/REGRESSION

Vineet Alexander[1], Hamza Albazzaz[2], Muthanna Al-Dahhan[*,3]

[1,*]Department of Chemical & Biochemical Engineering,

Missouri University of Science and Technology, Rolla, MO-65409

[2]Kuwait Institute for Scientific Research (KISR), Safat, Kuwait

[3]Cihan University, Erbil, Iraq

Email:[1]vaxt8@mst.edu, [*] aldahhanm@mst.edu

ABSTRACT

Liquid phase dispersion/mixing studies have been performed for the first time on the catalyst bed of a cold flow scaled-down upflow moving bed reactor (MBR) using residence time distribution (RTD) at various flow rates including the scaled down condition. MBR is hydrotreater and its design includes catalyst bed with conical bottom and plena. The catalyst bed is modeled using Wave Model, and its mixing parameters are estimated using a mathematical approach based on convolution and regression. A study is also shown to illustrate the limitation of Axial Dispersion Model (ADM) while modeling the flow which noticeably deviates from plug flow. In addition, a dimensionless variance is also estimated for the bed region from the RTDs. Overall liquid dispersion/mixing is seen high in MBR, with more dispersion/mixing in the expanded bed region. Scaled down conditions are seen best when considering the overall catalyst utilization and liquid mixing for hydrotreatment.

Keywords: Residence Time Distribution (RTD), Wave Model (WM), Moving Bed Reactor (MBR), Liquid Tracer, Liquid Dispersion Coefficient, Peclet Number, Axial Dispersion Model (ADM)

1. INTRODUCTION

Gas-Liquid-Solid reactors are widely used for industrial processes and are designed according to the hydrodynamics, heat, and mass transfer requirements of the process (Iliuta *et al.*, 1998). Two-phase upflow fixed bed reactors are used for hydrotreatment applications, as it satisfies the principal design requirement of hydrotreatment process which is to provide desired gas to liquid flow ratio, the low residence time of liquid, better liquid distribution, and fully wetted catalyst along the length of the reactor [(Thanos *et al.*, 2001), (Kressmann *et al.*, 2000)]. Although, the two-phase upflow fixed bed design provides a good working condition for hydrotreatment applications, but it could fail in the proper handling of the hydrocarbon feed with a high level of contaminants. As at hydrotreatment condition of temperature around 400-410°c and pressure of 100-200 bar (Kressmann *et al.*, 2000) the contaminates of crude oil deactivates catalyst fast and results in the frequent shutdown of the reactor for catalyst replacement. Ebullated bed technology, which is upflow gas-liquid over liquid fluidized bed (Kressmann *et al.*, 2000) with provision for catalyst replacement, is used for handling heavier crude oil feed. As the catalyst replacement enables reactor to run continuously without frequent shutdown, but the catalyst activity is less for an economic size of the reactor to handle a higher flow rate of the feed stream, and it is mainly due to the fluidized state of the catalyst bed (Kressmaann, Boyer et al 2000). The new design of catalyst bed with conical bottom called upflow moving bed reactor (MBR) solves issues pertaining to hydrotreatment of heavy crude oil. The peculiarity of MBR is the conical bottom attached to the catalyst bed (Figure 1), which enables the replacement of the catalyst during hydrotreatment operation. The gas-liquid feed stream is fed upflow through the MBR and maintaining the operating conditions to keep bed expansion less than 10 percent by volume

(Kramer *et al.*, 1994). The catalyst deactivates and move downward due to weight and due to removal of catalyst from the conical bottom, and then fresh or regenerated catalyst are added at the top of the bed (Krantz *et al.*, 2002). The replacement operation is not so often, and all the other times the bed behaves as upflow packed or slightly expanded bed condition. At the industrial conditions, this reactor is facing a lot of issues and is undergoing frequent shutdown, and these issues are directly linked with the design of MBR. The successful design can provide proper hydrodynamics, heat and mass transfer of the system (Muroyama and Fan, 1985) and that require predictable models validated with experimentation to lead to the final design at industrial scale. One of the most important design parameters is liquid mixing/dispersion which is never studied for MBR reactor.

Inside the reactor, there is random fluctuation in the movement of the phase which is superimposed on the general flow of the phase, and it is mainly due to the velocity variations and fluctuation due to varying convective force and bulk flow fields along the length of the reactor. This variations and fluctuations is termed as convective dispersion/mixing of any phase and is one of the most critical hydrodynamic phenomena and directly affects mass and heat transport (Westerterp *et al.*, 1995). Hydrotreating is a liquid limited reaction and hence essential to understand the liquid hydrodynamics. Liquid dispersion/mixing is critical design parameter and this information is needed from bench scale/pilot scale experimental setup to scale-up the process to industrial scale (Thanos *et al.*, 2001). The dispersion/mixing is mainly due to velocity variations and fluctuations, and it is difficult to estimate the local velocities along the entire length of the reactor to quantify mixing (Iliuta *et al.*, 1998). The easier way is to conduct residence time distribution studies (RTD) for the region of interest in the reactor. Then fitting with an appropriate model having dispersion/mixing parameters to RTD to estimate the dispersion/mixing parameters. These parameters quantify three-dimensional mixing and dispersion phenomena of liquid in the reactor.

RTD studies for the liquid phase are widely conducted on gas-liquid-solid reactor (Delgado, 2006), but the signals are usually estimated for the entire reactor, where the liquid tracer is injected at the reactor inlet and detected at its outlet. In MBR, the area of interest is the packed bed, and RTD signals are needed for the bed section alone which is accompanied by an additional volume of plena below it and extra space on top of it. The common approach to extract the RTD signal of the bed is to employ detection of tracer below and above the volume of interest [(Edwards and Richardson, 1968), (Valenz *et al.*, 2010)], but due to the complexity of this reactor, injections are done below and top of the bed and detection is done at reactor outlet. The obtained RTDs are followed through a methodology based on convolution and regression with appropriate mass transfer model describing dispersion phenomena. The most widely uses model to explain the dispersion phenomena is Axial Dispersion Model (ADM) (Muroyama and Fan, 1985), and is due to the simplicity of the ADM equation having a single parameter which accounts for the spatial complex velocity and concentration fluctuations inside the reactor (Westerterp *et al.*, 1996). ADM is obtained by superimposing diffusional phenomena on a plug flow and based on the assumption that phase dispersion is analogous to diffusional phenomena (Westerterp *et al.*, 1995). This assumption is not valid for the cases where the velocity and timescale of the dispersion phenomena are much deviating from the time and velocity scale of the diffusion processes (Westerterp *et al.*, 1996). In two-phase packed bed reactors, the dispersion is due to the combination of various factors such as velocity variations and fluctuations (Taylor dispersion), blending and separations due to flow through a tortuous path, mass exchange between stagnant and dynamic zone, molecular diffusion. The time and length scale of all these phenomena are different, and using ADM to find the dispersion phenomena fails in these cases. ADM is fundamentally second order partial diffusion equation, which has the property of infinite signal propagation (Westerterp *et al.*, 1995) which necessitates the condition of applicability of ADM limited to the case of slow temporal and spatial variation of concentration field [(Danckwerts, 1953) (Taylor, 1954)]. This condition is only possible

when the time scale of the transport process is extremely low and moves at infinite speed, which is the case of diffusion [(Westerterp *et al.*, 1995) (Westerterp *et al.*, 1996)]. For the cases, when the spatial concentration change is drastic during the time-scale of transport, such as the case when the system is noticeably deviating from plug flow conditions, ADM fails. A case study is shown in the section 5 below to emphasize this effect.

Many modifications of the ADM is found to account for various dispersion causing factors in packed bed reactor. Like Piston-Exchange Model (PE) model which consider stagnant and dynamic liquid zones without dispersion, Piston-Dispersion-Exchange (PDE) model which accounts Dispersion also (Beg *et al.*, 93-103). These modifications are just adding up additional parameters to fit but not solving the fundamental issue related to partial differential equation infinite signal propagation property which drastically limits the applicability of ADM for the cases of large deviation from plug flow. To account these issue (Westerterp *et al.*, 1995) developed Wave Model (WM).

The proposed wave model by (Westerterp *et al.*, 1995) consists of a set of two hyperbolic equation based on the simple extension of the concept formulated by (Taylor, 1954) for ADM. The one equation is for the concentration change averaged over cross section and other is for the dispersion flux, the equations are shown in the section 4.2. For linear problems, the equation is combined to one-second order partial differential equation, which has an analytical solution. For the normal pulse injection propagation of tracer in an non-reactive system, the analytical solution of Wave Model is in the form of transfer function similar to Gauss Jordan Distribution function (Benneker *et al.*, 1996). The simplicity and overcoming the conceptual difficulties of Partial Differential Equation (PDE) makes WM a best alternative for ADM for the limitations and conditions mentioned above.

In this work, a liquid tracer system is developed for two-phase upflow moving bed reactor (MBR), and RTD studies are conducted based on an injection-sampling concept called two-point injection and one detection method. The obtained RTD are processed by following a methodology based on convolution, regression and Wave Model (for catalyst

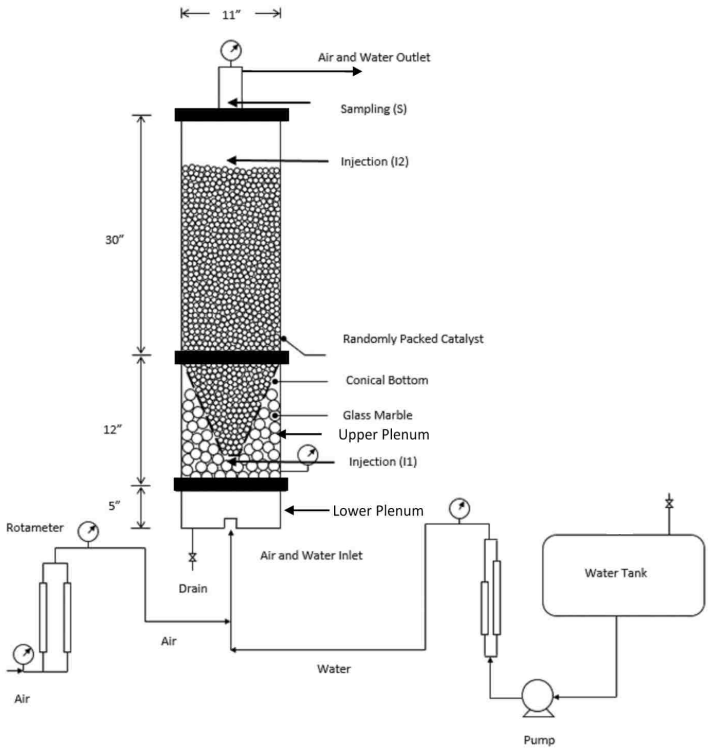

Figure 1. Schematic diagram of scaled down MBR setup for liquid dynamics studies

bed) for estimation of mixing parameter (D_l, Pe) of liquid. The results indicate the liquid mixing is deviating noticeably from plug flow and a case study demonstrates that ADM failed in explaining the flow behavior of liquid in the catalyst bed of MBR. In addition, dimensionless variance (σ_D^2) are estimated for the bed section of MBR, and it also indicates the extent of dispersion/mixing in the bed section. Overall liquid dispersion/mixing is seen higher in MBR, with dispersion/mixing being more in the expanded bed operating conditions.

2. EXPERIMENTAL SETUP

The experimental setup consists of scaled down to pilot plant form industrial scale moving bed reactor based on matching the dynamic and geometric similarity. The dynamic similarity is matched by keeping the pressure drop same through the internal holes for both industrial and pilot scale unit. Pressure drop is calculated for industrial scale at its operating condition and similarly, the pressure drop is estimated at pilot plant scale at the scaled down conditions. The scaled down conditions is determined by matching the LHSV and gas to liquid volumetric flow rate ratio same between industrial and pilot plant scale.

Figure 1 shows the schematic of the pilot scale upflow moving bed reactor (MBR). The design of this reactor is peculiar in terms of its design. It has a catalyst bed with a conical bottom, and plena classified as upper and lower plenum. The lower plenum contains deflector, 19 chimneys attached to the distributor plate in triangular pitch. Upper plenum is the compartment between the conical bottom and upper plenum wall, and this region is tightly packed with passive spheres and above the distributor plate. We conducted cold flow experimentation with gas and liquid phases as air and room temperature water. The gas phase is controlled by rotameter (Dywer-RMC-106-SSV, Dywer-RMC-102-SSV) and the liquid phase by rotameter (Omega FL7301, Omega FL-75C). The flow is set at desired values and fed to the reactor below the bottom plenum in a premixed manner. The phases enter the reactor through the inlet of lower plenum, and it enters to the deflector which has slots on the lateral wall. The phases are pushed out through these slots to move upward to the chimney region. The chimneys are hollow cylindrical pipes having a hole on its wall, these chimneys are screwed to the distributor plate holes, such that the chimney side holes are just below the distributor plate. At scaled down operating condition, the phases coming from the distributor will make a gas pocket formation around the chimney side hole, the liquid will enter through the chimney bottom, and the gas will mix with the incoming liquid phase from the side hole, and mixed phases will be sprayed to the upper plenum. In the upper plenum, the phases will distribute due to the packed spheres, and this mix then moves

to the bed region through the perforations on the conical bottom. Then phases will move upward through the bed region and air-water mix coming at the outlet is sent to the drain, as this mix will contain liquid tracer in it while conducting experimentation, which if recycled will cause calculation error for the methodology described in section 4.

The bed structure can change from upflow packed bed to three-phase fluidized bed based on the flow conditions but for the scaled down operating condition the bed is in the incipient fluidized conditions. At this state, the bed is almost in packed bed with slight expansion at the top part of the bed. In this study, we investigate the impact of flow conditions including the scaled-down conditions on liquid dispersion mixing inside the bed. Table 1 shows the operating conditions and dimensions of the experimental setup.

3. DYNAMIC LIQUID TRACER TECHNIQUE FOR RTD STUDIES OF LIQUID PHASE IN GAS-LIQUID UPFLOW MOVING BED REACTOR

3.1. Dynamic Liquid Tracer Technique. Figure 2 shows the component of the of the dynamic liquid tracer technique. KCL solution is used as the liquid tracer, after trial and error, we found 1.1 M KCL solution is needed for best response with the minimum of KCL for our reactor volume. KCL solution qualifies to be used as tracer as it is non-reactive, completely miscible in the liquid phase, and have the similar physical property of liquid phase (Shah *et al.*, 1978) . The tracer is stored in an in-house developed injection unit having a cylinder and solenoid valve attached to the bottom of the cylinder (Figure 2d). The injection unit is pressurized using nitrogen gas (Figure 2b). The solenoid valve powered to open for the small amount of time using a push button, this provides a pulse injection of tracer inside the reactor. Other types of injection such as step, sinusoidal, ramp, etc. (Shah *et al.*, 1978) can be achieved by programming the solenoid valve opening accordingly. A water pump (Figure 2c) draws the sample out from the outlet and feeds it to the conductivity probe. The Conductivity probe (Figure 2a) is used to detect the tracer concentration. The probe connects to the data acquisition (edaq) and samples the signal at a frequency of

Table 1. Experimental setup specifications and operating conditions for liquid dynamics study

Parameters	Value/Range	Comment
Column Diameter	11 inch	
Column Height	46.46 inch	
Bed Height	24.8 inch	Height from top of the cone to the top of the bed at no flow rate
Catalyst	3 mm Diameter	Bulk Density (570 Kg/m^3)
Liquid (Water) Superficial Velocity	0.01 to 0.4 cm/sec	
Gas (Air) Superficial Velocity	1.28 to 5.13 cm/sec	
Scaled Down Liquid Flow Rate	0.0175 cm/sec	By matching LHSV of industrial and scaled down reactor
Scaled Down Gas Flow Rate	7.7 cm/sec	By matching Gas/liquid volumetric flow rate of industrial and scaled down reactor

25 Hz. The conductivity probe gives linear variation in the voltage signal based on the conductivity of the passing liquid. The KCL solution has higher conductivity than pure water and conductivity is proportional to the concentration of KCL solution, and it is even sensitive to small traces of concentrations of KCL.

3.2. Liquid Tracer System of MBR. The liquid tracer system is shown in Figure 3, the system consists of two injection points (I1 and I2) and one sampling point (S). In our previous work on gas dispersion/mixing studies in upflow moving bed reactor, we used three injection and one detection, the different injection-sampling is due to the usage of different models and way it is solved. The methodology and models used in this study

(a) Conductivity Probe (b) Nitrogen(For Injection Unit

(c) Water Pump (d) Injection Unit

Figure 2. Liquid tracer components

is explained in section 4. Injection points are connected to the injection unit and is the path of entry of tracer into the system. The sampling point (S) is at the outlet of the reactor and above the mixing cup, from where the gas-liquid mix is drawn out and fed to the conductivity probe using the water pump (Figure 2c). The mixing cup provides a uniform concentration cross-sectionally at the sampling plane, which is essential to neglect the effect of small tracer loss at the sampling point. Each injection and sampling point gives the residence time distribution (RTD) of the section in between, Table 2 shows the zones covered by injection-sampling point to measure of the RTD. These assemblies of the injection/sampling are used for a method to obtain mixing parameter of the catalyst bed only and will be discussed later.

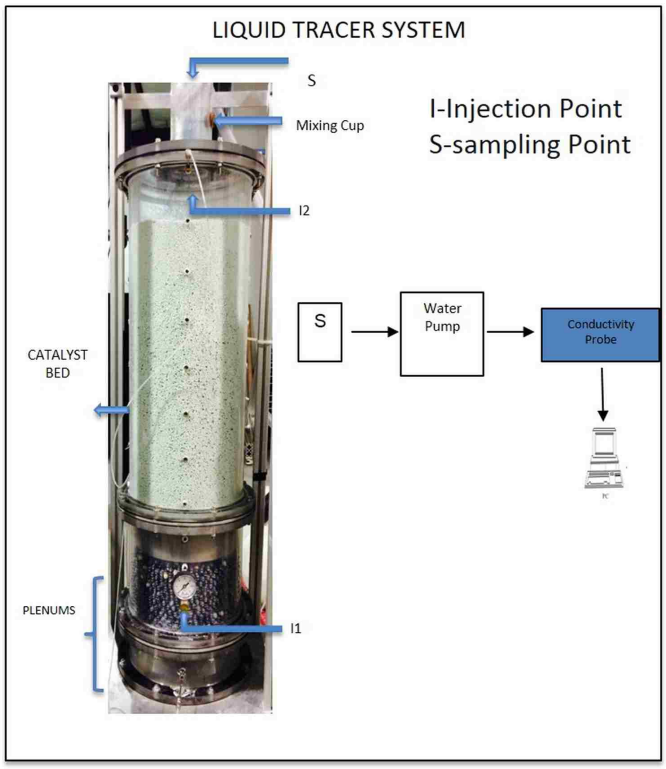

Figure 3. Liquid tracer system of MBR

Signal Processing: The raw time series signal of tracer response is filtered using second-order butterworth filter to remove non-biased noise, such as noise due to electronics (Al-Dahhan *et al.*, 2006). The filtered signal is normalized to a base value of zero by subtracting the signal values of filtered signal with the average signal value of the filtered signal corresponding to the air-water mixture for particular flow without any tracer. Figure 4 shows the tracer response (RTD) for injection I1-S and I2-S, the signal is again normalized to the range of 0 to 1 by dividing with maximum signal values. The shape of the RTD is dependent on the nature of flow and tracer input. For pulse input of tracer, the output response curve will be of gaussian distribution in nature and will be at the extreme of the plug flow (zero dispersion) and CSTR (complete mixing) (Shah *et al.*, 1978).

Table 2. Injection and sampling assembly for liquid dynamics study in MBR

Measurement	Injection	Sampling	Dispersion Zones
C(1)	I1	S	**Zone(1)**: Catalystbed + Upper external Volume + Sampling Line (measurement Volume)
C(2)	I2	S	**Zone(2)**: Upper External Volume + Sampling Line (measurement volume)

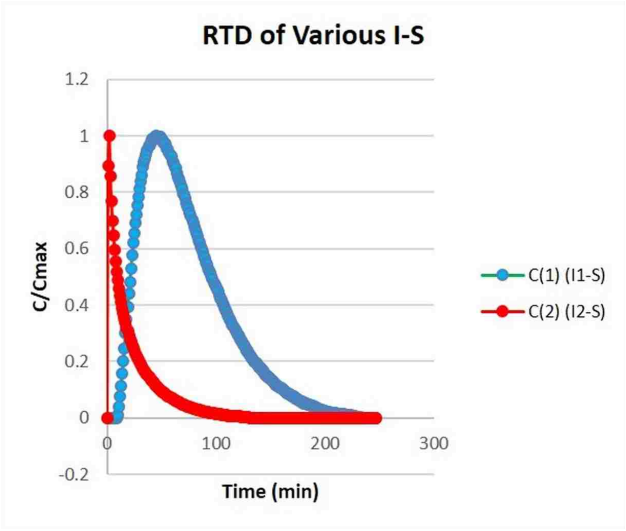

Figure 4. RTD of various injection-sampling at scaled down experimental condition

4. METHODOLOGY TO DETERMINE DISPERSION/MIXING PARAMETER IN CATALYST BED SECTION OF MBR

4.1. Two Injection and One Detection Method. The area of interest is the catalyst bed section, but the catalyst bed is accompanied by additional volumes (Plenums, Upper extra volume, Sampling line) as shown in Figure 3, and to exactly obtain the RTD of the bed section we need to deconvolute the RTD signal from overall signal obtained by I-S (Table

2). Deconvolution is numerically unstable (Han, PhD Thesis, 2007) and to overcome it we follow the methodology of single detection and multiple injection and a mathematical approach of convolution and regression proposed by (Han, PhD Thesis, 2007).

Usually two-point detection method (Cassanello *et al.*, 1992), in which one injection two detection is used to follow the convolution principle. However due to the complexity of the MBR two-point injection and one detection is followed and mathematically both yield similar results (Midoux and Charpentier, 1972). The injection is below (I1) and above (I2) the catalyst bed and the detections is just above the mixing cup as shown in the Figure 1. Using the RTDs obtained from the injection-sampling assembly a systematic approach is followed to obtain the mixing parameters. The catalyst bed section is initially modeled using an axial dispersion model (ADM), but it failed to describe the dispersion/mixing behavior of liquid phase. The conceptual difficulty and explanation of its failure are described as a case study in section 5. In an alternative to ADM, we used a wave model (WM) to describe the liquid phase dispersion/mixing behavior, which overcomes the conceptual deficiencies of ADM.

4.2. Wave Model. Wave Model is an alternative to Fickian-Type dispersion model (ADM), and it overcomes some of the conceptual deficiencies of ADM (Westerterp *et al.*, 1995). It is a hyperbolic system of two first order equations for the average concentration (c) (equation 1) and the dispersion flux (j) (equation 2). For development of model please see (Westerterp *et al.*, 1995).

$$\frac{\partial c}{\partial t} + U\frac{\partial c}{\partial x} + \frac{\partial j}{\partial x} + q(c, x, t) = 0 \tag{1}$$

$$[1 + \tau.q'(c, x, t)]j + \tau\frac{\partial j}{\partial t} + \tau(u + u_a)\frac{\partial j}{\partial x} = -D_e\frac{\partial c}{\partial x} \tag{2}$$

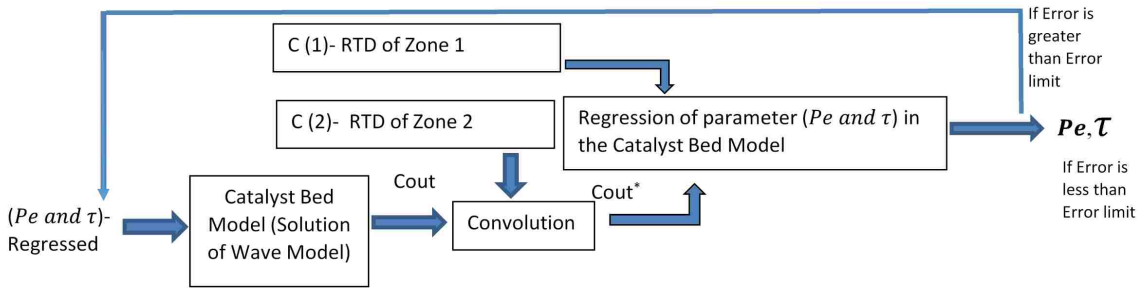

Figure 5. Schematic of convolution and regression approach to obtain liquid mixing parameters of catalyst bed

Where D_e is the Dispersion Coefficient, τ is the Relaxation time, and u_a is the Velocity Assymetry which are the parameters of the wave model. For the case of packed bed with no reaction, unit pulse injection of tracer and for arbitrary boundary condition and considering velocity asymmetry to be zero. The solution of wave model develops to gaussian distribution of the concentration as shown in equation 3.

$$C(t) = \sqrt{\frac{(-Pe * \tau)}{4 * \pi * t}} * \exp[\frac{-Pe * (\tau - t)^2}{4 * t * \tau}] \tag{3}$$

Where as Pe (peclet number) and τ (mean residence time) are the parameters. For detailed derivation of the solution of the wave model refers to (Westerterp *et al.*, 1995) and (Benneker *et al.*, 1996).

$$PecletNumber(Pe) = \frac{U * L}{\epsilon_l * D_L} \tag{4}$$

Essentially the parameter of the solutions are ϵ_l (liquid holdup), D_l (Liquid dispersion), τ is equivalent to t_m (mean residence time), U (superficial velocity), and L (Length of the packed bed) This Gaussian function (Benneker *et al.*, 1996) relates the concentration at one position to that at another location with the degree of longitudinal mixing governed by Pe. This transfer function is used in this study to evaluate liquid behavior in the bed at the flowing conditions by estimating its parameters mentioned above.

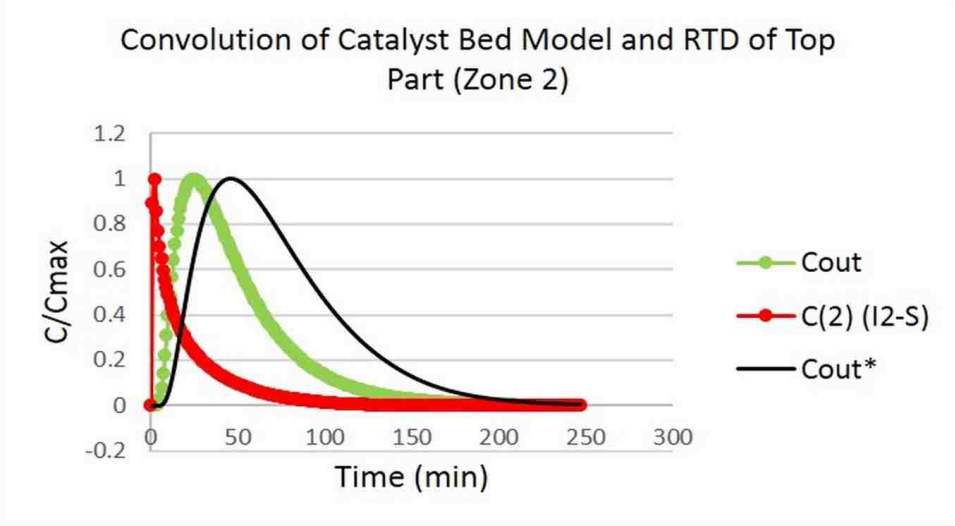

Figure 6. Cout (solution of the wave Model), C(2) (experimental output of zone-2), C_{out^*} (convoluted signal of Cout and Zone-2), at the experimental scaled down conditions

4.3. Convolution and Regression Approach to Estimate Liquid Dispersion Coefficient (D_l) and Peclet Number (Pe) of Liquid Phase in Catalyst Bed Section of MBR.

Pe and τ values are assumed initially and fed into equation 3 and the resulting output C_{out} (Figures 5 and 6) represents the solution for unit pulse input of tracer at the outlet of the catalyst bed. Convolution Principle is applied using equation 5. C_{out} is input to zone-2 and C(2) (Figure 5 and 6) is the experimental response of zone 2. The output C_{out^*} (Figures 5 and 6) represents the output from zone 2 for an inlet response of C_{out} which itself is the outlet of catalyst bed for unit pulse injection. Hence, C_{out^*} is theoretical output of catalyst bed section plus zone-2, which is equivalent to zone 1. It means C_{out^*} is theoretical output of Zone-1.

$$C_{out^*} = \int_0^t C_{out}(t').C_2(t-t').dt' \tag{5}$$

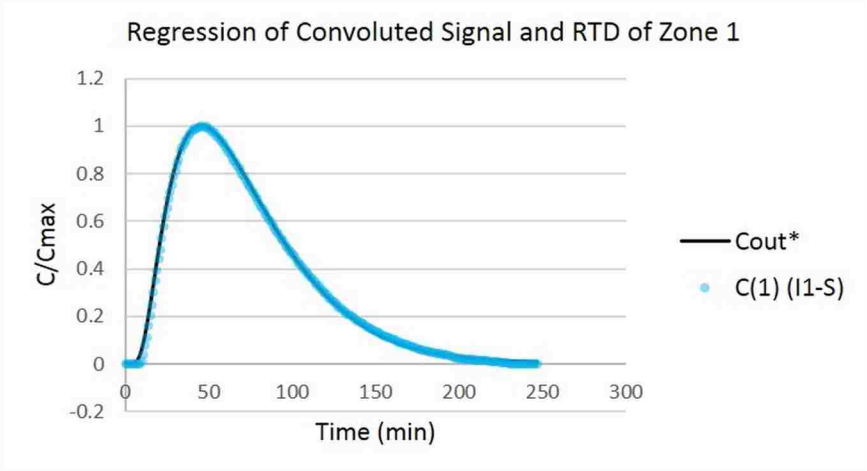

Figure 7. The regression plot for minimum error between convoluted signal (C_{out^*}) and experimental response C(1), at experimental scaled down condition

Estimation of Pe and τ: C(1) (Figure 7) represents the experimental output of zone 1 and C_{out^*} (Figure 7) represents the theoretical output of Zone 1 based on the solution of Wave Model for parameter Pe and τ. $C1$ and C_{out^*} are regressed using equation(6) for minimum error for the values of Pe and τ. These values represent the actual model parameters for equation (3) representing the liquid phase flow behavior inside the catalyst bed.

$$Error = \frac{1}{n}\sum_{j=1}^{n}[C_{out^*}(t_j) - C(1)(t_j)]^2 \tag{6}$$

The minimum averaged sum of square error (equation 6) value for the case shown in Figure 7 is 0.00013, this validates that Wave Model is applicable to quantify liquid flow dynamics in catalyst bed section of MBR. The estimated parameter are Pe=3.78, and τ=32 min.

Estimation of D_l: The D_l is calculated using the equation 4, where the unknown is ϵ_l, and rest of all the quantities are known. ϵ_l can be estimated using the equation 7 and equation 9 based on RTD response (Kressmann *et al.*, 2000).

$$\epsilon_{l1} = \frac{V_L}{X} * t_{m1} \tag{7}$$

Where ϵ_{l1} is the liquid holdup of zone1, V_L is the superficial liquid velocity based on empty column, X is the linear distance of zone 1, and t_{m1} is the mean residence time calculated using equation 8 for the RTD of Zone 1 (C(1)).

$$t_{m1} = \frac{\int C(1).t}{\int C(1)} \tag{8}$$

$$\epsilon_{l2} = \frac{V_L}{Y} * t_{m2} \tag{9}$$

Where ϵ_{l2} is the Liquid holdup of zone-2, V_L is the superficial liquid velocity based on empty column, Y is the linear distance of zone-2, and t_{m2} is the mean residence time calculated using equation 10 for the RTD of zone-2 (C(2)).

$$t_{m2} = \frac{\int C(2).t}{\int C(2)} \tag{10}$$

now using the equation

$$\epsilon_L = \frac{Volume of Liquid in Bed}{Volume of Bed} = \frac{\epsilon_{L1} * V_{zone1} - \epsilon_{L2} * V_{zone2}}{V_{catalyst bed}} \tag{11}$$

In equation 11, all the terms (ϵ_{l1}, ϵ_{l2}) are known from equation 7 and equation 9, and V_{zone1}, V_{zone2}, and $V_{catalyst bed}$ are known from reactor geometry. The estimated D_l = 0.0065 m^2/min for the experimental scaled down condition.

5. CASE STUDY TO SHOW FAILURE OF ADM

The methodology shown in section 4 is applied with replacing the model of catalyst bed with Axial Dispersion Model (ADM) for Dirac delta input as shown in Figure 8.

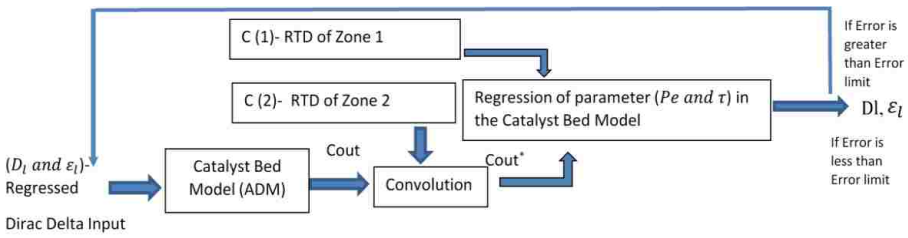

Figure 8. Schematic of convolution and regression approach using ADM model for catalyst bed

C_{out} is the solution of the ADM which is input to the zone-3. The same convolution principle of equation (5) is applied and C_{out^*} is obtained. The C_{out^*} represents the theoretical output of zone-1 and C(1) represents the experimental output of zone-1. The C_{out^*} and C(1) are regressed for D_l and ϵ_l for minimum error using the equation 6.

$$\frac{\partial C_L}{\partial t} = D_l \frac{\partial^2 C_L}{\partial Z^2} - \frac{U_L}{\epsilon_L} \frac{\partial C_L}{\partial Z} \tag{12}$$

Boundary Conditions:

$$Z = 0, U_g.C_{in} = U_L.C_L|_{z=0} - D_l \frac{\partial C_L}{\partial Z}|_{z=0} \tag{13}$$

$$Z = L, \frac{\partial C_L}{\partial z}|_{z=L} = 0 \tag{14}$$

Figure 9 shows the regression plot for the theoretical output using ADM and Experimental Output of RTD for Zone-1. The plots show the best regression possible for least error of 0.125. The least error is much higher than the tolerance limit for good fit (max error of 0.005), whereas using Wave Model for same operating conditions, the error was 0.00035 within the tolerance (Figure 7). This indicates, ADM is not a suitable model for liquid phase dispersion studies in catalyst bed section of this reactor. On carefully analyzing the Figure 9, one can see that theoretical output has signal value at a time from (0 min), whereas for the experimental output, the first signal value is at (3min), This is the primary reason for

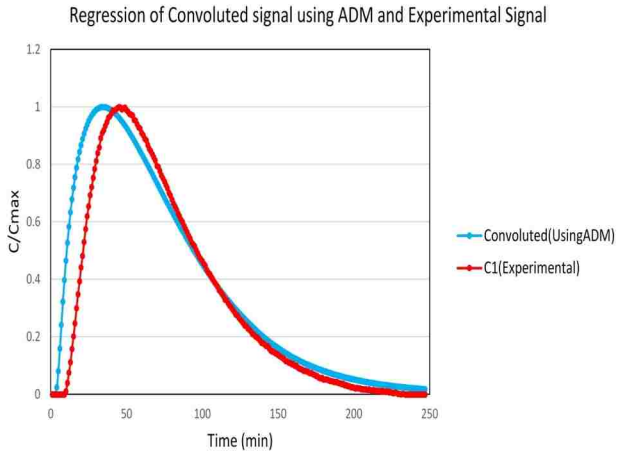

Figure 9. The regression plot for minimum error between convoluted signal (using ADM) and experimental response C(1), at scaled down experimental conditions

the non-fit condition between theoretical and experimental output. Why theoretical output generates a signal at zero time is due to the fundamental nature of ADM equation. ADM is second order parabolic differential equation, and the solution of these equations have an infinite speed of signal propagation, which means instantaneous signal (concentration) at all the modeling space with the intensity proportional to dispersion coefficient (Westerterp *et al.*, 1995). ADM can be better understood by focusing on ficks law, based on which ADM is conceived.

(Westerterp *et al.*, 1996) analyzed the ficks law for diffusional phenomena at particle level scrutiny and found that, to hold ficks law, the time taken (relaxation time) for random particle movement (mean free path) shall approach zero. Hence, the velocity scale (mean free path/relaxation time) of diffusional transport shall approach infinity. Hence, ADM is applicable for the cases when these conditions are fulfilled or not much deviating from it, or it is only properly applicable for the case of molecular diffusion, as infinite velocity scale of molecular diffusion justifies physically the ADM behavior of infinite signal propagation (Iordanidis *et al.*, 2003). The cases, such the flow of gas phases, the relaxation time of particle movement is very slow to the order of (10^{-10} to 10^{-11} sec) which is comparable with

the diffusional time scale, and hence ADM is applicable for gas phase with a reasonable level of accuracy (Westerterp *et al.*, 1995). The liquid phase flow has a time scale of particle movement higher than the diffusional phenomena and hence not reasonable to use ADM to find dispersion phenomena.

6. DIMENSIONLESS VARIANCE (TANK IN SERIES)

Tank in series is a one parameter model and are used to describe non-ideal reactors. In this modeling concept, n tanks are modeled as ideal CSTR in series for pulse injection of tracer. The Residence Time Distribution (RTD) obtained from the model is matched with experimental RTD of non-ideal reactor by varying n. Larger the value of n indicating the flow is towards plug flow and lower means the flow is towards CSTR. (Fogler, 2005) showed that equation 15 is the generalized RTD for n tank modeled as ideal CSTR in series.

$$E(t) = \frac{t^n}{(n-1)!\tau_i^n} e^{-t/\tau_i} \tag{15}$$

Where τ_i is the means residence time in single tank, n is the number of tank, and τ_i is equal to τ/n, and τ is mean residence time of entire reactor. Equation 15 is converted to dimensionless form $E(\theta)$ as shown in Equation 16.

$$E(\theta) = \tau E(\theta) = \frac{n(n\theta)^{n-1}}{(n-1)!} e^{-n\theta} \tag{16}$$

Where θ is the ratio of t and τ. The variance of equation 16 can be found using equation 17, which is called dimensionless variance (σ_D^2), and this dimensionless variance is equal to the ratio of variance (σ^2) and square of mean residence time (t_m).

$$\sigma_D^2 = \frac{\sigma^2}{{t_m}^2} = \int_0^\infty (\theta - 1)^2 E(\theta) d\theta \tag{17}$$

(Fogler, 2005) showed the solution of equation 17 is equal to the inverse of number of tanks (n), as shown in equation 18.

This indicates if σ_D^2 is zero then the flow is towards the plug flow as n tends to infinite ideal CSTR in series, and when σ_D^2 approaches one the flow is towards complete mixing as n tends to one ideal CSTR . Dimensionless variance can be determined by RTD experiments, as it is the ratio of variance (σ^2) (second moment) and square of mean residence time (t_m) (first moment).

$$\sigma_D^2 = \frac{\sigma^2}{{t_m}^2} = \frac{1}{n} \tag{18}$$

$$MeanResidenceTime(t_m) = \int_0^\infty E(t)t\,dt \tag{19}$$

$$Variance(\sigma^2) = \int_0^\infty (t - t_m)^2 E(t)dt \tag{20}$$

In our case, the area of interest is packed bed region, and its dimensionless variance is evaluated by finding the variance of RTD of zone 1 (t_{m1}) (Figure 4 and Table 2) and RTD of zone 2 (t_{m2}) (Figure 4 and Table 2) using the equation 19 and similarly the variance (σ_1^2 and σ_2^2) using equation 20. Volume of Zone 1 minus volume of zone 2 gives volume of bed , and as these moments are additive the bed variance will ($\sigma_1^2 - \sigma_2^2$) and mean residence time in the bed will be ($t_{m1} - t_{m2}$). Hence the σ_D^2 is calculated using equation 21.

$$\sigma_D^2(Bed) = \frac{(\sigma_1^2 - \sigma_2^2)}{(t_{m1} - t_{m2})^2} \tag{21}$$

Equation 21 shows the dimensionless variance of the liquid phase in catalyst bed region and for scaled down experimental condition (Table 1), σ_D^2 is 0.331.

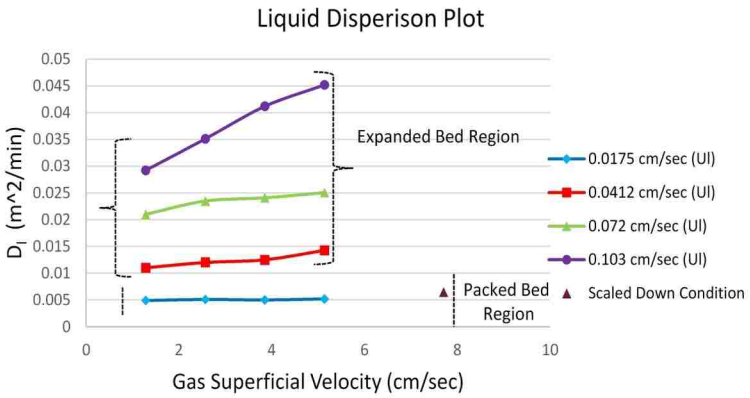

Figure 10. The liquid dispersion in the catalyst bed of MBR for varying flow rate of phases

7. RESULTS AND DISCUSSION

The evaluated wave model (WM) parameters are liquid dispersion coefficient (D_l) and Peclet number (Pe). In addition, dimensionless variance (σ_D^2) in the bed region is evaluated. These parameters estimate the extent of mixing of liquid phase in catalyst bed section of this reactor. The effect of operating conditions on these parameters are investigated.

7.1. Effect of Operating Condition on Dispersion Inside the Catalyst Bed Section of MBR. The physical representation of D_l is the quantification of the spread of tracer signal in the catalyst bed section. The spreading is dependent on diffusive nature of tracer and spread occurring due to the external force field which is dependent on the flow condition. Hence, the dispersion coefficient (D_l) can be represented as the summation of molecular diffusivity and dispersion due to convective term (Delgado, 2006). Any non-ideality in the flow is reflected in the convective dispersion term. The primary source of non-ideality for liquid flow in two-phase upflow packed or expanded bed are due to non-uniform velocity profile, by passing streams of phases, velocity fluctuations due to turbulence, backflow of liquid due to velocity difference with gas phase, non-uniform flow pattern of gas phase in bed, mass transfer between dynamic and stagnant liquid zones (Iliuta *et al.*, 1996). All

these non-idealities are a function of reactor design, bed structure and operating condition of phases. Figure 10 shows the effect of gas and liquid superficial velocity on the liquid dispersion in the catalyst bed packing of this reactor. Based on the operating condition the bed structure changes form packed bed to expanded. The previous study of (Article 2) indicates that for liquid flow rate (0.0175 cm/sec) and varying gas flow rate from (1 to 7 cm/sec), the bed is in packed condition, with slight expansion at the top for scaled down conditions (Table 1). For the rest of all the operating conditions the bed starts to expand, and its extent depends on flow condition. The dispersion trend of liquid is seen different for the packed bed and expanded bed case. In packed bed case (Figure 10) the liquid dispersion is not changing significantly with increasing flow rate of gas and the same observed by (Valenz *et al.*, 2010). In packed bed region with increase in gas flow the bubble breakup phenomena increases and moves upwards as small bubbles, these small rising bubbles cause less dispersion/mixing in liquid (Belfares *et al.*, 2001). Other main criteria which can induce non-ideality or increased spreading of liquid are liquid flow rates and bed structure, where the bed structure is not much changing for all the operating condition in packed bed case. In expanded bed case the situation changes as the bed structure changes with operating conditions.

The operating region of expanded bed is shown in Figure 10. In this region, the bed starts to expands and moves toward three phase fluidization. It is seen that for all liquid flow rates the liquid dispersion coefficient (D_l) is increasing with increase in gas flow rate. A similar trend is observed by (Muroyama and Fan, 1985) for three-phase fluidized bed. It is also seen that D_l increases with increase in liquid flow rate and the increasing effect with respect to increase in the gas flow is greater for higher liquid flow rates. The extent of the bed expansion is proportional to the increase in the flow rate of phases for MBR (Article-2). With increasing liquid flow rate the bed expansion increases which result in increase liquid spreading induced by moving solids. In expanded bed, with increasing gas flow rate results in bubble coalescence, channeling and random flow distribution of gas phase along

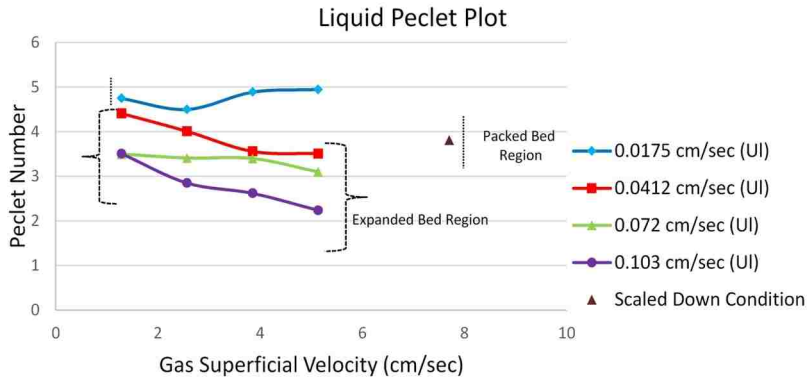

Figure 11. The liquid peclet number in catalyst bed of MBR for varying flow rate of phases

the bed, which increases the bubble-induced turbulence and macro recirculation of liquid phase (Muroyama and Fan, 1985). These phenomena increase dispersion of liquid phase in expanded bed region. From the results, it is indicative that the liquid dispersion is a strong function of flow rate of phases and its effect is intense for a higher flow rate of phases. Although this gives good trend to understand the dispersive nature but to identify nature of flow such as pulse flow or completely mixed, a peclet number is needed. As the calculated D_l is proportional to the convective component of liquid phase flow, and its increase will result in increasing trend of D_l, but it does not mean the flow is moving toward completely mixed flow. Hence, the comparison of bulk flow field with dispersive force field is done by finding the peclet number (Pe).

7.2. Effect of Operating Conditions on Peclet Number Inside the Catalyst Bed Section of MBR. Peclet (Pe) number is calculated using the equation 4, and it indicates whether advective or dispersive field dominates the nature of the flow. Higher the Pe, flow is towards the plug flow, and for lower Pe the flow is towards complete mixing. Figure 11 shows the peclet number plot for the liquid phase for the varying flow rate of phases. The plot shows that for both packed bed and expanded bed region, the Pe number is decreasing with increasing flow rate of gas phase and liquid phase, the decrease of Pe with increasing

gas flow rate is more significant at higher liquid flow rates. For packed and slightly expanded bed cases the Pe for liquid is seen to decrease with gas flow rate [(Thanos *et al.*, 2001), (Cassanello *et al.*, 1992), (Xie *et al.*, 2013), (Iliuta *et al.*, 1998)]. The small values of the peclet number clearly indicate that liquid phase non-ideality is quite significant and largely deviating from the plug flow [(Delgado, 2006), (Abdulmohsin and Al-Dahhan, 2016)]. These non-idealities are much dominant in expanded bed case, and is seen to be increasing function with bed expansion.

As the bed expands, dispersion of liquid phase increases as explained in the section 7.1. At expanded bed conditions the bubble coalescence and other maldistribution and catalyst particle movement is observed. These movement creates a force field for micro and macro recirculation zones in the bed for liquid phase (Saroha and Khera, 2006). These recirculations increases the residence time of the liquid phase and results in dominance of dispersive forces compared to convective. The dispersive forces are directly linked with hydrodynamics mixing which includes backmixing and thus decreases Pe with increasing liquid flow rate. For MBR at the hydrotreating condition, the condition of low bed expansion is preferable for maximum catalyst utilization (Kramer *et al.*, 1994). In terms of liquid mixing the scaled down conditions are suitable, as based on its low Pe value the mixing is already quite good. Pe gives a good indication of mixing phenomena in the bed, but additionally, dimensionless variance (σ_D^2) is evaluated using the moments of experimental RTDs, as this parameter is also indicates the degree of dispersion/mixing.

7.3. Effect of Operating Conditions on Dimensionless Variance Inside the Catalyst Bed Section of MBR. The dimensionless variance (σ_D^2) indicates the degree of dispersion/mixing in the reactor. The procedure to calculate σ_D^2 is shown in section 6. If the values of σ_D^2 is zero it indicates the flow is in plug flow and if its one then flow is completely mixed. Figure 12 shows the dimensionless variance plot for varying flow rate of phases and at scaled down conditions. The results indicates similar dispersion/mixing behavior of liquid phase in the bed as we observed with peclet plot (Figure 11). For packed bed

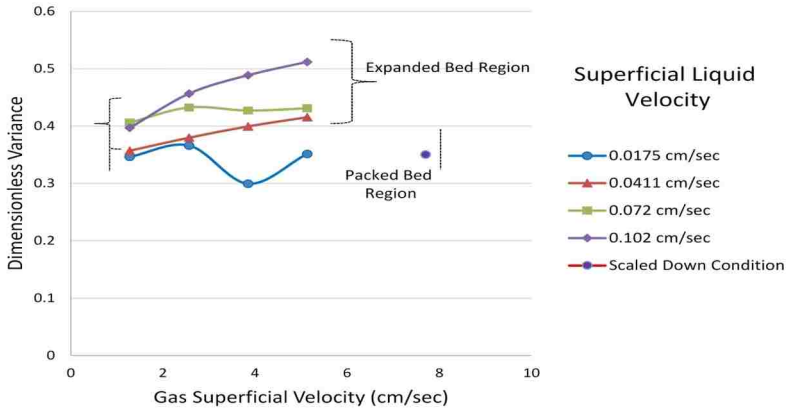

Figure 12. The liquid dimensionless variance in catalyst bed of MBR for varying flow rate of phases

the σ_D^2 is slightly increases with gas velocity, indicating gas phase doesnt have significant effect on liquid dispersion/mixing at these conditions. At expanded bed condition the σ_D^2 is increasing with increasing flow rate of both the phases. This indicates the dispersion or mixing is increasing and going towards complete mixing in the expanded bed case and is a direct function of bed expansion. The value of σ_D^2 is in the range of 0.3 to 0.52 indicating noticeable deviation from plug flow behavior, as σ_D^2 value of around 0.1 or less is considered to be in plug flow (Tang *et al.*, 2004). Scaled down experimental condition shows a σ_D^2 value of 0.33 showing high dispersion/mixing of liquid phase at these conditions, and at these conditions the bed behaves as upflow packed with slight expansion, which is needed for better catalyst utilization.

8. REMARKS

Liquid phase dispersion/mixing is successfully investigated for the first time in the catalyst bed of upflow moving bed reactor (MBR) using residence time distribution (RTD) studies. The catalyst bed is modeled using Wave Model (WM), and its dispersion or mixing parameters (D_l and Pe) are estimated using a mathematical approach based

on convolution and regression. A case study is also shown to illustrate the limitation of Axial Dispersion Model (ADM) for modeling the liquid phase flow behavior in MBR. In addition, a dimensionless variance (σ_D^2) in the bed section is estimated using the first moment (t_m) and second moment (σ^2) of the experimental RTD. The D_l result indicates the liquid dispersion is not much affected by the increase in gas flow rate in packed bed region, but in expanded bed regions D_l increases with increasing flow rate of both the phases and is due to the increase in bed expansion with flow rate. Pe and σ_D^2 showed that overall liquid dispersion/mixing is higher in MBR for all the operating conditions studied, but mixing/dispersion is more in expanded bed and increases with bed expansion. The value of Pe and σ_D^2 also indicates that the liquid flow is noticeably deviating from plug flow and moving towards completely mixing with bed expansion. For hydrotreatment application in MBR, scaled down conditions are preferable, as the Pe and σ_D^2 indicates high liquid mixing, and moreover, at these conditions, the bed behavior is in upflow packed with slight expansion at the top, which is a necessary condition for good catalyst utilization.

REFERENCES

Abdulmohsin, R. S. and Al-Dahhan, M. H., 'Axial dispersion and mixing phenomena of the gas phase in a packed pebble-bed reactor,' Annals of Nuclear Energy, 2016, **88**, pp. 100–111, doi:https://doi.org/10.1016/j.anucene.2015.10.038.

Al-Dahhan, M. H., Mills, P. L., Gupta, P., Han, L., Dudukovic, M. P., Leib, T. M., and Lerou, J. J., 'Liquid-phase tracer responses in a cold-flow counter-current trayed bubble column from conductivity probe measurements,' Chemical Engineering and Processing: Process Intensification, 2006, **45**(11), pp. 945–953, doi: https://doi.org/10.1016/j.cep.2006.01.011.

Beg, A., Hassan, M., and Naqvi, M., 'Hydrodynamics and mass transfer in a cocurrent packed column a theoretical study,' Chemical Engineering Journal and the Biochemical Engineering Journal, 93-103, **63**, pp. 1–2, doi:https://doi.org/10.1016/0923-0467(96)03080-1.

Belfares, L., Cassanello, M., Grandjean, B. P. A., and Larachi, F., 'Liquid back-mixing in packed-bubble column reactors: A state-of-the-art correlation,' Catalysis Today, 2001, **64**(3-4), pp. 321–332, doi:https://doi.org/10.1016/S0920-5861(00)00535-6.

Benneker, A. H., Kronberg, A. E., Post, J. W., Van Der Ham, A. G. J., and Westerterp, K. R., 'Axial dispersion in gases flowing through a packed bed at elevated pressures,' Chemical Engineering Science, 1996, **51**(10), pp. 2099–2108, doi: https://doi.org/10.1016/0009-2509(96)00067-X.

Cassanello, M. C., Martinez, O. M., and Cukierman, A. L., 'Effect of the liquid axial dispersion on the behavior of fixed bed three phase reactors,' Chemical Engineering Science, 1992, **47**(13-14), pp. 3331–3338, doi:https://doi.org/10.1016/0009-2509(92)85042-A.

Danckwerts, P., 'Continuous flow systems: Distribution of residence times,' Chemical Engineering Science, 1953, **2**(1), pp. 1 – 13, doi:https://doi.org/10.1016/0009-2509(53)80001-1.

Delgado, J. M. P. Q., 'A critical review of dispersion in packed beds,' Heat and Mass Transfer/Waerme- und Stoffuebertragung, 2006, **42**(4), pp. 279–310, doi: https://doi.org/10.1007/s00231-005-0019-0.

Edwards, M. and Richardson, J., 'Gas dispersion in packed beds,' Chemical Engineering Science, 1968, **23**(2), pp. 109 – 123, doi:https://doi.org/10.1016/0009-2509(68)87056-3.

Fogler, H. S., 'Elements of chemcial reaction engineering,' 2005, **4th Edition**.

Han, L., 'Hydrodynamics and mass transfer in slurry bubble column,' PhD Thesis, 2007.

Iliuta, I., Thyrion, F. C., and Muntean, O., 'Hydrodynamic characteristics of two-phase flow through fixed beds: Air/newtonian and non-newtonian liquids,' Chemical Engineering Science, 1996, **51**(22), pp. 4987–4995, doi:https://doi.org/10.1016/0009-2509(96)00331-4.

Iliuta, I., Thyrion, F. C., and Muntean, O., 'Axial dispersion of liquid in gas-liquid cocurrent downflow and upflow fixed-bed reactors with porous particles,' Chemical Engineering Research and Design, 1998, **76**(1), pp. 64–72, doi: https://doi.org/10.1205/026387698524488.

Iordanidis, A. A., van Sint Annaland, M., Kronberg, A. E., and Kuipers, J. A. M., 'A critical comparison between the wave model and the standard dispersion model,' Chemical Engineering Science, 2003, **58**(13), pp. 2785–2795, doi: https://doi.org/10.1016/S0009-2509(03)00151-9.

Kramer, D. C., Stangeland, B. E., Smith, D. S., McCall, J. T., Scheuerman, G. L., and Bachtel, R. W., 'Apparatus for an on-stream particle replacement system for countercurrent contact of a gas and liquid feed stream with a packed bed,' US Patent, US5302357A, 1994.

Krantz, W. B., Earls, D. E., Trimble, H. J., Chabot, J., and Parimi, K., 'Balanced flow resistance OCR distributor cone,' US Patent, US6387334B1, 2002.

Kressmann, S., Boyer, C., Colyar, J. J., Schweitzer, J. M., and Viguie, J. C., 'Improvements of ebullated-bed technology for upgrading heavy oils,' Oil and Gas Science and Technology, 2000, **55**(4), pp. 397–406, doi:https://doi.org/10.2516/ogst:2000028.

Midoux, N. and Charpentier, J. C., 'On an experimental method of residence time distribution measurement in the fast flowing phase of a two-phase flow apparatus: Application to gas flow in gas-liquid packed column,' The Chemical Engineering Journal, 1972, **4**(3), pp. 287–290, doi:https://doi.org/10.1016/0300-9467(72)80026-1.

Muroyama, K. and Fan, L.-S., 'Fundamentals of gas-liquid-solid fluidization,' AIChE Journal, 1985, **31**(1), pp. 1–34, doi:https://doi.org/10.1002/aic.690310102.

Saroha, A. K. and Khera, R., 'Hydrodynamic study of fixed beds with cocurrent upflow and downflow,' Chemical Engineering and Processing: Process Intensification, 2006, **45**(6), pp. 455–460, doi:https://doi.org/10.1016/j.cep.2005.11.005.

Shah, Y. T., Stiegel, G. J., and Sharma, M. M., 'Backmixing in gas-liquid reactors,' AIChE Journal, 1978, **24**(3), pp. 369–400, doi:https://doi.org/10.1002/aic.690240302.

Tang, D., A., J., X., R., B., B., and S., S., 'Axial dispersion and wall effects in narrow fixed bed reactors: A comparative study based on rtd and nmr measurements,' Chemical Engineering & Technology, 2004, **27**(8), pp. 866–873, doi:10.1002/ceat.200402076.

Taylor, G. I., 'Diffusion and mass transport in tubes,' Proceedings of the Physical Society. Section B, 1954, **67**(12), p. 857.

Thanos, A. M., Galtier, P. A., and Papayannakos, N. G., 'Liquid dispersion and holdup in a small-scale upflow hydrotreater at high temperatures and pressure,' Chemical Engineering Science, 2001, **56**(2), pp. 693–698, doi:https://doi.org/10.1016/S0009-2509(00)00277-3.

Valenz, L., Rejl, F. J., and Linek, V., 'Gas and liquid axial mixing in the column packed with Mellapak 250Y, Pall rings 25, and intalox saddles 25 under flow conditions prevailing in distillation columns,' Industrial and Engineering Chemistry Research, 2010, **49**(20), pp. 10016–10025, doi:https://doi.org/10.1021/ie101092e.

Westerterp, K. R., Dil'man, V. V., and Kronberg, A. E., 'Wave model for longitudinal dispersion: Development of the model,' AIChE Journal, 1995, **41**(9), pp. 2013–2028, doi:https://doi.org/10.1002/aic.690410902.

Westerterp, K. R., Kronberg, A. E., Benneker, A. H., and Dil'man, V. V., 'Wave concept in the theory of hydrodynamical dispersion a Maxwellian type approach,' Chemical Engineering Research and Design, 1996, **74**(8), pp. 944–952, doi:https://doi.org/10.1205/026387696523111.

Xie, L., Li, Z., and Liu, H., 'Axial dispersion and pressure drop of a slightly expanded bed reactor,' Beijing Huagong Daxue Xuebao (Ziran Kexueban)/Journal of Beijing University of Chemical Technology (Natural Science Edition), 2013, **40**(4), pp. 1–7.

IV. PHASE MASS DISTRIBUTION BASED PERFORMANCE EVALUATION OF LOWER PLENUM OF UPFLOW MOVING BED HYDROTREATER REACTOR (MBR) AND PROPOSAL OF AN IMPROVED DESIGN USING CFD

Vineet Alexander[1], Premkumar Kamalanathan[2], Hamza Albazzaz[3], Muthanna Al-Dahhan[*,4]

[1,2*]Department of Chemical & Biochemical Engineering,

Missouri University of Science and Technology, Rolla, MO-65409

[3]Kuwait Institute for Scientific Research (KISR), Safat, Kuwait

[4]Cihan University, Erbil, Iraq

Email:[1]vaxt8@mst.edu, [*] aldahhanm@mst.edu

ABSTRACT

Upflow Moving Bed Hydrotreater Reactor (MBR) is used in hydroprocessing to remove metal impurities from the crude oil. The reactor at industrial scale is facing issues such as coking and catalyst agglomeration in its catalyst bed, and these issues are directly linked to the maldistribution of phases in the bed. Maldistribution itself is connected with the performance of lower plenum of MBR in term of distribution of phases uniformly. In this study, a 3-D axisymmetric Euler-Euler CFD simulation is performed on the lower plenum of a pilot-scale MBR, at industrial scaled down conditions. The results indicate that the current design of lower plenum is not performing well, as uneven phase mass distribution is seen through its outlets. A modified design is proposed for the lower plenum and its CFD simulation shows improved performance in terms of uniform phase mass distribution through the outlets.

Keywords: CFD, Moving Bed Reactor (MBR), Bubble Column, Lower Plenum

1. INTRODUCTION

Upflow moving bed reactor (MBR) is a hydrotreater and is a new technology in guard reactor for hydrotreatment process. MBR is usually placed before the fixed bed residual desulfurization process (RDS), as this reactor hydrotreates to remove heavy metal from ressidum oil. These metals can reduce the life cycle of RDS process, and hence MBR guard RDS from these metal impurities [(Kramer *et al.*, 1994), (Scheuerman *et al.*, 1993)]. MBR has a peculiar design as it has a catalyst bed with a conical bottom and upstream to the bed is plena, which can be classified as lower plenum and upper plenum by. In MBR, hydrogen and ressidum oil flows in a concurrent upward direction, it enters the lower plenum by a deflector that has holes to spread the mixture of gas and liquid. At the top of the lower plenum is the gas-liquid distributor that has complex internals to distribute the gas and liquid to the upper plenum. The uppper plenum is packed bed type of distributor having inert spheres to feed the phases to the catalyst bed through the conical bottom having perforation small enough to avoid catalyst plugging.

At the industrial scale, this reactor is not performing at its best, and it is facing drastic issues such as coke formation, catalyst agglomeration inside the catalyst packing of this reactor, and this leads to the frequent shutdown of MBR itself. Which in turns affect the overall hydrotreatment processes. Our previous studies conducted on the pilot scale reactor of MBR using a two-tip optical probe to investigate local hydrodynamics, shows a maldistributed state of the bed at the scaled down industrial condition. We observed various locations inside the catalyst bed having liquid and gas derived region. At hydrotreatment condition of high temperature and pressure, the liquid deprived region can create hot spots (Absi-Halabi *et al.*, 1991), and gas deprived region forms hydrocracking, hence coke formation on the catalyst (Dudukovic and Mills, 2014). We also inferred that this kind of maldistribution is directly linked with improper functioning of the lower plenum of MBR.

The type of the gas-liquid distributor used for MBR consists of chimneys to create a gas pocket underneath the distributor plate. These type of distributors are widely used in hydrotreatment application for upflow gas-liquid reactors. [(Paul and Brian, 1984), (Bruce *et al.*, 1999)] showed that a gas pocket type of distributor is achieved by using a hollow pipe called chimneys having a side hole on the lateral wall near the top region of chimney. These chimneys are placed underneath the gas-liquid distributor plate assembly, where a distributor plates having openings is the interface between the distributor and remainder of the reactor. Multiple chimneys are attached to the openings of the distributor plate and are placed such that the chimneys side holes are just below the distributor plates and are facing toward the same direction. There are three possible scenarios for flow through the chimneys, the first case; the liquid moves up the inlet hole of the chimney, and the gas flowing in from the side holes blocks the liquid to move up, and only gas phase exits the chimney outlets. The second case; the liquid flows up through the inlet hole of chimney and gas flowing through the side holes mixes, and gas-liquid mix flows out of the chimney outlet. The third case; both gas and liquid flows from both inlet hole and side hole of the chimneys and mix of gas-liquid moves out of the chimney outlet. For proper functioning, a single mix of gas-liquid needs to be ejected from the chimney outlet, which is seen in the second and third case. (Robert and Frederick, 2003) observed for the plenum containing gas pocket type of distributor and circular inlets at the bottom of the plenum, the majority of gas flow towards the central region of the distributor, they came up with a deflector design and placed it to obstruct the gas-liquid flowing to the central region and deflect it towards the sides. Even with this deflector, they observed central region having more gas movement, and they further designed and placed obstruction to block the inlet holes of the chimneys at the central region of distributor. (Christophe *et al.*, 2006) found the deflector inside the plenum creates a movement of phases towards the distributor, which induces oscillation of gas-liquid interface and can cause maldistribution. They came up with enclosed mixing design, in which the gas pocket type of distributor is used inside the plenum, but the gas

inlet is through the sides and at the top portion of the plenum. The liquid flow upward from the bottom inlet of the distributor and flows through the chimney inlet holes and the gas coming from the sides, moves lateral and enters the chimney side holes, the gas-liquid mix is then ejected out of the distributor outlet. Lower plenum of MBR also incorporates a gas pocket type of distributors having chimneys, and a different deflector design, detailed explanation of design is given in section 3.

There are no studies available in open literature on the lower plenum of MBR. In this study we implement CFD simulation to investigate the flow behavior inside the plenum and investigate its performance based on phase mass distribution through its outlet to upper plenum. This lower plenum is basically a bubble column with internals. The internals in MBR lower plenum are deflector and gas pocket type of gas-liquid distributor and is discussed in detail in section 3. There are lot of work in the area of bubble column with well advanced flow models and closures [(Larachi *et al.*, 2006) (Li *et al.*, 2009)]. CFD modeling approach in bubble column are Euler-Euler and Euler-Langragian [(Zhang and Ahmadi, 2005) (Sommerfeld *et al.*, 2008) (Deen *et al.*, 2004) (Hu and Celik, 2008) (S *et al.*, 2002)]. It is preferable to run a 3D simulation but literature shows lot of work in 2D simulation and 3D axisymmetric simulations (Li *et al.*, 2009), as these simulations are very useful in evaluating time averaged flow parameters in both rectangular and cylindrical geometry and even at lab and industrial scale reactors [(Ekambara and Joshi, 2003) (Bech, 2005) (Joshi, 2001) (Sankey *et al.*, 2009) (Krishna *et al.*, 2000)]. Moreover these simulations are computationally inexpensive compared to 3D simulations for similar CFD models.

In this study, a 3D axisymmetric Euler-Euler simulation is conducted on the gas-liquid distributor of a pilot-scale moving bed reactor (MBR) using ANSYS-Fluent. Simulation is carried at cold flow conditions, and the CFD model validity is confirmed with the radial profile of line average gas volume fraction obtained from a radioactive experimental technique called gamma-ray densitometry (GRD). The simulation result shows uneven

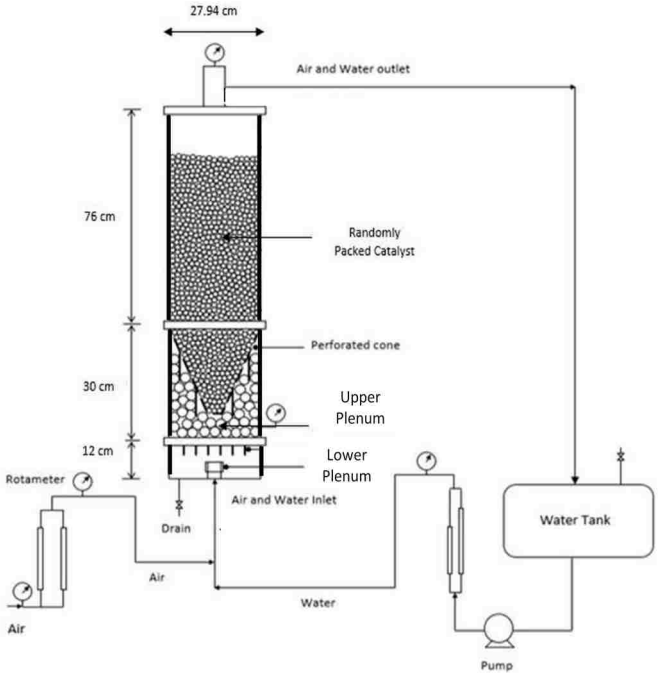

Figure 1. Schematic diagram of scaled down MBR setup for CFD studies

liquid mass distribution through the outlet of this distributor. A modified design is proposed, and its CFD simulation shows improved performance in terms of uniform liquid mass distribution through its outlet.

2. EXPERIMENTAL SETUP

The industrial moving bed hydrotreater (MBR) reactor is scaled down to pilot-plant scale based on hydrodynamic and geometric similarity. The scaled down flow operating condition is obtained by matching the LHSV and gas-liquid volumetric flow rate ratio with the industrial operating condition. The schematic of pilot plant scale reactor is shown in Figure 1. The reactor is a plexiglass column of height 118 cm and the internal diameter of 29.7 cm; it is divided into three section by distributor plate and conical bottom. The parts below conical bottom are called plena, and it is further divided into lower and upper plenum. The lower plenum details are given in Section (3). The upper plenum is the

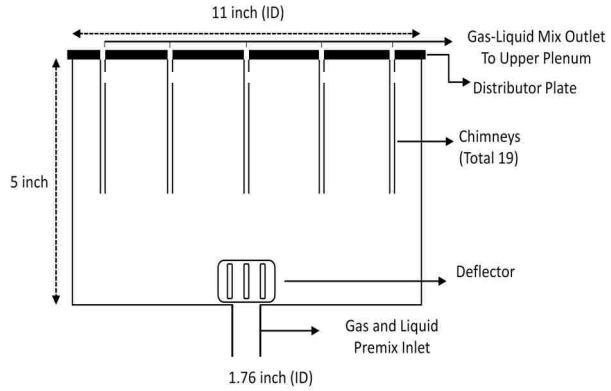

Figure 2. Schematic diagram of lower plenum of MBR

compartment form conical bottom wall to upper plenum wall , and above the distributor plate, and tightly packed with passive spheres. The conical bottom supports the catalyst bed, and it has perforation along the lateral wall and at its bottom. The catalyst bed region which is the cylindircal bed along with conical bed is filled with 3 mm catalyst (Table 1).

The gas and liquid phases are sent in a premixed manner to the inlet of the MBR and the flowrate of these phases are controlled by gas and liquid rotameters. The premixed feed enters the lower plenum and a single mix gas-liquid phase is ejected out through the lower plenum outlets to the upper plenum. The working of lower plenum is explained in section 3. The incoming phases to the upper plenum is further distributed by the passive spheres and is fed to the catalyst bed region through the perforations on the conical bottom. These phases move upwards through the catalyst bed and through the outlet of MBR its sent to a water tank which is open to atmosphere. The liquid collected in the tank is recycled. At scaled down flow condition the catalyst bed behaves upflow packed with slight expansion at the top. Experimental setup specification and operating conditions are shown in Table 1.

Table 1. Experimental setup specification and operating conditions for CFD study

Parameters	Value/Range	Comment
Column Diameter	11 inch	
Column Height	46.46 inch	
Bed Height	24.8 inch	Height from top of the cone to the top of the bed at no flow rate
Catalyst	3 mm Diameter	Bulk Density (570 Kg/m^3)
Scaled Down Liquid Flow Rate	0.0175 cm/sec	By matching LHSV of industrial and scaled down reactor
Scaled Down Gas Flow Rate	7.7 cm/sec	By matching Gas/liquid volumetric flow rate of industrial and scaled down reactor

3. LOWER PLENUM OF MBR

Figure 2 shows the schematic of the lower plenum of pilot-scale MBR. The lower plenum contains of a deflector and gas pocket type of gas-liquid distributor, which is assembly of 19 chimneys attached to the distributor plate, as shown in Figure 2.

The gas-liquid is premixed and enters into the lower plenum through the deflector. The deflector is placed at the inlet of the lower plenum (Figure 2), and its specification are shown in Figure 3a. This deflector has slots on the lateral wall, which shall push the phases outward in an uniform way along the cross sectional plane towards the chimneys. The chimneys are hollow cylinder having a side hole closer to one of its end, the specification of chimneys are shown in Figure 3b. These chimneys are attached to the distributor plate having 19 openings arranged in triangular pitch, and its specifications are shown in Figure 3c. The

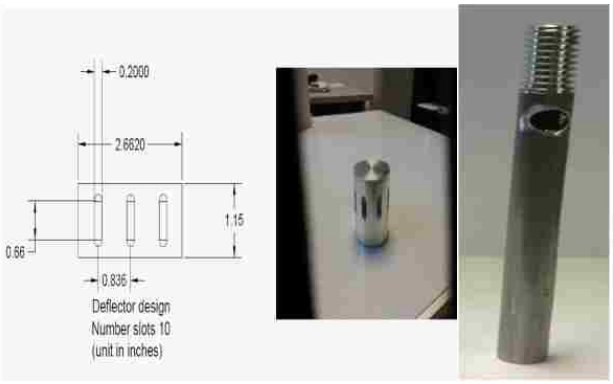

(a) Deflector

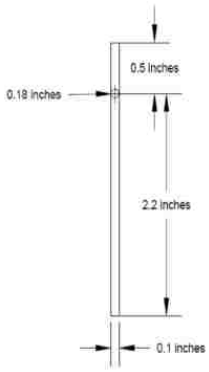

(b) Chimney

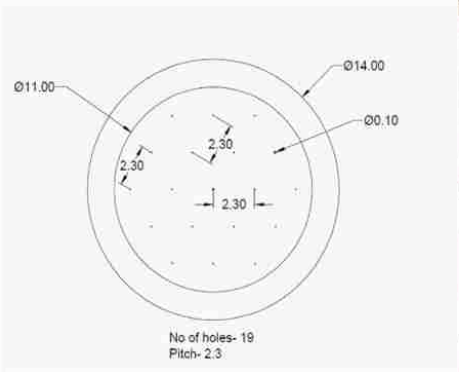

(c) Distributor Plate

(d) Supporting Beams

Figure 3. Internals of lower plenum of MBR

chimney placement is such that the side holes are closer to the distributor plate and all the chimneys side holes are facing in same direction. Now as per the design, this distributor plate with chimneys assembly shall create a uniform gas pocket around the chimney side holes at the scaled down experimental condition, and the gas-liquid mix coming from the deflector shall well mix in the chimneys and eject as a single mix of gas-liquid spray through its outlet to upper plenum of MBR (Figure 2). The distributor also has supporting beams as shown in the Figure 3d.

Table 2. Summary of the flow model and solution scheme

Multiphase Model	Eulerian-Eulerian
Turbulence Model	Realizable K-Epsilon (2 EQN) Turbulence Multiphase model-per phase
Drag Model	Schiller Naumann
Solution Methods	Pressure Velocity Coupling-SIMPLE

4. CFD MODEL

Eulerian-Eulerian approach is used in this study. In this approach both the fluids are considered as interpenetrating continua. Mass and momentum equations are solved for each phase. Both the phases are interrelated by the interphase momentum forces like drag. Both the phases are assumed as incompressible.

Continuity Equation: The mass balance of any phase (k) in a two phase (k, p) system can be shown by the equation 1.

$$\frac{\partial}{\partial t}(\epsilon_k \rho_k) + \nabla.(\epsilon_k \rho_k \vec{v}_k) = (\dot{m}_{pk} - \dot{m}_{kp}) + S_k \tag{1}$$

Where ϵ_k is the phasic volume fraction, ρ_k is the density, and $\vec{v}_k$ are the velocity of phase k. The right hand side terms are mass transfer terms, where, $\dot{m}_{pk}, \dot{m}_{kp}$ characterize the mass transfer from phase p to k and k to p, respectively, and S_K is the mass generation term. In our system for cold flow studies, mass transfer terms can be neglected. The resulting form is equation 2.

$$\frac{\partial}{\partial t}(\epsilon_k \rho_k) + \nabla.(\epsilon_k \rho_k \vec{v}_k) = 0 \tag{2}$$

Momentum Equation: The force balance on any phase (k) in two-phase(k, p), is represented by the equation 3.

$$\frac{\partial}{\partial t}(\epsilon_k \rho_k \vec{v}_k) + \nabla.(\epsilon_k \rho_k \vec{v}_k \vec{v}_k) = -\epsilon_k \nabla(P) + \epsilon_k \rho_k \vec{g} + \nabla.\tau_k + F_{kp} \tag{3}$$

k and p are liquid(l) and gas(g).

The right hand side of the equation 3 shows the forces due to pressure term, gravity, viscous and F_{kp} is the interfacial forces, in this case we only consider drag force (F_D). The stress term of phase k is described by equation 4.

$$\tau_k = -\mu_{eff,k}(\nabla(\vec{v}_k) + \nabla(\vec{v}_k)^T) - \frac{2}{3} I(\nabla.v_k)) \tag{4}$$

$\mu_{eff,k}$ is the effective viscosity due to the combination of molecular viscosity, turbulent viscosity and viscosity due to bubble induced turbulence.

$$\mu_{eff,L} = \mu_{I,L} + \mu_{t,L} + \mu_{BI,L} \tag{5}$$

Effective gas viscosity is based on the effective liquid visocity and is calculated using the equation 6.

$$\mu_{eff,G} = \frac{\rho_g}{\rho_l} \mu_{eff,L} \tag{6}$$

Interfacial moementum transfer due to drag force is accounted by equation 7.

$$F_D = \frac{3}{4} C_D \epsilon_g \rho_L \frac{1}{d_s} |v_g - V_l|(v_g - V_l) \tag{7}$$

The drag coeffecient C_D is calculated using schiller nauman model (Schiller and Naumann, 1935) as shown by equation 8.

$$\begin{aligned} C_D &= \frac{24(1 + 0.15Re^{0.687})}{Re}, Re <= 1000 \\ C_D &= 0.44, Re > 1000 \end{aligned} \tag{8}$$

Table 3. Boundary and operating conditions for the numerical simulation

	Boundary Condition	
Inlet	Liquid Velocity	0.019256 m/sec
	Gas Velocity	18.162525 m/sec
	Gas Volume Fraction	0.3
Outlet	Mixture Pressure	13789.5 pa
Wall	No Slip	
	Operating Condition	
Temperature (273K)	Pressure (101325 Pa)	Water (Primary Phase) Air (Secondary Phase)

Where, Re (reynolds number) is given by Equation (9)

$$Re = \frac{\rho_k |\vec{V}_p - \vec{v}_k| d_p}{\mu_k} \tag{9}$$

5. NUMERICAL SOLUTION

The three dimensional CFD simulation is done for the gas-liquid distributor. The model used in this simulation is summarized in Table 2. ANSYS-Fluent is used as a simulation package, which is finite volume solver. The continuity and momentum balance is solved for first order implicit methods for spatial and time discretization. The pressure and velocity coupling is done using SIMPLE scheme.

A tetrahedral meshing is employed for the computational grid, with total mesh cells of around 0.8 millions. The transient simulation were performed for the time step of 0.001 sec. The boundary and operating conditions of this study are shown in Table 3. The convergence criteria is set to 0.001.

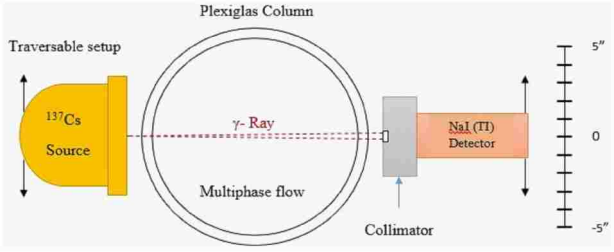

Figure 4. Schematic diagram of GRD

6. VALIDATION OF THE MODEL

The CFD model used in this study is validated with a experimental technique called Gamma-Ray Densitometery (GRD).

6.1. Gamma-Ray Densitometry (GRD). GRD is a radioactive and nonivasive measurement technique. It is widely implemented in multiphase reactors to measure the line avearge phase volume fractions, and its used as flow monitering device in industrial applications [(Al-Dahhan *et al.*, 2007), (Toukan *et al.*, 2017)]. Figure 4 shows the schematic of GRD, with its components; encapsulated radioactive source (Cesium-137) and lead collimated Scintillating Detector (NaI(Tl)). The source and detector are aligned and the photon emitted by the radioactive source is detected by the detector, which is translated to photon count series using a multi channel analyzer (MCA). The amount of count received by the detector varies based on the mixture density and the distance between the source and detector. The detailed working principle of GRD is given by (Toukan, 2017). The source and detector are properly aligned and in between is lower plenum (test section), the GRD scanning is done along the radial location (Figure 5) and at the middle level of the gas liquid distributor. The line average gas fraction is measured using the procedure of (Toukan *et al.*, 2017) from the GRD photon count signals.

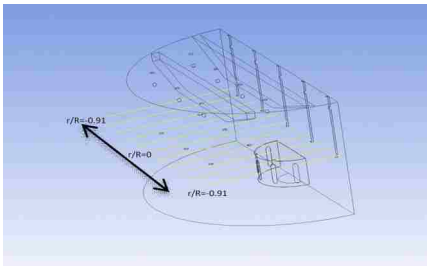

Figure 5. Radial location

6.2. Analysis Principle. The Gamma source of Cs-137 will eject gamma rays and a detector detects the photon counts. The photon attenuation along the path was measured based on Beer Lamberts Law. The intensity of photon attenuation transmitted through a homogeneous material is expressed as follows.

$$\frac{I}{I_o} = e^{-\mu\rho l} \tag{10}$$

where I is detected radiation, I_o is the incident radiation, μ is the mass attenuation coefficient, ρ is the medium density, and l is the path length through the medium, if the material is cylindrical then l is the chord length.

A new variable called A ($ln(\frac{I_o}{I})$) is equal to integral sum of the attenuation through the material along the beam path.

$$A = ln(\frac{I}{I_o}) = \mu\rho l \tag{11}$$

A_{gls} denotes the attenuation coefficient for a test section having three phase (gas, liquid, and solid), and it shown by equation 12.

$$A_{gls} = \mu_g\rho_g l_g + \mu_l\rho_l l_l + \mu_s\rho_s l_s \tag{12}$$

Where, mass attenuation coefficients μ_g, μ_l, and μ_s, and densities ρ_g, ρ_l, and ρ_s, and thicknesses l_g, l_l, and l_s, for the gas, liquid, and solid phases, respectively. L is the total length of the pixel of the test section through which gamma ray beam passes is shown by equation 13.

$$L = l_g + l_l + l_s, l_g = \epsilon_g L, l_l = \epsilon_l L, l_s = \epsilon_s L \tag{13}$$

where ϵ_g, ϵ_l, and ϵ_s, are the line average holdup for the gas, liquid and solid phases, respectively. Since the summation of the holdups equal unity (i.e. $\epsilon_g + \epsilon_l + \epsilon_g = 1$) in each line scan the attenuation of GRD scan for three-phase system (equation 14) can be written as follows.

$$A_{gls} = ln(\frac{I_o}{I_{gls}}) = [\mu_g \rho_g \epsilon_g + \mu_l \rho_l (1 - \epsilon_g - \epsilon_s) + \mu_s \rho_s \epsilon_s] L \tag{14}$$

6.3. Experimental Procedure for Line Average Phase Holdup Calculations. The formula used to measure holdup distribution is similar as (Chen *et al.*, 2001). The first step before installing the test section is to scan with test section. This scan will give I_o.

Scanning empty lower plenum: The photon attenuation in this case will be only due to column wall and internal solids, which can be together called solids, and attenuation due to solids will remain same as the position and size of solids are not changing for other GRD scans. The attenuation in this case is as follows.

$$A_{gs} = ln(\frac{I_o}{I_{gs}}) = [\mu_g \rho_g (1 - \epsilon_s) + \mu_s \rho_s \epsilon_{s,i}] L \tag{15}$$

μ_g is small compared to other phases hence the gas attenuation term can be neglected from equation (15), and the resulting equation is as follows.

$$A_s = ln(\frac{I_o}{I_{gs}}) = [\mu_s \rho_s \epsilon_s] L \tag{16}$$

Scanning lower plenum filled with water: This will give attenuation (A_l) due to liquid and solids.

$$A_{ls} = ln(\frac{I_o}{I_l}) = \mu_l \rho_l L(1 - \epsilon_s) + \mu_s \rho_s \epsilon_s L \tag{17}$$

Scanning lower plenum with flow rates: In this case attenuation ($A_{g,l,s}$) is due to gas liquids and solids, but gas attenuation are neglected and the resulting equation is shown below.

$$A_{gls} = ln(\frac{I_o}{I_{gls}}) = [\mu_l \rho_l \epsilon_l + \mu_s \rho_s \epsilon_s]L \tag{18}$$

Line average liquid holdup (ϵ_l) are estimated by following equation.

$$\epsilon_l = \frac{(A_{gls} - A_{gs})}{\mu_l * \rho_l * L} \tag{19}$$

Where mass attenuation coefficient of water (μ_l= $8.956 * 10^{-2}$ gm/cm^2), density of water (ρ_l = 1 gm/cm^3), and L is the chord length at particular line scan. The line average solid holdup is obtained from equation 20.

$$\epsilon_s = 1 - \frac{(A_{ls} - A_{gs})}{\mu_l * \rho_l * L} \tag{20}$$

The line average gas holdup (ϵ_g) is obtained by following equation 21.

$$\epsilon_g = 1 - \epsilon_l - \epsilon_s \tag{21}$$

6.4. Comparison of Experimental and Simulation Results. Figure 6 shows the line average volume fraction of gas phase obtained from GRD and the average volume fraction obtained from simulation results along the lines shown in Figure 5 for each radial locations.

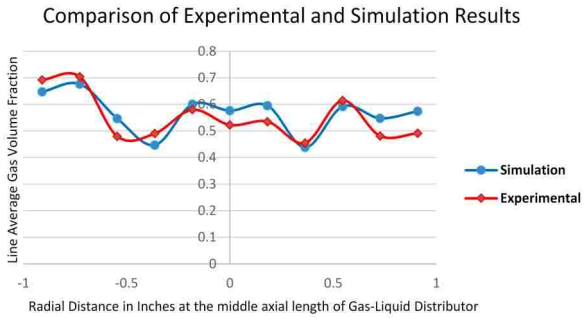

Figure 6. Comparison of experimental and simulations result

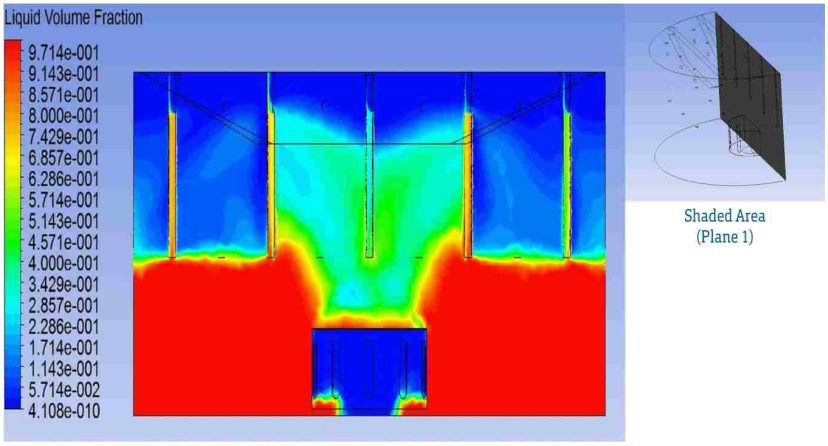

Figure 7. Liquid volume fraction at plane-1 of the gas-liquid distributor

Figure 6 indicates that the results are closely matched with maximum error limit within 18%, and it is also visible that the flow profile of both the results are similar. Hence, on a macro level this CFD model is able to predict the flow profile in the gas liquid distributor for the scaled down operating conditions.

7. RESULTS AND DISCUSSION

7.1. Volume Fraction Contour. Figure 7 shows the contour of liquid volume fraction at the axisymmetric plane (plane-1) of the gas-liquid distributor for the experimental scaled down condition. The dark red zones in the Figure 7 indicate high volume fraction of

liquid and similarly dark blue zone implies the low volume fraction of liquid. It is clearly visible that there is gas pocket formation at the top of the distributor around the side holes of chimneys, with fountain shape flow movement of the liquid phase at the central region, and also liquid upflow through the main holes of the chimney inlet.

At scaled-down experimental condition the flow rate of the gas phase in extremely high compared to the liquid flow rate (Table 1). This indicates that the disperse gas phase may be guiding the liquid phase mainly around the central region of the gas-liquid distributor. Basically, this is a bubble column reactor with internals and in these systems disperse phase (air) guide the flow of continuous phase (water) (Dudukovic, 2010). The Figure 7 also shows that the gas is moving only around the deflector in an upward direction and spread along the cross-sectional plane as moving towards the top region and clear demarcation of gas and liquid boundaries inside the distributor.

This particular flow pattern of gas is not good in terms of even mass distribution through the outlet of the chimneys to the upper plenum region. As on carefully examining the area of chimneys from the side hole to the outlet in Figure 7. It is observed an unveven distribution of mass through each chimneys, with largest mass of liquid flowing out from the second chimney from the left side. It is due to the fountain shape of flow movement and orientation of chimney side hole facing towards one side. Hence, it indicates uneven mass distribution radially at the axisymmetric plane. It creates a doubt about the mass distribution through outlets of all the chimneys, and to examine this a mass fraction profile is obtained for all the chimney outlets.

7.2. Liquid Mass Distribution at the Outlet of Chimneys. Figure 8 shows the designation of chimney outlet based on its position, all the blue dots show the chimney outlets thought which gas-liquid mixture exits the distributor and enters to the upper plenum region. Level 1 represents the plane at the axisymmetric plane, level-3 and level-2 represent the plane towards the wall region and the plane in between respectively. Figure 9 shows the mass fraction of liquid through each chimney outlets, and each outlet is designated by its location

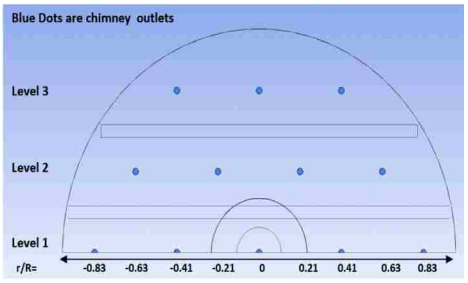

Figure 8. Designation of chimney outlet

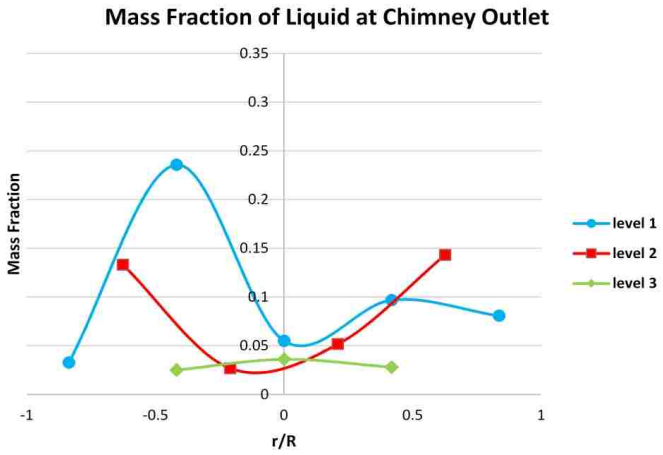

Figure 9. Mass fraction of liquid at the chimney outlet

at particular plane (level), and radial distance (r/R; r represents the distance from the center of gas-liquid distributor to the distance of the chimney if it falls on the axisymmetric plane or level-1, and R is the inner radius of the distributor). For example, level-2 and r/R=-0.63 indicates the first blue dot or chimney outlet from the left at the middle plane. Mass fraction of each chimney is the ratio mass flux through each chimney outlet and summation of mass flux through all the chimney outlets.

Figure 9 clearly indicates an uneven mass distribution of liquid through the outlet of chimneys. With a maximum liquid mass fraction of around 25% from the chimney at level-1 and r/R=-0.5. The similar observation is also seen from the liquid volume fraction contour (Figure 7). The mass fraction at chimneys in the plane at wall region (level-3)

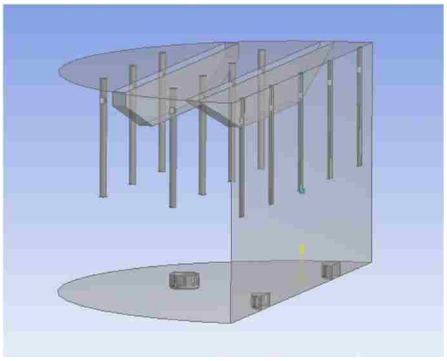

Figure 10. CAD model of new design

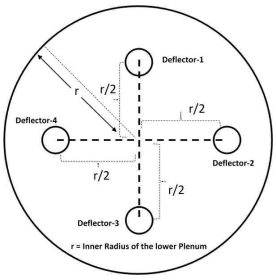

Figure 11. Deflector location in new design

is less than 5% indicating very low liquid movement through these outlets. These results show that this present design lower plenum does not qualify as a good distributor. As the best performance of plenum is characterized by its uniform flow distribution through its outlets [(Li *et al.*, 2009) (Christophe *et al.*, 2006)]. This uneven distribution behavior of lower plenum is mainly due to fountain shape flow movement of liquid and gas phase as seen in Figure 7, and this flow movement is due to the deflector design (Figure 3a), which pushes the gas only around the deflector region. If we properly utilize this phenomenon of the deflector, then overall liquid mass distribution can be improved.

8. MODIFIED DESIGN OF LOWER PLENUM

It is observed from simulation result for the previous design of the lower plenum (section 3) that the deflector (Figure 3a) is major reason for the under-performance of the distributor in terms of even liquid mass distribution through the outlets of the distributor. We observed a fountain shape of flow movement of gas phase due to deflector which in turn is pushing more liquid along the fountain region. Keeping this in mind we proposed a new design for this kind of lower plenum.

Figure 10 shows the axisymmetric CAD model of the new distributor. It has a deflector which is similar in shape but scaled down to 1/4th in terms of size compared to previous deflector design, presuming this reduction in size may reduce the fountain shape compared to the previous design. The number of deflectors has been increased to four and are placed at the locations as shown by Figure 11. We presume that multiplication of deflector generates four small fountain shape inside the distributor, which may improve the overall liquid mass distribution through the outlet of distributor. The gas pocket type of gas-liquid distributor having chimneys and distributor plates assembly are same as that used in the previous lower plenum design.

8.1. CFD Model and Numerical Solution for New Design. In this case too the modeling scheme employed is similar with the old design. The model used for this study are shown in Table 2 and the operating and boundary condition are shown in Table 3. Numerical scheme is also similar. A tetrahedral meshing is employed for the computational grid. The total mesh cells are around 2.2 million. The transient simulation were performed for the time step of 0.001 sec.

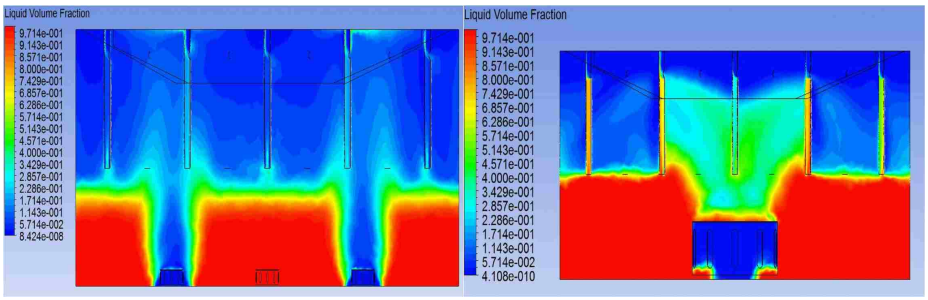

(a) Liquid Volume Fraction Contour New Design

(b) Liquid Volume Fraction Contour New Design

Figure 12. Comparison of liquid volume fraction of new and old design

9. COMPARISON OF OLD AND NEW DESIGN

9.1. Comparison of Liquid Volume Fraction. Figure 12a shows the liquid volume fraction contour of the new design and Figure 12b shows the liquid volume fraction contour for the old design at the axisymmetric plane (plane 1-Figure 7). The overall flow distribution of phases is seen much better in the new design. It is mainly due to the smaller size of the deflector, which produces a smaller fountain shape and its influence with the nearby fountain of another deflector try to stabilize the overall flow pattern.

On examining the area from the chimney side hole to the chimney outlet, the liquid distribution in the new design is seen much even compared to the previous design. It indicates the liquid mass distribution is improved at the axisymmetric plane, but to see the overall performance of new design, mass fraction through all the chimney outlets are calculated.

9.2. Comparison of Mass Distribution at Outlet. Figure 13a shows the mass fraction profile through chimney outlets for new design and Figure 13b shows the mass fraction profile for old design. Level and r/R in Figure has the same meaning as explained in section 7.2. The results indicates improved performance of new design compared to old one. With mass fraction variation through all the chimney outlets of new design is in the

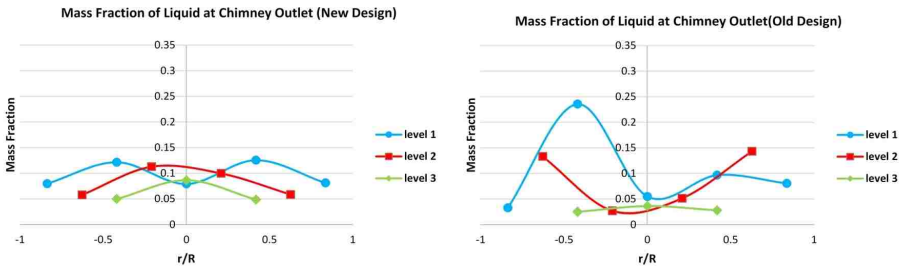

(a) Mass fraction profile New Design (b) Mass fraction profile of old design

Figure 13. Comparison of mass fraction profile of new and old design

range of 5% to 13%, whereas in the old design there is drastic variation in the range of 3% and 25%. For the new design also lesser mass movement is seen at level-3 (plane at wall region), but these mass distribution is much more compared to old design. Hence, overall the distribution of liquid through chimney outlets is improved with the new design. These improvements can be solution for some of the maldistribution issues faced by MBR in the bed region, and can improve the overall performance of MBR.

10. REMARKS

Performance evaluation of a lower plenum of pilot-scale MBR, is performed using CFD simulation. Performance evaluation parameter was the liquid mass distribution through the outlets of the lower plenum. The internal of the lower plenum includes a deflector and 19 chimneys which are attached to the distributor plate, and this plate is the outlet boundary of lower plenum. The CFD simulation is performed using 3-D axisymmetric Euler-Euler simulation for the experimental scaled down condition. The simulation results indicate gas pocket formation along the chimneys top area (below the distributor plate) covering the side holes and with clear demarcation of gas-liquid phase inside the distributor. This kind of gas pocket formation is due to the chimney design. It is also seen that this gas pocket is not uniform along all the chimneys and the reason is due to the flow pattern created

by the deflector. The deflector design is seen to create a fountain type profile along the central region of the distributor, which can create uneven mass distribution through the outlets of the distributor. The results of mass fraction profile of liquid going through the chimney outlet of lower plenum shows a majority of liquid mass moving out through one chimney located in the central region and overall uneven mass distribution. A new design of lower plenum is proposed, where chimneys design is not altered but a new deflector is used which is similar in shape with the previous deflector but its size is reduced to 1/4th, and total four deflectors are used in the new design. These four deflectors are placed at inlet location of lower plenum. CFD simulations are performed on the new design with the similar flow model, boundary and operating condition as that of previous one. The liquid mass fraction profile based on the liquid flowing out from the new design indicates a much even distribution of liquid compared to the previous design. The new distributor design can improve the flow distribution through its outlet and hence flow distribution improvements can be seen in the catalyst bed section of MBR, which may solve some of the drastic issues in that region of MBR.

REFERENCES

Absi-Halabi, M., Stanislaus, A., and Trimm, D., 'Coke formation on catalysts during the hydroprocessing of heavy oils,' Applied Catalysis, 1991, **72**(2), pp. 193 – 215, doi:https://doi.org/10.1016/0166-9834(91)85053-X.

Al-Dahhan, M., Kemoun, A., Cartolano, A., Roy, S., Dobson, R., and Williams, J., 'Measuring gas liquid distribution in a pilot scale monolith reactor via an industrial tomography scanner,' Chemical Engineering Journal, 2007, **130**(2), pp. 147 – 152, doi: https://doi.org/10.1016/j.cej.2006.06.022, special Issue for the 4th World Congress on Industrial Process Tomography.

Bech, K., 'Dynamic simulation of a 2d bubble column,' Chemical Engineering Science, 2005, **60**(19), pp. 5294 – 5304, doi:https://doi.org/10.1016/j.ces.2005.03.066.

Bruce, E. R., Bruce, E. S., and Parimi, K., 'Gas pocket distributor for hydroprocessing a hydrocarbon feed stream,' US Patent, US5885534A, 1999.

Chen, J., Rados, N., Al-Dahhan, M. H., DudukoviÄĞ, M. P., Nguyen, D., and Parimi, K., 'Particle motion in packed/ebullated beds by ct and carpt,' AIChE Journal, 2001, **47**(5), pp. 994–1004, doi:https://doi.org/10.1002/aic.690470506.

Christophe, B., Vincent, C., and Daniel, S., 'Enclosed space for mixing and distribution of a gaseous phase and a liquid phase circulating in ascending flow,' US Patent, US20050051915A1, 2006.

Deen, N., van Sint Annaland, M., and Kuipers, J., 'Multi-scale modeling of dispersed gasâĂŞliquid two-phase flow,' Chemical Engineering Science, 2004, **59**(8), pp. 1853 – 1861, doi:https://doi.org/10.1016/j.ces.2004.01.038, complex Systems and Multi-scale Methodology.

Dudukovic, M. P., 'Reaction engineering: Status and future challenges,' Chemical Engineering Science, 2010, **65**(1), pp. 3–11, ISSN 0009-2509, doi:http://doi.org/10.1016/j.ces.2009.09.018.

Dudukovic, M. P. and Mills, P. L., 'Chapter one - challenges in reaction engineering practice of heterogeneous catalytic systems,' in A. G. Dixon, editor, 'Modeling and Simulation of Heterogeneous Catalytic Processes,' volume 45 of *Advances in Chemical Engineering*, pp. 1 – 40, Academic Press, 2014, doi:https://doi.org/10.1016/B978-0-12-800422-7.00001-7.

Ekambara, K. and Joshi, J., 'Cfd simulation of mixing and dispersion in bubble columns,' Chemical Engineering Research and Design, 2003, **81**(8), pp. 987 – 1002, doi:https://doi.org/10.1205/026387603322482220, particle Technology.

Hu, G. and Celik, I., 'EulerianâĂŞlagrangian based large-eddy simulation of a partially aerated flat bubble column,' Chemical Engineering Science, 2008, **63**(1), pp. 253 – 271, ISSN 0009-2509, doi:https://doi.org/10.1016/j.ces.2007.09.015.

Joshi, J., 'Computational flow modelling and design of bubble column reactors,' Chemical Engineering Science, 2001, **56**(21), pp. 5893 – 5933, doi:https://doi.org/10.1016/S0009-2509(01)00273-1, proceedings of the 5th International Conference on Gas-Liquid and Gas-Liquid-Solid Reactor Engineering.

Kramer, D. C., Stangeland, B. E., Smith, D. S., McCall, J. T., Scheuerman, G. L., and Bachtel, R. W., 'Apparatus for an on-stream particle replacement system for countercurrent contact of a gas and liquid feed stream with a packed bed,' US Patent, US5302357A, 1994.

Krishna, R., van Baten, J., and Urseanu, M., 'Three-phase eulerian simulations of bubble column reactors operating in the churn-turbulent regime: a scale up strategy,' Chemical Engineering Science, 2000, **55**(16), pp. 3275 – 3286, doi:https://doi.org/10.1016/S0009-2509(99)00582-5.

Larachi, F., Desvigne, D., Donnat, L., and Schweich, D., 'Simulating the effects of liquid circulation in bubble columns with internals,' Chemical Engineering Science, 2006, **61**(13), pp. 4195 – 4206, doi:https://doi.org/10.1016/j.ces.2006.01.053.

Li, G., Yang, X., and Dai, G., 'Cfd simulation of effects of the configuration of gas distributors on gasâĂŞliquid flow and mixing in a bubble column,' Chemical Engineering Science, 2009, **64**(24), pp. 5104 – 5116, ISSN 0009-2509, doi: https://doi.org/10.1016/j.ces.2009.08.016.

Paul, T. R. and Brian, E. T., 'Gas-pocket distributor for an upflow reactor,' US Patent, CA1177385A, 1984.

Robert, B. and Frederick, L., 'Gas-pocket distributor and method of distributing gas,' US Patent, US20030223924A1, 2003.

S, L., Border.D, and M, S., 'Modeling hydrodynamics and turbulence in a bubble column using euler-langrange procedure,' Int. J. Multiphase Flow, 2002, **28**, pp. 1381–1407.

Sankey, M., Holland, D., Sederman, A., and Gladden, L., 'Magnetic resonance velocity imaging of liquid and gas two-phase flow in packed beds,' Journal of Magnetic Resonance, 2009, **196**(2), doi:https://doi.org/10.1016/j.jmr.2008.10.021.

Scheuerman, G. L., Johnson, D. R., Reynolds, B. E., Bachtel, R. W., and Threlkel, R. S., 'Hydroprocesses advances in chevron rds technology for heavy oil upgrading flexibility,' Fuel Processing Technology, 1993, **35**(1), pp. 39–54, ISSN 0378-3820, doi:http://doi.org/10.1016/0378-3820(93)90084-H.

Schiller and Naumann, 'A drag coefficient correlation,' VDI Zeitung, 1935, **77**, pp. 318–320.

Sommerfeld, M., Bourloutski, E., and BrÃűder, D., 'Euler/lagrange calculations of bubbly flows with consideration of bubble coalescence,' The Canadian Journal of Chemical Engineering, 2008, **81**(3âĂŘ4), pp. 508–518, doi:10.1002/cjce.5450810324.

Toukan, A., Alexander, V., Albazzaz, H., and Al-Dahhan, M., 'Identification of flow regime in a cocurrent gas-liquid uplfow moving packed bed reactor using gamma ray densitometry,' Chemical Engineering Science, 2017, **168**, pp. 380–390, doi: https://doi.org/10.1016/j.ces.2017.04.028.

Toukan, A. J., 'Hydrodynamics of a co-current gas liquid uplfow in a moving packed bed reactor with porous catalyst,' 2017, **MS thesis**.

Zhang, X. and Ahmadi, G., 'Eulerian lagrangian simulations of liquid gas solid flows in three-phase slurry reactors,' Chemical Engineering Science, 2005, **60**(18), pp. 5089 – 5104, doi:https://doi.org/10.1016/j.ces.2005.04.033.

SECTION

2. SUMMARY, CONCLUSIONS, AND RECOMMENDATION

2.1. SUMMARY AND CONCLUDING REMARK

Upflow Moving Bed Hydrotreater (MBR) reactor is an integral part of hydrotreatment process, as it is used as a guard reactor to fixed bed residual desulfurization (RDS) unit. MBR hydrotreats heavy crude or residuum oil to remove unwanted metal contents, which can reduce the life cycle of RDS process. The MBR is a new technology in guard reactor, and its specialty is its conical bottom bed which facilitates removal of the spent catalyst during the operation. In effect, it reduces the shutdown time of entire hydrotreatment process. MBR design also includes lower plenum which consists of deflector, chimneys, and distributor plate and upper plenum which is a packed bed type of gas-liquid distributor. MBR at industrial scale is facing drastic issues such as coking, hot spots, and catalyst agglomeration inside the packed bed of MBR. Eventually it leads to emergency shutdown and the anticipated cause of these problems are improper hydrodynamics (phase flow distribution and mixing) inside the packed bed. There are no previous hydrodynamic studies available in the open literature on MBR. Hence, the overall objective of this study is to do the hydrodynamic evaluation of scaled down MBR which is achieved by following.

An industrial scale MBR is scaled-down to pilot-scale by matching geometric and dynamic similarity. The pilot-scale MBR reactor is successfully commissioned and under operation at Multiphase Reactors Engineering and Applications Laboratory at Missouri S&T. The present pilot-scale MBR is capable of conducting cold flow studies, but modifications are needed to employ it for hot flow studies. We investigated the hydrodynamics by developing experimental methods and systems for the pilot scale MBR.

Improper local hydrodynamics inside the packed bed is the key factor for the major issues (coking, agglomeration, etc.) of MBR. Hence, to investigate and quantify local hydrodynamics, an invasive experimental technique called Two-Tip Optical Probe (TTOP) is implemented at various radial and axial locations inside the bed for industrial scaled down operating condition. Developed method (algorithm) to obtain local phase saturations, local phase velocities, local backmixing, and local maldistribution form the time series signal of TTOP. This study shows a highly maldistributed state of the bed, with local zones having gas or liquid deprived regions, these regions are prone to coking or catalyst agglomeration at hydrotreatment condition. Also, on comparing the radial phase saturation below and above the conical bottom shows that cone is not translating the flow profile generated by the lower plenum (gas-liquid distributor) to the bottom of the bed. Instead, it is seen to push the gas towards side walls. In terms of local maldistribution, the bottom part of the bed or tightly packed zones shows less maldistribution, or it means the maximum catalyst utilization occurs at these zones compared to higher axial levels, where the bed slightly expands.

Gas and liquid dispersion/mixing are essential performance parameter of MBR, as it directly affects the mass transfer and hence the yield. The overall phase mixing is investigated inside the bed using residence time distribution (RTD) concept. A gas tracer and liquid tracer experimental facility are developed for pilot-scale MBR to obtain RTD signal for gas and liquid respectively from two-phase gas-liquid upflow. A multiple injection (inlet of MBR, below the catalyst bed, and above the catalyst bed) and one detection (at the outlet of MBR after mixing cup) method is followed for gas phase, and two injection (below and above the catalyst bed) and one detection (outlet of MBR after mixing cup) for liquid phase. The obtained RTDs of phases are evaluated using a methodology based on convolution, regression, and catalyst bed model (ADM-for gas phase, and Wave Model-for liquid phase) and estimated model parameters (D, Pe) for each gas and liquid phase. These parameters quantify gas and liquid mixing inside the bed. These studies are conducted

for varying flow rate of phases including the scaled-down experimental condition. Gas dispersion/mixing studies results indicate the operating conditions where the bed in overall sense behaves as packed or expanded. The gas dispersion/mixing is seen good in a packed bed region and even at scaled-down experimental condition where the bed is in packed bed state with slight expansion at the top. Liquid mixing studies show that liquid behavior in the bed is largely deviating from plug flow, and in expanded bed, the liquid mixing is much more, but even in the scaled-down experimental condition the liquid mixing is seen quite high. It is needed that bed to be in packed bed state for better catalyst utilization as seen from local hydrodynamic studies and for good gas mixing. Hence the liquid and gas scaled-down experimental conditions are suitable for hydrotreatment applications.

Lastly, the performance of lower plenum of pilot-scale MBR based on mass distribution is evaluated using 3-D axisymmetric CFD simulation. The results indicate that the present configuration of the plenum is not performing well in terms of even phase mass distribution through its outlet to upper plenum and is due to its deflector design. A modified deflector arrangement is proposed for lower plenum and conducted CFD simulation using similar flow model, operating and boundary conditions as used for the previous design. The results show a much even distribution of phases in the new design compared to the old design of the lower plenum. This improvement can solve some of the maldistribution issues seen the packed bed region of MBR. Hence, it can improve the overall performance of MBR

2.2. RECOMMENDATION

Taking all the results into consideration, a new design of MBR can be proposed. From CFD study, we have proposed a new design for the lower plenum showing improved performance. We recommended utilizing this lower plenum for the new design. It is also seen from the local hydrodynamic study that conical bottom is one of the factors creating maldistribution inside the bed. Hence, the new design needs either removal of

conical bottom completely, or a different bottom design for catalyst support and this support shall also have the provision to remove spent catalyst. Another criterion to take into consideration while designing these catalyst support is that it shall exactly translate the flow profile generated by the lower plenum to the catalyst bed region. The current operating condition can be followed for new design, as based on phase mixing studies at scaled down conditions, we observed an overall good gas and liquid mixing and bed behavior as upflow packed bed with slight expansion at the top.

All proposed new design of MBR needs experimental validation at pilot scale using the developed experimental method in this study, to see whether there is an improvement or not with the current design. It is also highly recommended that additional experimental investigation using single-source or dual-source computed tomography (CT/DSCT) and radioactive particle tracking (RPT) are needed to investigate 3-D phase distribution and particle movement inside the catalyst bed, which are major factor affecting the performance of this reactor.

The best design of MBR needs scaling up, and one of the recommended scaling up strategy is to enable CFD as scaling up tool. The experimental results obtained from these sophisticated measurement techniques can be converted to dimensionless parameters, and a CFD model can be developed for smaller-scale design and validated for these parameters. The validated CFD model can be applied to higher-scale design and identifying flow parameters through simulations to obtain similar dimensionless number having values close enough to the smaller scale design.

APPENDIX A

SCALING DOWN PROCEDURE

The general principle followed in this scale down operation is to match hydrodynamic and similarity between the commercial and industrial MBR reactor.

SCALED DOWN OPERATING PARAMETER OF PILOT SCALE MBR

Scaled Down Lab Scale Liquid and Gas Flow Rate: To calculate liquid flow rate, the Liquid hourly space velocity (LHSV) is kept same between the commercial and lab scale models, to find the gas flow rate, H_2 to oil volumetric flow ratio of commercial unit is equated to gas to liquid volumetric ratio of lab scale.

- LHSV=Volumetric Liquid Flow Rate/ Catalyst Volume
- Catalyst Volume= Weight of Catalyst/ Compacted Bulk Density
- Weight of Catlayst Used in Lab Scale= 30 kg, and Bulk Density of Catlalyst= 570 Kg/m^3
- Lab Scale Liquid Volumetric Flow Rate= 0.173 gallon/min
- Lab Scale Gas Volumetric Flow Rate= 595.228 standard ft cube per hour (SCFH)
- Lab Scale MBR Reactor Inside Diameter is selected as 11 inch.

Principle Behind Number of Holes and Hole Diameter in the Internals of Pilot Scale MBR: The calculation of number of holes in the internals lab scale reactor is based on matching Hydrodynamic similarity, and is done by matching drop pressure through internal same in both the refinery scale and lab scale identical. The equation of the drop pressure which is used in this calculation is expressed as follows

$$\triangle P = \frac{U^2 * \rho_{fluid}}{C * 2} \tag{A.1}$$

$$U = \frac{Q}{A} \tag{A.2}$$

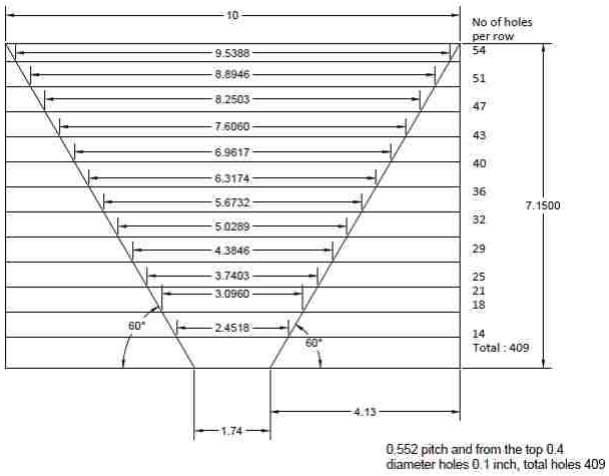

Figure A.1. Schematic of pilot scale cone

Whereas, $\triangle P$ is pressure drop, U is superficial velocity, ρ_{fluid} is the density of the fluid, C is a coefficient equal to 0.64, A is cross sectional area, and Q is volumetric flow rate

INTERNAL-CONE

Cone Dimension: Figure A.1 shows the cone dimension of lab scale MBR. Top diameter of the cone is selected as 10 inch. Height of the cone is 7.15 inch, and is obtained by matching the aspect ratio (Top Diameter/Height) with industrial cone. Slant height of the cone is 8.2503 inch and is obtained by keeping the slant angle same between the lab and industrial cone. Bottom Diameter is 1.74 inch, and is obtained using Pythagoras theorem, slant height and top diameter of the reactor

Methodology to calculate the number and diameter of holes in the cone:

- Consider liquid and gas pass through the cone.
- Assume the density of the liquid and gas is identical in both refinery and lab scales.

For refinery:

- Add the volumetric flow rate of liquid and gas to get the total volumetric flow rate of the fluid Q_{total} (The volumetric flow rate of the liquid and gas is known)
- Find the volumetric flow rate passing one hole by dividing the total volumetric flow rate of the fluid to the total number of hole. (Total number of holes are known)
- Find the area of the one hole. (the diameter of one hole is known)
- Equate the drop pressure equation for refinery and lab scales. All term in the equation will be canceled only the superficial velocity will be remained.
- Find the superficial velocity of the fluid passing one hole by divided the volumetric flow rate of the fluid passing one hole to the area of one hole.

For lab:

- Total volumetric flow rate of fluid (gas+ liquid) is known.
- Assume number of hole in order from 1 to 800. Then divide the total volumetric flow rate to the number of hole. For example total volumetric flow rate of fluid is $16.895 m^3/h$ and number of hole 1, the volumetric flow rate passing one hole become 16.895/1 = 16.895 m^3/h if number of hole 2, the volumetric flow rate passing one hole 16.895/2 = 8.4475 m^3/h, and so on.
- Because of the delta P equation is equated for refinery and Lab scales, superficial velocity of the refinery and the flow rate of one hole in the lab is calculated then the area of one hole in the lab can be calculated by dividing the volumetric flow rate passing one hole in the lab scale to the superficial velocity of the refinery scale.
- After the area of the one hole in the lab is calculated, the diameter of one hole can be calculated by the equation Diameter (D)= $\sqrt[2]{4 * areaofonehole)/\pi}$

- At each number of holes for the lab scale was assumed the flow rate of one hole and diameter of hole will be calculated.
- To confirm the results of the total flow rate: multiply number of hole assumed into the volumetric flow rate of one hole to give the total flow rate of the fluid.
- To confirm superficial velocity of fluid passing one hole for both lab and refinery scales are equal: divide volumetric flow rate passing one hole to the area of one hole.
- Select reasonable number and diameter of holes of the cone in the lab scale.
- To calculate the pitch between the holes. The AutoCAD software was used. The pitch was assumed and the radius of each will measure at different levels. The radius of the cone will decrease from the top to the bottom and the distance between two radius levels is the assumed pitch value. Then the equation (π*radius)/pitch value was used to calculate number of hole in each radius level.
- The summary of the design and the drawing of cone of the lab scale are shown the Figure A.1.

INTERNAL-SKIRT

Lab Scale Skirt Design Calculation:

- Length of skirt= Arbitrary length(X) + Length of the skirt exceeding the bottom part of cone (Y)
- X= sin60* (slant height/2) => 0.86*(8.25/2)= 3.5475
- We have taken (Y) as equal to 0.5 inch
- Length of skirt= 3.5474+0.5= 4.06 inch
- Number of Skirts=2

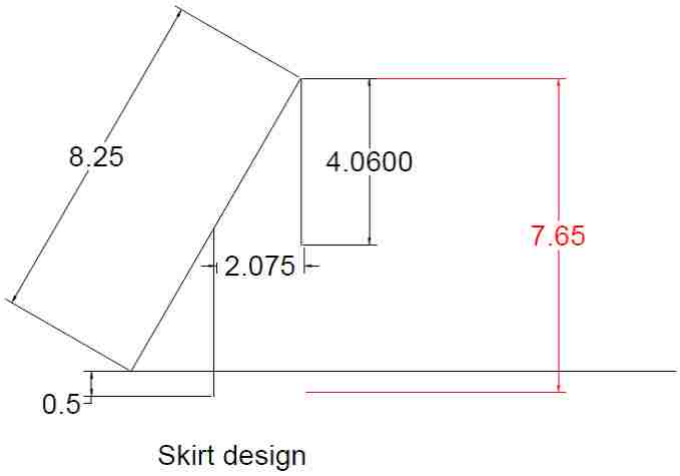

Figure A.2. Schematic of pilot scale skirt

- Distance Between skirts along the slant height= 4.125 inch

INTERNAL-BOTTOM CONE CIRCLE

Methodology to calculate Number of Holes in bottom cone circle:

- Consider that gas and liquid pass through the bottom of cone plate.
- The calculation number of holes in the lab scale for the bottom of the cone in the reactor is based on the dynamics similarity and makes drop pressure in both the refinery scale and lab scale identical.
- Assume the density of the liquid and gas is identical in both refinery and lab scales.
- The methodology for calculation the number of holes in the bottom of the cone is same as the methodology shown in the cone section. The procedure will not be repeated.
- The AutoCAD software was used to estimate the equal distance between the holes.
- The summary of design results and drawing of the design is shown below.

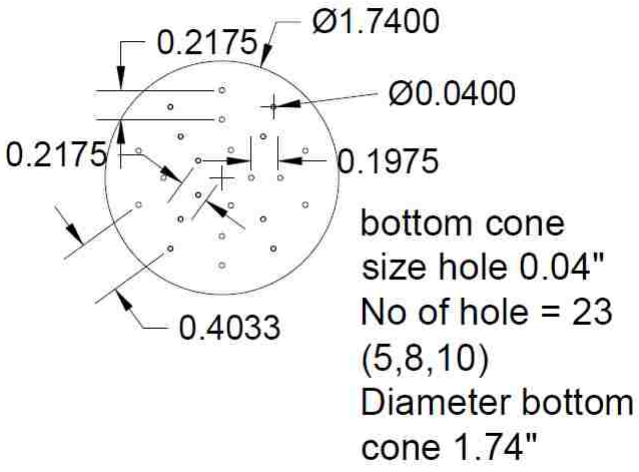

Figure A.3. Schematic of pilot scale bottom cone circle

INTERNAL-DEFLECTOR

Diameter of deflector in lab model:

- Keeping (diameter of Column commercial/ Diameter of Deflector commercial)= (Diameter of Column Lab / Diameter of Deflector lab)
- So Diameter of deflector= (11* 27/223) = 1.331 inch
- The diameter comes out to be very small so we doubled the diameter and now the diameter becomes 2.662 inch

Height of the deflector in lab model:

- Keeping (diameter of deflector commercial/ Height of Deflector commercial)= (Diameter of Deflector Lab / Height of Deflector lab)
- Height of the deflector= (2.662* 11.7)/27= 1.15 inch

Diameter of slot in lab model:

- Keeping (diameter of deflector commercial/ Diameter of slot commercial)= (Diameter of Deflector Lab / Diameter of slot lab)

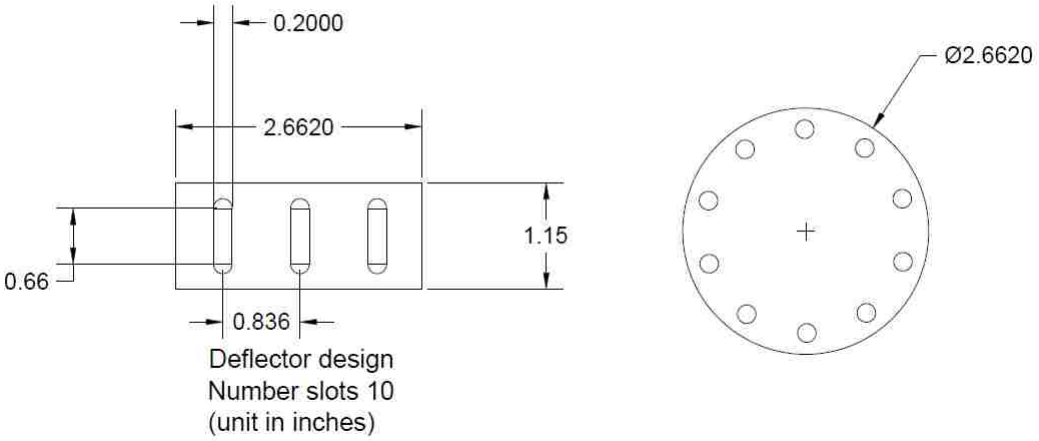

Figure A.4. Schematic of pilot scale deflector

- Diameter of slot= (2.6*2)/27= 0.2 inch

Number and the height of slots in lab model:

- Consider that gas and liquid pass through the bottom of cone plate.
- The calculation of number of holes in the lab scale for the bottom of the cone in the reactor is based on the dynamics similarity and makes drop pressure in both the refinery scale and lab scale identical.
- Assume the density of the liquid and gas is identical in both refinery and lab scales.
- The methodology for calculation the number of slots in the deflector is same as the methodology shown in the cone section. The only difference is the number of slot will be assumed instead of the number of holes and
- To find the height of the slot in lab scale, the diameter of the slot will remain fixed. The volumetric flow rate of fluid passing one slot calculated in lab scale divided to the superficial velocity of the refinery for one slot to find the area of one slot. Then length of one slot in lab scale will be calculated from the equation L_{slot}=(Area of the one slot-(3.14*D^2)/4)/D

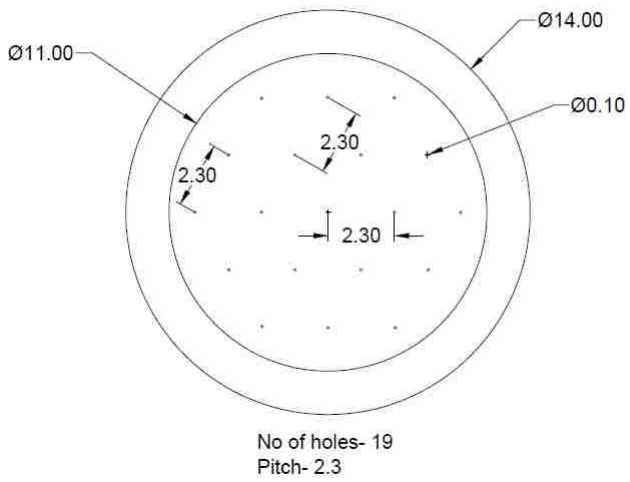

Figure A.5. Schematic of pilot scale distributor

- Select proper number of slots
- The AutoCAD software was used to estimate the equal distance between the slots.
- The summary of design results and drawing of the design is shown below.

INTERNAL-DISTRIBUTOR

To find number of hole and pitch in distributor:

- Consider passing gas and liquid through the hole of distributor (chimney)
- The calculation number of holes of the lab scale for the distributor plate in the reactor is based on the dynamics similarity and makes drop pressure in both the refinery scale and lab scale identical.
- Assume the density of the liquid and gas is identical in both refinery and lab scales.
- The methodology for calculation the number of holes in the bottom of the distributor plate is same as the methodology shown in the cone section. The procedure will not be repeated.

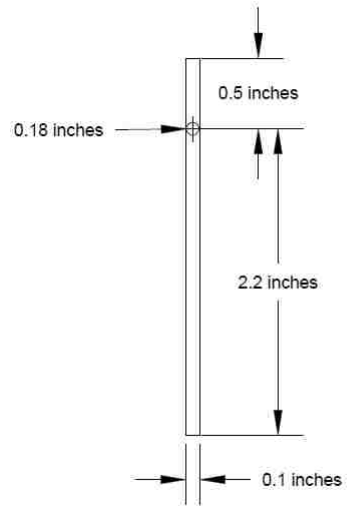

Figure A.6. Schematic of pilot scale chimney

- The AutoCAD software was used to estimate the equal distance between the holes (pitch).
- The summary of design results and drawing of the design is shown in Figure A.5.

INTERNAL-CHIMNEY

- The chimney is a hollow pipe having inlet and exit holes, with additional holes on the side of pipe wall below the exit holes.
- The inlet hole is same as the diameter of the distributor hole, and the exit hole of chimney are slightly lesser the inlet size, and the exit holes side screws into the distributor (Figure A.5) holes.
- The number of chimneys are equal to the number of holes of distributor
- The length and the side hole diameter of the chimney are calculated based on an equation (Proprietary and will not be discussed), to have a good pocket of gas around the chimney side holes, while operating under scaled down condition.
- Figure A.6 shows the schematic of scaled down chimney.

APPENDIX B

THE PROCEDURE TO DETERMINE LOCAL HYDRODYNAMICS USING TTOP

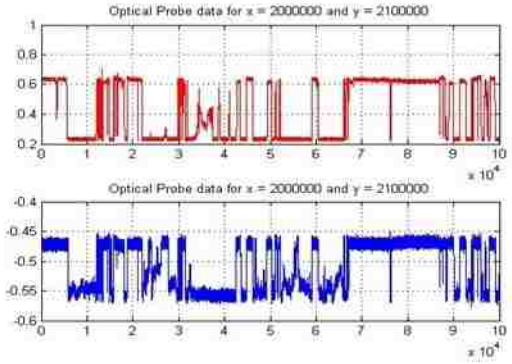

Figure B.1. Raw signal obtained from two-tip optical probe

RAW SIGNAL OF TTOP

The signals of two-tip optical probes are shown in the Figure B.1. The graph illustrates the time-series signal received from the both the tips. The y-axis represents the voltage generated and the top-band values having higher voltage represent the time of gas phase on tip surface and similarly the bottom band values shows the time of liquid on the tip surface. From the time series signal shown in the Figure B.1 different local hydrodynamic parameters are measured using developed algorithm. The procedure to measure local gas/liquid saturations and local gas/liquid velocities are also shown in (Abdul Rahman, 2017).

The total measurement time for one set of experiment is 52 seconds, in this duration approximately 3,000,000 signal data points are generated. It is hard to visualize the whole set of data in one frame. Hence, total data points are split into different frames with each frame containing 100,000 data points. Then the data points are converted to sampling time based on the sampling frequency, and each frame which is part of one set of measurement will represent different time slots as show in Figure B.2

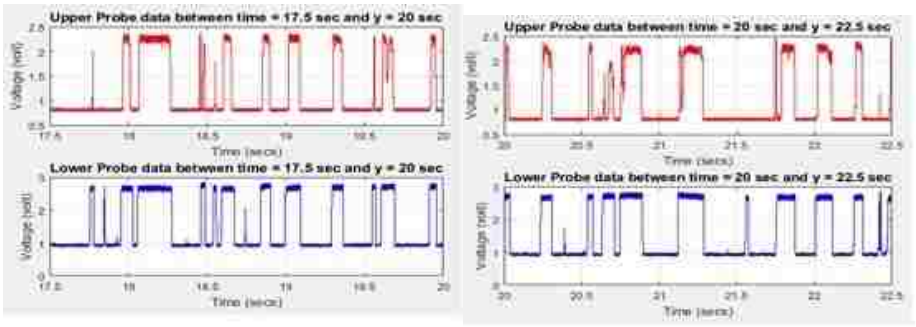

(a) (b)

Figure B.2. (a) Raw time series data of the frame between 17.5 sec and 20 sec (b) Raw time series data of the frame between 20 sec and 22.5 sec

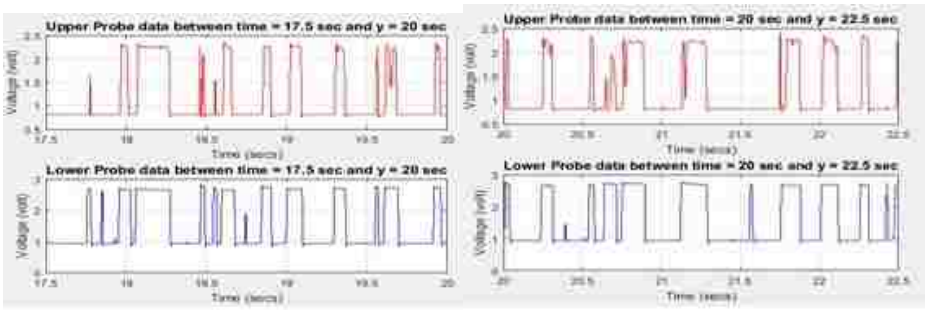

(a) (b)

Figure B.3. (a) Filtered time series data of the frame between 17.5 sec and 20 sec (b) Filtered time series data of the frame between 20 sec and 22.5 sec

FILTERED SIGNAL OF TTOP

The raw signal has noises associated with it as seen in the Figure B.2. These noises are mostly due to electronics of data acquisition (DAQ) ports. It is reduced by designing a low pass filter and passing the raw signal through it. Figure B.3 shows the filtered signal.

NORMALIZING OF FILTERED SIGNAL

The filtered signal is normalized for clear cut demarcation of gas and liquid bands. It is accomplished by assigning a threshold voltage value above which all signals are considered gas phase and below are considered as the liquid phase. The gas phase will

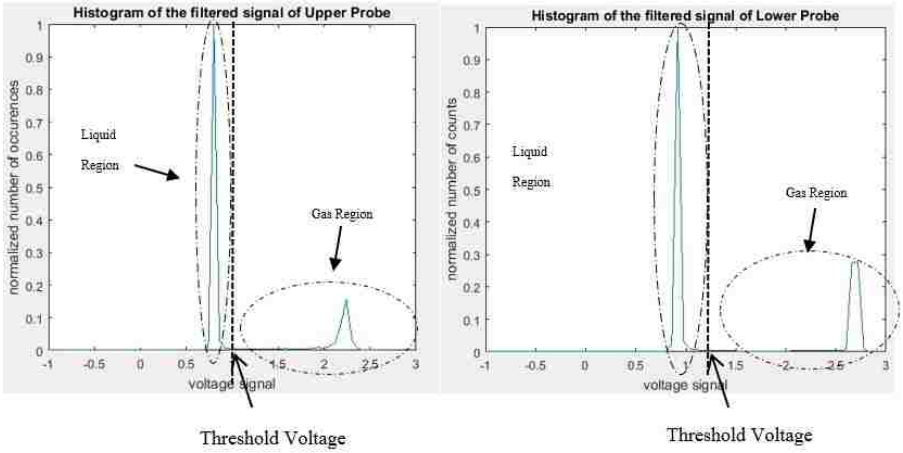

Figure B.4. The histogram plot of raw signal; (a) for the upper probe (b) for the lower probe

be assigned value one and liquid phase will be assigned value of zero. The histogram plot of raw signal is generated to obtain threshold voltage value. Figure B.4 represents the histogram plot of both upper and lower probe signal and each probes signal has two peaks. The peak on the left represents the liquid phase, and the peak on right represents gas phase. These peaks shape varies, and the number of occurrences varies based on the flow conditions. In the case shown in Figure B.4 the number of occurrences of the liquid band is more as compared to gas bands. The threshold voltage value is taken as the voltage at which the peak of liquid region drops. In Figure B.4a for the upper probe signal the threshold voltage value is 1 and similarly in Figure B.4b the threshold voltage value for the lower probe is 1.2. The threshold values are changed from 1 to 1.5 in upper probe signal and 1.1 to 1.5 in lower probe signal and minimal variation in results are seen. For standardization, the voltage at which the first drop for the liquid region is observed is taken as the threshold voltage.

Figure B.5 represents the normalized signal, and all the gas bands are assigned value of one and liquid bands are allocated value of zero. The normalized signal will give the exact time when the gas bubble touches the tip of the probe and the exact time when it leaves the tip of the probe.

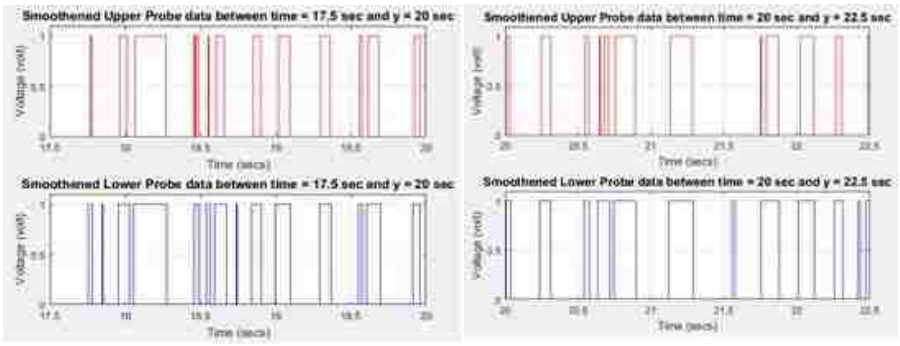

(a) (b)

Figure B.5. Smoothed signal of filtered data of two-tip optical probe; (a) for time frame 17.5 sec to 20 (b) for time frame 20 sec to 22.5

DETERMINATION OF LOCAL GAS AND LIQUID SATURATION

Local Gas Saturation: It is the local gas holdup concerning the gas-liquid mixture present in the catalyst void space for a two-phase flow through packed bed system. It is defined as the fraction of volume occupied by the gas in the catalyst void space where there is flow of gas-liquid phase.

$$\epsilon_{g(s),local} = \frac{V_{g,local}}{V_{g,local} + V_{l,Local}} \tag{B.1}$$

The ergodic hypothesis says that the ensemble average is equivalent to time average, spatially volume time average can be replaced by time average holdup. Hence, time average holdup is the ratio of time spent by gas on the probe tip surface by the total measurement time when gas or liquid phase are on the probe tip surface.

$$\epsilon_{g(s),local} = \frac{t_g}{t_g + t_l} \tag{B.2}$$

Local Liquid Saturation: It is the local liquid holdup with respect to gas-liquid mixture within the catalyst void space of packed bed reactor. The summation of local saturation of both phases in the void space should be one as the probe only detects the flow of gas or liquid phase in the measured region. Hence, to obtain local liquid saturation subtract local gas saturation from one.

$$\epsilon_{l(s),local} = 1 - \epsilon_{g(s),local} \tag{B.3}$$

The usage of the optical probe in measuring local gas and liquid holdup was done by (Wang *et al.*, 2003) in a fluidized bed and (Xue *et al.*, 2008) in a bubble column. They all used the ergodic hypothesis to determine the local holdup of phases. In packed bed reactor, the same procedure is applied, but the obtained values are not local holdups but rather local saturations. It is because the tip in the void space of packed bed only senses gas or liquid phase and quantifies the amount of time spent by gas and liquid phase in this regions. The solids are not moved and are not detected by these probes. The wetting factor in local void space is directly proportional to local liquid saturation.

The smoothened signal is used to calculate local gas and liquid saturation. The total time is calculated when the signal value is one. This time and the total measurement time is fed to Equation B.2 to calculate local gas saturation. Then using local gas saturation in Equation B.3 to calculate local liquid saturation.

DETERMINATION OF LOCAL GAS AND LIQUID VELOCITIES

Local Gas Velocity: The two-tip optical probe is designed in such a way to obtain local phase velocity. The velocity as by definition is the distance traveled divided by the time taken to travel that much distance. In our case the two tips are placed at a distance

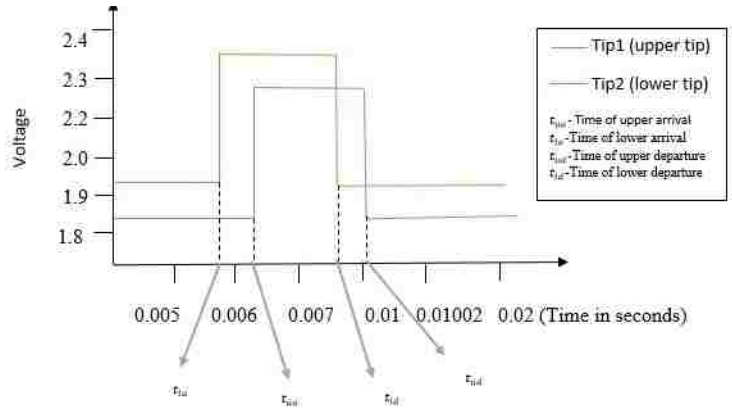

Figure B.6. Schematic of probe response of two-tips of optical probe

of 1 mm and so the only requirement here is to determine the time taken by the bubble to travel this distance between the tips. Figure 14 shows the schematic of probe response to illustrate local velocity calculations.

The two tips are categorized as lower and upper based on their geometrical orientation. In the above case, the tip 2 is the lower as it is placed below tip 1. t_{la} is the time when a bubble first touches the lower probe or tip 2, and t_{ua} is the time at which the same bubble touches the upper probe or tip 1.

The time difference (t_{la}-t_{ua}) or (t_{ua}-t_{la}) will give the time taken by the gas bubble to travel $1mm$, which is the distance between two tips. Hence the local gas velocity is given as:

$$V_{g,local} = \frac{1mm}{t_{la} - t_{ua}} \; or \; V_{g,local} = \frac{1mm}{t_{ua} - t_{la}} \tag{B.4}$$

For gas-liquid upflow through packed bed ($t_{ua} - t_{la}$) , and for downflow ($t_{la} - t_{ua}$) is used in equation B.4 . When the gas-liquid flow is in the opposite direction to general flow negative time difference values are observed.

Local Liquid Velocity: To measure liquid velocity the time taken by the liquid to travel the distance between two tips is calculated. As the interested measurement zone only has gas and liquid phase. Hence, it means that as soon as the gas departs from the tip, the liquid will arrive or the difference between departure times of gas bubble will give the time

taken by the liquid to travel the distance of $1mm$. From Figure B.6 t_{ld} and t_{ud} is the time at which the gas bubble departs from the respective tips of the probe. Hence local liquid velocity can be given as:

$$V_{g,local} = \frac{1mm}{t_{ld} - t_{ud}} \; or \; V_{g,local} = \frac{1mm}{t_{ud} - t_{ld}} \tag{B.5}$$

Here also if the general direction of gas-liquid phase is upflow then $(t_{ud} - t_{ld})$ or in case of downflow $(t_{ld} - t_{ud})$ is considered in equation B.5. Normalized data as shown in Figure B.5 is used to determine the local velocity parameter of phases, as smoothed data clearly demarcates the gas and liquid region by the voltage value of one and zero. As seen in the equation B.4 and B.5, to obtain local velocity we need the time of arrivals and time of departures of the bubble in both the tips. To find the arrival and departure time of bubble an algorithm is developed as part of the method to track the transition of the voltage value from zero to one in the entire smoothed time series, and this gives us the time of arrival of bubbles. Similarly, the developed algorithm tracks the transition from one to zero to determine the time of departures of bubbles. The complication here is to select the same bubbles which touch both the tips to determine local velocity, as there is the possibility of bubble deviation due to the local force field. Signal selection criteria are to be set to filter out the tracked bubble which can give us the local velocities. In work done on bubble column using the optical probe, (Magaud *et al.*, 2001) followed acceptance-rejection algorithm of (Aloui and Souhar, 1996) on the selection of signals to detect the bubble velocity (Figure B.7). The acceptance-rejection algorithm works on the assumption that the bubble chord length is larger than the distance between two tips. The other criteria is to match the signal using Autocorrelation or Correlation function, which matches the signal in an time averaged way rather than putting an actual limiting criteria, and it may not work in two-phase packed bed reactors.

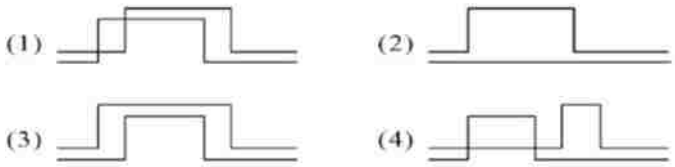

Figure B.7. Detected bubbles and validation test: (1) accepted, (2) rejected, (3) rejected, and (4) rejected ((Magaud *et al.*, 2001),(Aloui and Souhar, 1996)

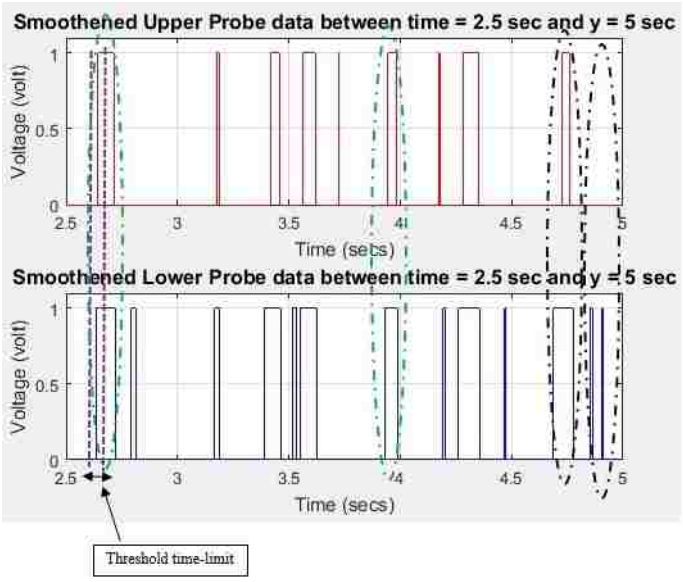

Figure B.8. Selection criteria for local gas velocity calculation in two-tip optical probe; bubbles similar to green circled are accepted and bubbles similar to black circled are rejected

Hence, a new criterion is developed in which all the tracked bubble are filtered out through a condition that the absolute time difference of time of arrivals and time of departures of both the tips shall fall below certain threshold time-limit. This time-limit is determined at the lowest flow rate of phases, all the tracked bubbles at these conditions are visually analyzed and maximum time difference when the same bubble touches both the tips are measured. This maximum time difference value is the threshold time-limit. The tracked bubble which is not falling in this time-limit is not considered for velocity calculations. It is assumed that the for higher flow rates the same bubble which touch both the tips shall fall below threshold time limit.

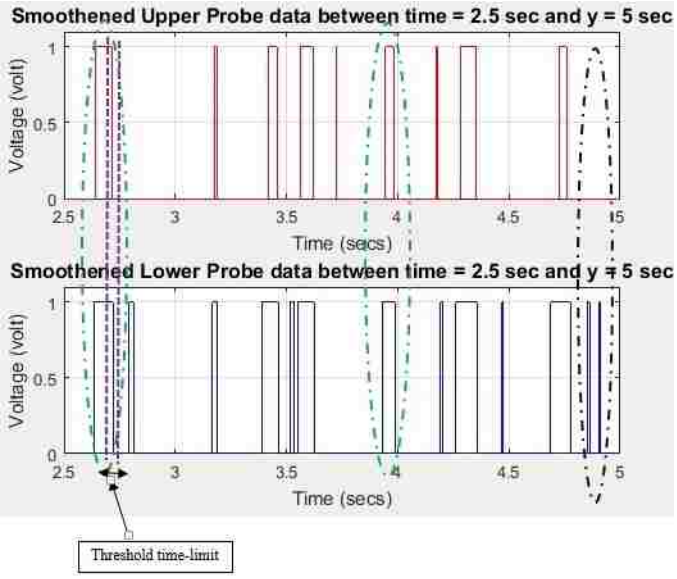

Figure B.9. Selection criteria for local liquid velocity calculation in two-tip optical probe; bubbles similar to green circled are accepted and bubbles similar to black circled are rejected

As shown in the Figure B.8, the bubble similar to as circled in green is selected to find local gas velocity, as the time difference of arrivals of the same bubble in both the tips falls below the threshold time-limit. Bubbles similar to as circled in black does not satisfy the selection criteria; hence they are rejected from velocity calculations. Similarly, in Figure B.9 the bubble similar to as circled in green is selected to find local liquid velocity as the time difference of departures of the same bubble in both the tip falls below the threshold time-limit. Bubbles similar to the black circled one are rejected in this case for failing to match the selection criteria.

Additionally, the developed method will make sure that even under the threshold time-limit conditions no bubbles are repeated. It means all matched bubbles for velocity calculation will have a unique time of arrivals or time of departures, such that no two sets of matched signal have a common time of arrival or departure. Time of arrivals and departures of matched signal obtained after filtering thorough matching conditions is used in equation B.4 and equation B.5 to get local gas and local liquid velocity respectively.

Local Negative Velocities: By following the above method, we will generate the velocity distribution for all the bubbles tracked and fulfilled by the selection criteria. Many of the matched bubbles will give negative values and is due to the flow reversal of phase at that local void space. This reversal mainly occur due to the force field developed due to backpressure. Hence on quantifying the occurrence of negative velocity will indicate the extent of backpressure or backmixing in those local void space in two-phase packed bed.

Zero Velocities: Zero velocity occurrence is a condition when either the entire void space is covered by liquid or gas phase or gas bubble deviation during the measured transient. These velocities are quantified using the velocity distribution obtained by following the method for two-tip optical probe for packed in two-phase flow.These conditions are not good for the reactor and represent the extent of local maldistribution in that small region, It can be represented in terms of percentage.

The following procedure is followed at each measurement point to obtain number of occurences of zero velocities

1= Total Data points (Obtained from method)

2= Total Data points of gas phase (Obtained from method)

3= Total Number of Bubbles (Number of tracked bubble-Obtained from method)

4= Average datapoints per bubble (2/3)

5= Total of bubbles giving velocities (Number of tracked bubble which matches selection criteria for velocity measurement-Obtained from method)

6= Total number of velocity (equal to (5), 1 bubble gives one velocity)

7= Total number of datapoints taken by velocity (4*6)

8= Total data points of not having velocity or zero velocity (1-7)

9= Percentage of time we get zero velocity [(8/1)*100]

10= Number of zero velocity occurence (8/4)

Determination of (9) and (10) gives the extent of local maldistribution at a local void space of a two-phase packed bed reactor

REFERENCES

Abdul Rahman, M. F. B., *Investigation of local velocities and phase holdups, and flow regimes and maldistribution identification in a trickle bed reactor*, Ph.D. thesis, Rolla, 2017.

Abdulmohsin, R. S. and Al-Dahhan, M. H., 'Axial dispersion and mixing phenomena of the gas phase in a packed pebble-bed reactor,' Annals of Nuclear Energy, 2016, **88**, pp. 100–111, doi:https://doi.org/10.1016/j.anucene.2015.10.038.

Absi-Halabi, M., Stanislaus, A., and Trimm, D., 'Coke formation on catalysts during the hydroprocessing of heavy oils,' Applied Catalysis, 1991, **72**(2), pp. 193 – 215, doi:https://doi.org/10.1016/0166-9834(91)85053-X.

Al-Dahhan, M., Kemoun, A., Cartolano, A., Roy, S., Dobson, R., and Williams, J., 'Measuring gas liquid distribution in a pilot scale monolith reactor via an industrial tomography scanner,' Chemical Engineering Journal, 2007, **130**(2), pp. 147 – 152, doi:https://doi.org/10.1016/j.cej.2006.06.022, special Issue for the 4th World Congress on Industrial Process Tomography.

Al-Dahhan, M. H., Mills, P. L., Gupta, P., Han, L., Dudukovic, M. P., Leib, T. M., and Lerou, J. J., 'Liquid-phase tracer responses in a cold-flow counter-current trayed bubble column from conductivity probe measurements,' Chemical Engineering and Processing: Process Intensification, 2006, **45**(11), pp. 945–953, doi:https://doi.org/10.1016/j.cep.2006.01.011.

Aloui, F. and Souhar, M., 'Experimental study of a two-phase bubbly flow in a flat duct symmetric sudden expansion - Part II: Liquid and bubble velocities, bubble sizes,' International Journal of Multiphase Flow, 1996, **22**(5), pp. 849–861, doi:https://doi.org/10.1016/0301-9322(96)00026-2.

Bachtel, R. W., Ohara, Y., Ishizuka, T., and Hiraga, T., 'Apparatus for catalyst replacement,' US Patent, US5527512A, 1996.

Bech, K., 'Dynamic simulation of a 2d bubble column,' Chemical Engineering Science, 2005, **60**(19), pp. 5294 – 5304, doi:https://doi.org/10.1016/j.ces.2005.03.066.

Beg, A., Hassan, M., and Naqvi, M., 'Hydrodynamics and mass transfer in a cocurrent packed column a theoretical study,' Chemical Engineering Journal and the Biochemical Engineering Journal, 93-103, **63**, pp. 1–2, doi:https://doi.org/10.1016/0923-0467(96)03080-1.

Belfares, L., Cassanello, M., Grandjean, B. P. A., and Larachi, F., 'Liquid back-mixing in packed-bubble column reactors: A state-of-the-art correlation,' Catalysis Today, 2001, **64**(3-4), pp. 321–332, doi:https://doi.org/10.1016/S0920-5861(00)00535-6.

Benneker, A. H., Kronberg, A. E., Post, J. W., Van Der Ham, A. G. J., and Westerterp, K. R., 'Axial dispersion in gases flowing through a packed bed at elevated pressures,' Chemical Engineering Science, 1996, **51**(10), pp. 2099–2108, doi: https://doi.org/10.1016/0009-2509(96)00067-X.

Boyer, C., Duquenne, A. M., and Wild, G., 'Measuring techniques in gas liquid and gas liquid solid reactors,' Chemical Engineering Science, 2002, **57**, pp. 3185–3215, doi:https://doi.org/10.1016/S0009-2509(02)00193-8.

Briens, L. A. and Ellis, N., 'Hydrodynamics of three-phase fluidized bed systems examined by statistical, fractal, chaos and wavelet analysis methods,' Chemical Engineering Science, 2005, **60**(22), pp. 6094–6106, doi: https://doi.org/10.1016/j.ces.2005.04.005.

Bruce, E. R., Bruce, E. S., and Parimi, K., 'Gas pocket distributor for hydroprocessing a hydrocarbon feed stream,' US Patent, US5885534A, 1999.

Carleton, A., Flain, R., Rennie, J., and Valentin, F., 'Some properties of a packed bubble column,' Chemical Engineering Science, 1967, **22**(12), pp. 1839 – 1845, doi: https://doi.org/10.1016/0009-2509(67)80214-8.

Cartellier, A. and Barrau, E., 'Monofiber optical probes for gas detection and gas velocity measurements: Conical probes,' International Journal of Multiphase Flow, 1998, **24**(8), pp. 1265–1294, doi:https://doi.org/10.1016/S0301-9322(98)00032-9.

Cassanello, M. C., Martinez, O. M., and Cukierman, A. L., 'Effect of the liquid axial dispersion on the behavior of fixed bed three phase reactors,' Chemical Engineering Science, 1992, **47**(13-14), pp. 3331–3338, doi:https://doi.org/10.1016/0009-2509(92)85042-A.

Chen, J., Rados, N., Al-Dahhan, M. H., DudukoviÄĞ, M. P., Nguyen, D., and Parimi, K., 'Particle motion in packed/ebullated beds by ct and carpt,' AIChE Journal, 2001, **47**(5), pp. 994–1004, doi:https://doi.org/10.1002/aic.690470506.

Chen, Z., Yang, J., Ling, D., Liu, P., Ilankoon, I. M. S. K., Huang, Z., and Cheng, Z., 'Packing Size Effect on the Mean Bubble Diameter in a Fixed Bed under Gas-Liquid Concurrent Upflow,' Industrial and Engineering Chemistry Research, 2017, **56**(45), pp. 13490–13496, doi:https://doi.org/10.1021/acs.iecr.7b00123.

Choi, K. H. and Lee, W. K., 'Comparison of probe methods for measurement of bubble properties,' Chemical Engineering Communications, 1990, **91**(1), pp. 35–47, doi: https://doi.org/10.1080/00986449008940700.

Christophe, B., Vincent, C., and Daniel, S., 'Enclosed space for mixing and distribution of a gaseous phase and a liquid phase circulating in ascending flow,' US Patent, US20050051915A1, 2006.

Collins, J. H. P., Sederman, A. J., Gladden, L. F., Afeworki, M., Douglas Kushnerick, J., and Thomann, H., 'Characterising gas behaviour during gas-liquid co-current up-flow in packed beds using magnetic resonance imaging,' Chemical Engineering Science, 2017, **157**, pp. 2–14, doi:https://doi.org/10.1016/j.ces.2016.04.004.

Danckwerts, P., 'Continuous flow systems: Distribution of residence times,' Chemical Engineering Science, 1953, **2**(1), pp. 1 – 13, doi:https://doi.org/10.1016/0009-2509(53)80001-1.

Deen, N., van Sint Annaland, M., and Kuipers, J., 'Multi-scale modeling of dispersed gasâĂŞliquid two-phase flow,' Chemical Engineering Science, 2004, **59**(8), pp. 1853 – 1861, doi:https://doi.org/10.1016/j.ces.2004.01.038, complex Systems and Multi-scale Methodology.

Delgado, J. M. P. Q., 'A critical review of dispersion in packed beds,' Heat and Mass Transfer/Waerme- und Stoffuebertragung, 2006, **42**(4), pp. 279–310, doi: https://doi.org/10.1007/s00231-005-0019-0.

Dominic, P., Arturo, M., and Valois, P., 'Bubble characteristics measured using a monofibre optical probe in a bubble column and freeboard region under high gas holdup conditions,' Chemical Engineering Science, 2014, doi: https://doi.org/10.1016/j.ces.2014.02.024.

Dudukovic, M. P., 'Reaction engineering: Status and future challenges,' Chemical Engineering Science, 2010, **65**(1), pp. 3–11, ISSN 0009-2509, doi: http://doi.org/10.1016/j.ces.2009.09.018.

Dudukovic, M. P. and Mills, P. L., 'Chapter one - challenges in reaction engineering practice of heterogeneous catalytic systems,' in A. G. Dixon, editor, 'Modeling and Simulation of Heterogeneous Catalytic Processes,' volume 45 of *Advances in Chemical Engineering*, pp. 1 – 40, Academic Press, 2014, doi:https://doi.org/10.1016/B978-0-12-800422-7.00001-7.

Edwards, M. and Richardson, J., 'Gas dispersion in packed beds,' Chemical Engineering Science, 1968, **23**(2), pp. 109 – 123, doi:https://doi.org/10.1016/0009-2509(68)87056-3.

Ekambara, K. and Joshi, J., 'Cfd simulation of mixing and dispersion in bubble columns,' Chemical Engineering Research and Design, 2003, **81**(8), pp. 987 – 1002, doi: https://doi.org/10.1205/026387603322482220, particle Technology.

Fan, L. S., Bavarian, F., Gorowara, R. L., Kreischer, B. E., Buttke, R. D., and Peck, L. B., 'Hydrodynamics of gas-liquid-solid fluidization under high gas hold-up conditions,' Powder Technology, 1987, **53**(3), pp. 285–293, doi:http://doi.org/10.1016/0032-5910(87)80101-8.

Fogler, H. S., 'Elements of chemcial reaction engineering,' 2005, **4th Edition**.

Fraguío, M. S., Cassanello, M. C., Larachi, F., and Chaouki, J., 'Flow regime transition pointers in three-phase fluidized beds inferred from a solid tracer trajectory,' Chemical Engineering and Processing: Process Intensification, 2006, **45**(5), pp. 350–358, doi:https://doi.org/10.1016/j.cep.2005.10.001.

Götz, J., Zick, K., Heinen, C., and König, T., 'Visualisation of flow processes in packed beds with NMR imaging: determination of the local porosity, velocity vector and local dispersion coefficients,' Chemical Engineering and Processing: Process Intensification, 2002, **41**(7), pp. 611–629, doi:https://doi.org/10.1016/S0255-2701(01)00185-4.

Gunn, D. J. and Pryce, C., 'Dispersion in Packed Beds,' Trans Inst Chem Eng, 1969, **47**, pp. t341–t350.

Gutsche, R. and Bunke, G., 'Modelling the liquid-phase adsorption in packed beds at low reynolds numbers: An improved hydrodynamic model,' Chemical Engineering Science, 2008, **63**(16), pp. 4203–4217, doi:https://doi.org/10.1016/j.ces.2008.05.024.

Hamidipour, M. and Larachi, F., 'Characterizing the liquid dynamics in cocurrent gas-liquid flows in porous media using twin-plane electrical capacitance tomography,' Chemical Engineering Journal, 2010, **165**(1), pp. 310–323, doi:https://doi.org/10.1016/j.cej.2010.08.058.

Han, L., 'Hydrodynamics and mass transfer in slurry bubble column,' PhD Thesis, 2007.

Hu, C., Li, W., Liu, J., and Peng, P., 'Technological study on residue hydrotreating reactor with up-flow slightly expanded bed,' Petroleum Refinery Engineering, 2001, **31**(3), pp. 44–45.

Hu, G. and Celik, I., 'EulerianâĂŞlagrangian based large-eddy simulation of a partially aerated flat bubble column,' Chemical Engineering Science, 2008, **63**(1), pp. 253 – 271, ISSN 0009-2509, doi:https://doi.org/10.1016/j.ces.2007.09.015.

Iliuta, I., Thyrion, F. C., and Muntean, O., 'Hydrodynamic characteristics of two-phase flow through fixed beds: Air/newtonian and non-newtonian liquids,' Chemical Engineering Science, 1996, **51**(22), pp. 4987–4995, doi:https://doi.org/10.1016/0009-2509(96)00331-4.

Iliuta, I., Thyrion, F. C., and Muntean, O., 'Axial dispersion of liquid in gas-liquid cocurrent downflow and upflow fixed-bed reactors with porous particles,' Chemical Engineering Research and Design, 1998, **76**(1), pp. 64–72, doi:https://doi.org/10.1205/026387698524488.

Iordanidis, A. A., van Sint Annaland, M., Kronberg, A. E., and Kuipers, J. A. M., 'A critical comparison between the wave model and the standard dispersion model,' Chemical Engineering Science, 2003, **58**(13), pp. 2785–2795, doi:https://doi.org/10.1016/S0009-2509(03)00151-9.

Jena, H. M., Roy, G. K., and Meikap, B. C., 'Prediction of gas holdup in a three-phase fluidized bed from bed pressure drop measurement,' Chemical Engineering Research and Design, 2008a, **86**(11), pp. 1301–1308, doi: https://doi.org/10.1016/j.cherd.2008.05.007.

Jena, H. M., Roy, G. K., and Meikap, B. C., 'Prediction of gas holdup in a three-phase fluidized bed from bed pressure drop measurement,' Chemical Engineering Research and Design, 2008b, **86**(11), pp. 1301–1308, doi: http://doi.org/10.1016/j.cherd.2008.05.007.

Ji, M., Yang, Z., Lou, X.-J., Yong, Y.-M., and Yang, C., 'Fluid flow and backmixing characteristics of up-flow reactor,' Huaxue Gongcheng/Chemical Engineering (China), 2015, **43**(11), pp. 41–46, doi:https://doi.org/10.3969/j.issn.1005-9954.2015.11.009.

Johns, M. L., Sederman, A. J., Bramley, A. S., Gladden, L. F., and Alexander, P., 'Local transitions in flow phenomena through packed beds identified by MRI,' AIChE Journal, 2000, **46**(11), pp. 2151–2161, doi:https://doi.org/10.1002/aic.690461108.

Joshi, J., 'Computational flow modelling and design of bubble column reactors,' Chemical Engineering Science, 2001, **56**(21), pp. 5893 – 5933, doi: https://doi.org/10.1016/S0009-2509(01)00273-1, proceedings of the 5th International Conference on Gas-Liquid and Gas-Liquid-Solid Reactor Engineering.

Koh, J. H., Wankat, P. C., and Wang, N. H. L., 'Pore and surface diffusion and bulk-phase mass transfer in packed and fluidized beds,' Industrial and Engineering Chemistry Research, 1998, **37**(1), pp. 228–239.

Kramer, D. C., Stangeland, B. E., Smith, D. S., McCall, J. T., Scheuerman, G. L., and Bachtel, R. W., 'Apparatus for an on-stream particle replacement system for countercurrent contact of a gas and liquid feed stream with a packed bed,' US Patent, US5302357A, 1994.

Krantz, W. B., Earls, D. E., Trimble, H. J., Chabot, J., and Parimi, K., 'Balanced flow resistance OCR distributor cone,' US Patent, US6387334B1, 2002.

Kressmann, S., Boyer, C., Colyar, J. J., Schweitzer, J. M., and Viguie, J. C., 'Improvements of ebullated-bed technology for upgrading heavy oils,' Oil and Gas Science and Technology, 2000, **55**(4), pp. 397–406, doi:https://doi.org/10.2516/ogst:2000028.

Krishna, R., van Baten, J., and Urseanu, M., 'Three-phase eulerian simulations of bubble column reactors operating in the churn-turbulent regime: a scale up strategy,' Chemical Engineering Science, 2000, **55**(16), pp. 3275 – 3286, doi: https://doi.org/10.1016/S0009-2509(99)00582-5.

Kumar, S., Kumar, R. A., Munshi, P., and Khanna, A., 'Gas hold-up in three phase co-current bubble columns,' Procedia Engineering, 2012, **42**, pp. 782–794, doi: https://doi.org/10.1016/j.proeng.2012.07.470.

Larachi, F., Desvigne, D., Donnat, L., and Schweich, D., 'Simulating the effects of liquid circulation in bubble columns with internals,' Chemical Engineering Science, 2006, **61**(13), pp. 4195 – 4206, doi:https://doi.org/10.1016/j.ces.2006.01.053.

Lee, D., Macchi, A., Grace, J. R., and Epstein, N., 'Fluid maldistribution effects on phase holdups in three-phase fluidized beds,' Chemical Engineering Science, 2001, **56**(21-22), pp. 6031–6038, doi:https://doi.org/10.1016/S0009-2509(01)00280-9.

Levenspiel, O. and Smith, W., 'Notes on the diffusion-type model for the longitudinal mixing of fluids in flow,' Chemical Engineering Science, 1957, **6**(4), pp. 227 – 235, ISSN 0009-2509, doi:https://doi.org/10.1016/0009-2509(57)85021-0.

Li, G., Yang, X., and Dai, G., 'Cfd simulation of effects of the configuration of gas distributors on gasâĂŞliquid flow and mixing in a bubble column,' Chemical Engineering Science, 2009, **64**(24), pp. 5104 – 5116, ISSN 0009-2509, doi:https://doi.org/10.1016/j.ces.2009.08.016.

Li, X., Yang, C., Yang, S., and Li, G., 'Fiber-optical sensors: Basics and applications in multiphase reactors,' Sensors (Switzerland), 2012, **12**(9), pp. 12519–12544, doi:https://doi.org/10.3390/s120912519.

Magaud, F., Souhar, M., Wild, G., and Boisson, N., 'Experimental study of bubble column hydrodynamics,' Chemical Engineering Science, 2001, **56**(15), pp. 4597–4607, doi:https://doi.org/10.1016/S0009-2509(01)00110-5.

Mantle, M. D., Sederman, A. J., and Gladden, L. F., 'Single-and two-phase flow in fixed-bed reactors: MRI flow visualisation and lattice-Boltzmann simulations,' Chemical Engineering Science, 2001, **56**(2), pp. 523–529, doi:https://doi.org/10.1016/S0009-2509(00)00256-6.

Mena, P. C., Rocha, F. A., Teixeira, J. A., Sechet, P., and Cartellier, A., 'Measurement of gas phase characteristics using a monofibre optical probe in a three-phase flow,' Chemical Engineering Science, 2008, **63**(16), pp. 4100–4115, doi:https://doi.org/10.1016/j.ces.2008.05.010.

Midoux, N. and Charpentier, J. C., 'On an experimental method of residence time distribution measurement in the fast flowing phase of a two-phase flow apparatus: Application to gas flow in gas-liquid packed column,' The Chemical Engineering Journal, 1972, **4**(3), pp. 287–290, doi:https://doi.org/10.1016/0300-9467(72)80026-1.

Muroyama, K. and Fan, L.-S., 'Fundamentals of gas-liquid-solid fluidization,' AIChE Journal, 1985, **31**(1), pp. 1–34, doi:https://doi.org/10.1002/aic.690310102.

Paul, T. R. and Brian, E. T., 'Gas-pocket distributor for an upflow reactor,' US Patent, CA1177385A, 1984.

Pugliese, L., Poulsen, T. G., and Andreasen, R. R., 'Relating Gas Dispersion in Porous Media to Medium Tortuosity and Anisotropy Ratio,' Water, Air, & Soil Pollution, 2012, **223**(7), pp. 4101–4118, doi:https://doi.org/10.1007/s11270-012-1176-7.

Rao, A. V. R., Kumar, R. K., Sankarshana, T., and Khan, A., 'Identification of flow regimes in a concurrent gas liquid upflow through packed beds,' Chemical Engineering & Technology, 2011, **34**(11), pp. 1909–1917, doi:https://doi/org/10.1002/ceat.201100070.

Robert, B. and Frederick, L., 'Gas-pocket distributor and method of distributing gas,' US Patent, US20030223924A1, 2003.

S, L., Border.D, and M, S., 'Modeling hydrodynamics and turbulence in a bubble column using euler-langrange procedure,' Int. J. Multiphase Flow, 2002, **28**, pp. 1381–1407.

Safoniuk, M., Grace, J. R., Hackman, L., and McKnight, C. A., 'Gas holdup in a three-phase fluidized bed,' AIChE Journal, 2002, **48**(7), pp. 1581–1587, doi: https://doi.org/10.1002/aic.690480720.

Salleh, K. A. M., Lee, H. K., and Al-Dahhan, M. H., 'Local liquid velocity measurement in trickle bed reactors (TBRs) using the x-ray digital industrial radiography (DIR) technique,' Measurement Science and Technology, 2014, **25**(7), doi: https://doi.org/10.1088/0957-0233/25/7/075401.

Sankey, M., Holland, D., Sederman, A., and Gladden, L., 'Magnetic resonance velocity imaging of liquid and gas two-phase flow in packed beds,' Journal of Magnetic Resonance, 2009, **196**(2), doi:https://doi.org/10.1016/j.jmr.2008.10.021.

Saroha, A. K. and Khera, R., 'Hydrodynamic study of fixed beds with cocurrent upflow and downflow,' Chemical Engineering and Processing: Process Intensification, 2006, **45**(6), pp. 455–460, doi:https://doi.org/10.1016/j.cep.2005.11.005.

Scheuerman, G. L., Johnson, D. R., Reynolds, B. E., Bachtel, R. W., and Threlkel, R. S., 'Advances in Chevron RDS technology for heavy oil upgrading flexibility,' Fuel Processing Technology, 1993a, **35**(1), pp. 39–54, doi:http://doi.org/10.1016/0378-3820(93)90084-H.

Scheuerman, G. L., Johnson, D. R., Reynolds, B. E., Bachtel, R. W., and Threlkel, R. S., 'Hydroprocesses advances in chevron rds technology for heavy oil upgrading flexibility,' Fuel Processing Technology, 1993b, **35**(1), pp. 39–54, ISSN 0378-3820, doi:http://doi.org/10.1016/0378-3820(93)90084-H.

Schiller and Naumann, 'A drag coefficient correlation,' VDI Zeitung, 1935, **77**, pp. 318–320.

Schubert, M., Kryk, H., and Hampel, U., 'Slow-mode gas/liquid-induced periodic hydrodynamics in trickling packed beds derived from direct measurement of cross-sectional distributed local capacitances,' Chemical Engineering and Processing: Process Intensification, 2010, **49**(10), pp. 1107–1121, doi: https://doi.org/10.1016/j.cep.2010.08.004.

Sederman, A. J., Johns, M. L., Bramley, A. S., Alexander, P., and Gladden, L. F., 'Magnetic resonance imaging of liquid flow and pore structure within packed beds,' Chemical Engineering Science, 1997, **52**(14), pp. 2239–2250, doi: https://doi.org/10.1016/S0009-2509(97)00057-2.

Shah, Y. T., Stiegel, G. J., and Sharma, M. M., 'Backmixing in gas-liquid reactors,' AIChE Journal, 1978, **24**(3), pp. 369–400, doi:https://doi.org/10.1002/aic.690240302.

Simcik, M., Ruzicka, M. C., Mota, A., and Teixeira, J. A., 'Smart rtd for multiphase flow systems,' Chemical Engineering Research and Design, 2012, **90**(11), pp. 1739–1749, doi:https://doi.org/10.1016/j.cherd.2012.03.014.

Sommerfeld, M., Bourloutski, E., and BrÃűder, D., 'Euler/lagrange calculations of bubbly flows with consideration of bubble coalescence,' The Canadian Journal of Chemical Engineering, 2008, **81**(3âĂŘ4), pp. 508–518, doi:10.1002/cjce.5450810324.

Tang, D., A., J., X., R., B., B., and S., S., 'Axial dispersion and wall effects in narrow fixed bed reactors: A comparative study based on rtd and nmr measurements,' Chemical Engineering & Technology, 2004, **27**(8), pp. 866–873, doi:10.1002/ceat.200402076.

Taylor, G. I., 'Diffusion and mass transport in tubes,' Proceedings of the Physical Society. Section B, 1954, **67**(12), p. 857.

Thanos, A. M., Galtier, P. A., and Papayannakos, N. G., 'Liquid dispersion and holdup in a small-scale upflow hydrotreater at high temperatures and pressure,' Chemical Engineering Science, 2001, **56**(2), pp. 693–698, doi:https://doi.org/10.1016/S0009-2509(00)00277-3.

Toukan, A., Alexander, V., Albazzaz, H., and Al-Dahhan, M., 'Identification of flow regime in a cocurrent gas-liquid uplfow moving packed bed reactor using gamma ray densitometry,' Chemical Engineering Science, 2017, **168**, pp. 380–390, doi:https://doi.org/10.1016/j.ces.2017.04.028.

Toukan, A. J., 'Hydrodynamics of a co-current gas liquid uplfow in a moving packed bed reactor with porous catalyst,' 2017, **MS thesis**.

Valenz, L., Rejl, F. J., and Linek, V., 'Gas and liquid axial mixing in the column packed with Mellapak 250Y, Pall rings 25, and intalox saddles 25 under flow conditions prevailing in distillation columns,' Industrial and Engineering Chemistry Research, 2010, **49**(20), pp. 10016–10025, doi:https://doi.org/10.1021/ie101092e.

Wang, T., Wang, J., Yang, W., and Jin, Y., 'Experimental study on bubble behavior in gas-liquid-solid three-phase circulating fluidized beds,' Powder Technology, 2003, **137**(1-2), pp. 83–90, doi:https://doi.org/10.1016/j.powtec.2003.08.032.

Wang, X.-T., Li, W.-R., Weng, H.-X., Hu, C.-L., and Peng, P., 'Gas-liquid flow and bed expansion ratio in slightly expanded-bed of residue hydro treating reactor,' Huadong Ligong Daxue Xuebao /Journal of East China University of Science and Technology, 2006a, **32**(5), pp. 530–534.

Wang, X.-T., Li, W.-R., Weng, H.-X., Liu, J.-D., Qi, S.-R., and Ma, Q.-T., 'Research on slight expanded-bed oil residue hydrotreating reactor,' Huaxue Gongcheng/Chemical Engineering (China), 2006b, **34**(9), pp. 28–31.

Westerterp, K. R., Dil'man, V. V., and Kronberg, A. E., 'Wave model for longitudinal dispersion: Development of the model,' AIChE Journal, 1995, **41**(9), pp. 2013–2028, doi:https://doi.org/10.1002/aic.690410902.

Westerterp, K. R., Kronberg, A. E., Benneker, A. H., and Dil'man, V. V., 'Wave concept in the theory of hydrodynamical dispersion a Maxwellian type approach,' Chemical Engineering Research and Design, 1996, **74**(8), pp. 944–952, doi:https://doi.org/10.1205/026387696523111.

Xie, L., Li, Z., and Liu, H., 'Axial dispersion and pressure drop of a slightly expanded bed reactor,' Beijing Huagong Daxue Xuebao (Ziran Kexueban)/Journal of Beijing University of Chemical Technology (Natural Science Edition), 2013, **40**(4), pp. 1–7.

Xue, J., *Bubble Velocity, Size and Interfacial Area Measurements in Bubble Columns*, Ph.D. thesis, 2004.

Xue, J., Al-Dahhan, M., Dudukovic, M. P., and Mudde, R. F., 'Bubble velocity, size, and interfacial area measurements in a bubble column by four-point optical probe,' AIChE Journal, 2008, **54**(2), pp. 350–363, doi:https://doi.org/10.1002/aic.11386.

Yun, J., Lin, D.-Q., Lu, M.-H., Zhong, L.-N., and Yao, S.-J., 'Measurement and modeling of axial distribution of adsorbent particles in expanded bed: Taking into account the particle density difference,' Chemical Engineering Science, 2004, **59**(24), pp. 5873–5881, doi:https://doi.org/10.1016/j.ces.2004.07.009.

Yun, J., Yao, S. J., and Lin, D. Q., 'Variation of the local effective axial dispersion coefficient with bed height in expanded beds,' Chemical Engineering Journal, 2005, **109**(1), pp. 123–131, doi:https://doi.org/10.1016/j.cej.2005.03.015.

Zhang, J.-P., Epstein, N., and Grace, J. R., 'Minimum fluidization velocities for gas-liquid-solid three-phase systems,' Powder Technology, 1998, **100**(2-3), pp. 113–118, doi:https://doi.org/10.1016/S0032-5910(98)00131-4.

Zhang, X. and Ahmadi, G., 'Eulerian lagrangian simulations of liquid gas solid flows in three-phase slurry reactors,' Chemical Engineering Science, 2005, **60**(18), pp. 5089 – 5104, doi:https://doi.org/10.1016/j.ces.2005.04.033.

VITA

Vineet Alexander was born in 1988, in Kerala, India. He received his Bachelors Degree in Chemical Engineering in July 2011, from Kerala University, India. After graduation, he worked for a couple of years, first in a manufacturing facility called Hindustan Latex Ltd, Trivandrum, Kerala and then in an environmental protection agency called Kerala State Pollution Control Board, Allepey, Kerala. In July 2013, he moved to Rolla, Missouri, to pursue Masters Degree in Chemical Engineering at Missouri University of Science and Technology. He got an offer to convert to Ph.D. degree in Jan 2014 from the same university, which he accepted. In July 2018, he received his Ph.D. in Chemical Engineering from Missouri University of Science and Technology.